

14-40
FILE

DEVELOPMENT OF A BASIC METHODOLOGY FOR PREDICTING AIRCRAFT STOPPING DISTANCE ON A WET RUNWAY

O. W. Preston
Dr. G. W. Kibbee
R. H. Muroyama
R. A. Storley

DOUGLAS AIRCRAFT COMPANY
MCDONNELL-DOUGLAS CORPORATION
LONG BEACH, CALIFORNIA



MARCH 1971

FINAL REPORT

Availability is unlimited. Document may be released to the National Technical Information Service, Springfield, Virginia 22151, for sale to the public.

Prepared for

FEDERAL AVIATION ADMINISTRATION

Systems Research & Development Service

Washington D. C., 20590

1. Report No. FAA-RD-70-62		2. Government Accession No.		3. Recipient's Catalog No.	
4. Title and Subtitle DEVELOPMENT OF A BASIC METHODOLOGY FOR PREDICTING AIRCRAFT STOPPING DISTANCE ON A WET RUNWAY				5. Report Date March 1971	
				6. Performing Organization Code	
7. Author(s) O. W. Preston R. H. Muroyama Dr. G. W. Kibbee R. A. Storley				8. Performing Organization Report No. FAA-NA-70-5	
9. Performing Organization Name and Address DOUGLAS AIRCRAFT COMPANY McDonnell-Douglas Corporation Long Beach, California				10. Work Unit No. Project 510-003-04X	
				11. Contract or Grant No. DOT FA66-NF-128	
12. Sponsoring Agency Name and Address FEDERAL AVIATION ADMINISTRATION Systems Research and Development Service Washington, D. C. 20590				13. Type of Report and Period Covered FINAL REPORT 1966 to 1970	
				14. Sponsoring Agency Code	
15. Supplementary Notes None					
16. Abstract Studies and tests were conducted to develop a basic methodology for predicting the test aircraft stopping distance on a wet runway. Development consisted of a series of wet and dry runway tests utilizing the FAA Variable Slip Runway Friction Tester and an instrumented non-flyable test aircraft followed by an analysis of the test results using an analog computer simulation of the aircraft. A relationship was established between wet runway friction measured by the friction tester and friction available to the braking wheels of the test aircraft. The methodology consists of using this relationship and an analog computer aircraft simulation, incorporating actual anti-skid and braking system hardware, to prepare a nomograph showing aircraft stopping distance as a function of the runway friction measured by the FAA Variable Slip Runway Friction Tester. Correlation exists between friction measured by the friction tester and friction available to the tires of the test aircraft when normalized with respect to theoretical hydroplaning velocities. The relationship is that $\mu_{MAXA/C}$ equals 0.59 times μ_{MAXT} when the ratio between aircraft and friction tester velocities was equal to the ratio between their respective theoretical hydroplaning velocities.					
17. Key Words Aircraft Airport Friction Tester Runways Stopping			18. Distribution Statement Availability is unlimited. Document may be released to the National Technical Information Service, Springfield, Virginia 22151, for sale to the public.		
19. Security Classif. (of this report) Unclassified		20. Security Classif. (of this page) Unclassified		21. No. of Pages 116	22. Price

FOREWORD

This report was prepared by Douglas Aircraft Company, a division of McDonnell Douglas Corporation, for the Federal Aviation Administration. The work effort was part of a program of the Engineering and Safety Division, Aircraft Development Service, Washington, D.C. The work was administered under the direction of Mr. William A. Hering, who served as project engineer for the Instrument and Flight Test Section, Aircraft Branch, Test and Evaluation Division, National Aviation Facilities Experimental Center, Atlantic City, New Jersey.

TABLE OF CONTENTS

	Page
INTRODUCTION	1
DESCRIPTION	2
Methodology Concept	2
FAA Variable Slip Runway Friction Tester Description	3
Test Aircraft Description	4
Runway Description	6
Description of Tests	6
Description of Data Reduction	12
Description of the Computer Simulation	13
Description of Procedure Used to Determine a Relationship Between Tester Friction and Aircraft Tire Friction	17
RESULTS	19
DISCUSSION	20
Friction Tester Operation	20
Runway Tests	20
Discussion of Simulation	21
Discussion of Procedure Used to Determine a Relationship Between Tester Friction and Aircraft Tire Friction	21
Discussion of the Procedure Used in Preparing the Landing Distance Nomogram	24
Discussion of the Development and Application of the Basic Methodology	26
Additional Considerations	29
CONCLUSIONS	32
REFERENCES	33
APPENDIX I LONG BEACH AIRPORT RUNWAY PROFILE SURVEY AND SURFACING SPECIFICATION (9 Pages)	I-1
APPENDIX II FAA VARIABLE SLIP RUNWAY FRICTION TESTER DEVELOPMENTAL TESTS (7 Pages)	II-1
APPENDIX III RUNWAY CALIBRATION AND CORRELATION TESTS (9 Pages)	III-1
APPENDIX IV NONCONTRACTUAL FRICTION MEASURING VEHICLES INCLUDED IN RUNWAY TEST PROGRAM (6 Pages)	IV-1
APPENDIX V DEVELOPMENT OF THE FRICTION RELATIONSHIPS USED IN THE ANALOG SIMULATION (15 Pages)	V-1
APPENDIX VI ANALOG COMPUTER SIMULATION OF THE TEST AIRCRAFT (15 Pages)	VI-1

TABLE OF CONTENTS (Cont)

	Page
APPENDIX VII COMPARATIVE METHODS USED TO DETERMINE RELATIONSHIP BETWEEN FRICTION COEFFICIENTS OF THE FRICTION TESTER AND THE AIRCRAFT	(7 Pages) VII-1
APPENDIX VIII DEFINITIONS	(2 Pages) VIII-1

LIST OF ILLUSTRATIONS

Figure		Page
1	FAA Variable Slip Runway Friction Tester	3
2	DC-7 Test Aircraft	5
3	Long Beach Airport, Runway 12-30	7
4	Runway Surface Texture	8
5	Runway Wetting for Minimum Wet Condition	9
6	Runway Wetting for Maximum Wet Condition	9
7	FAA Variable Slip Runway Friction Tester	10
8	Miles Laboratory Trailer	10
9	FAA Station Wagon Equipped with James Brake Decelerometer	11
10	DC-7 Test Aircraft During Maximum Wet Tests	11
11	Runway Wetness After a Maximum Wet Test Had Been Completed	12
12	Analog Computer Simulation of DC-7 Test Aircraft	14
13	Douglas Automatic Parameter Scan Analog Computer (DAPSAC)	15
14	Anti-Skid Adaptive Electronics and Anti-Skid Control Card	16
15	Simulation Hydraulic System	16
16	Correlation Method – Block Diagram Description of Procedure Used to Determine Relation Between Aircraft and Friction Tester Friction Coefficient	18
17	Anti-Skid Efficiency Expressed as a Relationship Between μ_{MAX} and μ_{EFF}	22
18	Anti-Skid Efficiency	22
19	Relationship Between Measured Friction and Aircraft Tire Friction	23
20	Nomogram Preparation Procedure	25
21	Stopping Distance Chart	26
22	Landing Distance Nomogram	27
23	Possible Runway Friction Classification Charts	30

INTRODUCTION

The development of commercial jet aircraft with higher takeoff and landing speeds and greater weights than the previous generation of propeller-driven aircraft has intensified the problem of aircraft stopping performance. Jet aircraft rely primarily on brake performance to stop with assistance from engine thrust reversers. Advances in the design of anti-skid systems and brakes, and the use of aerodynamic lift spoilers have improved aircraft stopping performance. However, specification of wet runway length requirements is still a problem primarily due to the inability to correlate the highly variable friction of wetted pavement surfaces.

Government agencies and industry have conducted extensive research to gain insight into factors affecting aircraft stopping performance on wet runways. References 1 through 5 describe work done by the FAA and NASA during the last decade to provide information on airplane tire braking coefficients, effects of tire tread configuration, effects of tire tread compounds, information on the relationship of various friction measuring vehicles or trailers, the relationship of friction measurement from these devices to friction experienced by the aircraft, and the evaluation of runway surface modifications which increase friction during inclement weather conditions. Notwithstanding this work, an accurate operational method for predicting the aircraft stopping performance on wet runways has yet to be proven.

To develop a method including flight manual nomograms for predicting wet runway stopping distance, the McDonnell Douglas Corporation, under contract to the National Aviation Facilities Experimental Center of the Federal Aviation Administration, initiated a program involving an analytical approach in combination with runway tests utilizing an instrumented test aircraft and the FAA Variable Slip Runway Friction Tester.

The objectives were to develop a methodology consisting of a formula, method or procedure which would permit data acquired on a test runway with the FAA Variable Slip Runway Friction Tester to be correlated with the stopping performance of a test aircraft and, using this relationship, to formulate a method for predicting aircraft stopping distances on wet runway surfaces.

The resulting program was essentially a three-phase effort. The first phase provided familiarization and evaluation of the vehicle and runway on which tests were to be conducted. The evaluation resulted in some modification and mechanical improvements being accomplished on the vehicle. The second phase consisted of coincident aircraft wet runway braking and runway friction measurements with the FAA Variable Slip Runway Friction Tester. The third phase was the analysis of the test data for methods development.

Friction measurements were also obtained during the second phase with the FAA Fixed Slip Runway Friction Tester, the Miles Braking Trailer, and the James Brake Decelerometer. The FAA fixed slip tester was towed by a specially equipped FAA station wagon. The object of these tests (Appendix IV) was to determine correlation factors, if any, between the FAA Variable Slip Runway Friction Tester and other testers.

The analytical approach utilized an analog computer, coupled to actual anti-skid and braking system hardware, to simulate the test aircraft dynamically. The anti-skid braking system hardware provided the actual time relationships between wheel speed and brake pressures. The aircraft simulation system also included the tire/runway interface of a braked wheel. Runway friction data put into the analog initially were those obtained by the FAA Variable Slip Runway Friction Tester.

DESCRIPTION

The object of this program was to develop a methodology whereby runway friction data obtained with the FAA Variable Slip Runway Friction Tester could be used to predict aircraft stopping distance on a wet runway. The following paragraphs describe this methodology concept and the equipment, tests, and analyses necessary for its development.

METHODOLOGY CONCEPT

The methodology for the use of the runway friction tester in predicting airplane stopping distances on wet runways as conceived for this program was as follows:

1. Standard airplane stopping distance nomograms would be prepared to show airplane stopping distance for various coefficients of friction or friction categories of wet runways.
2. A runway friction tester would be used to obtain the friction coefficients from which the nomograms would be made.
3. A friction tester could be used to determine the slipperiness of a runway at the time of landing or to relate friction level to runway condition.
4. With the slipperiness of the runway identified by the friction tester, together with the nomograms, the acceptability of the runway length for the landing could be determined.

The basic requirement was that a satisfactory methodology be developed that could be used to relate the friction data obtained on a wet runway with the FAA Variable Slip Runway Friction Tester to the stopping distance required by a transport aircraft operating on the same runway.

It was decided that an analytical approach instead of an empirical approach be developed because of the varying performance of aircraft skid control systems. Furthermore, to obtain a sufficient quantity of statistical data for an empirical approach, each model transport aircraft would have to be tested on each runway for all necessary conditions, and costs would be extremely high.

Of the factors affecting airplane braking performance, the anti-skid system is considered one of the most important. To include this effect in the analysis, an analog computer simulation of a braking aircraft was used to determine stopping distance based upon friction available to the braked wheels.

Through the use of the simulation, the friction tester information was related directly to aircraft tire/runway friction with the simulation accounting for the many variables existing between friction available to the aircraft tire and the end result, namely aircraft stopping distance. The purpose of the simulation was two-fold: to enable establishment of a relationship between friction tester measured friction and friction available to the aircraft tire; and to enable this relationship to be applied to predicting stopping distances for a variety of runway slipperiness conditions.

The development of this methodology consisted of the following steps:

1. Establishment of a data correlation base by performing wet and dry runway tests using both the FAA Variable Slip Runway Friction Tester and a test aircraft instrumented to record braking performance data, primarily anti-skid signals and landing gear vertical, drag, and torque loads.
2. Development of an aircraft simulation using an analog computer and actual anti-skid and braking system hardware, and using braking performance characteristics recorded during runway tests to both develop and verify the simulation.
3. Application of the simulation to determine the relationship between friction, as measured by the friction tester, and friction available to the aircraft tires.
4. Formulation of the method, applying the tester/aircraft friction relationship, facilitating prediction of aircraft stopping distance with practical accuracy.

FAA VARIABLE SLIP RUNWAY FRICTION TESTER DESCRIPTION

The FAA Variable Slip Runway Friction Tester shown in Figure 1 is a single integrated unit consisting of a modified 3/4-ton truck, test trailer, friction wheel vertical and torque loading system, pavement wetting system, and data recording instrumentation. The friction tester is capable of speeds up to 80 mph and test wheel slip can be adjusted manually from 0 to 100 percent or cycled automatically from 0 percent to the desired slip and back to 0 percent in a selected time period between 7 and 14 seconds. Control of the test tire slip is accomplished by a variable displacement hydraulic pump and motor system. The vehicle was designed to use a 7.50 x 14-in. ASTM standard test tire and is capable of providing a constant 0.020-inch film of water in front of the tire to simulate wet runway conditions. Drag force from the test tire/runway interface is measured by a strain gage load cell. True vehicle speed is obtained by a free rolling wheel. More detailed information on the friction tester is contained in References 6 and 7.

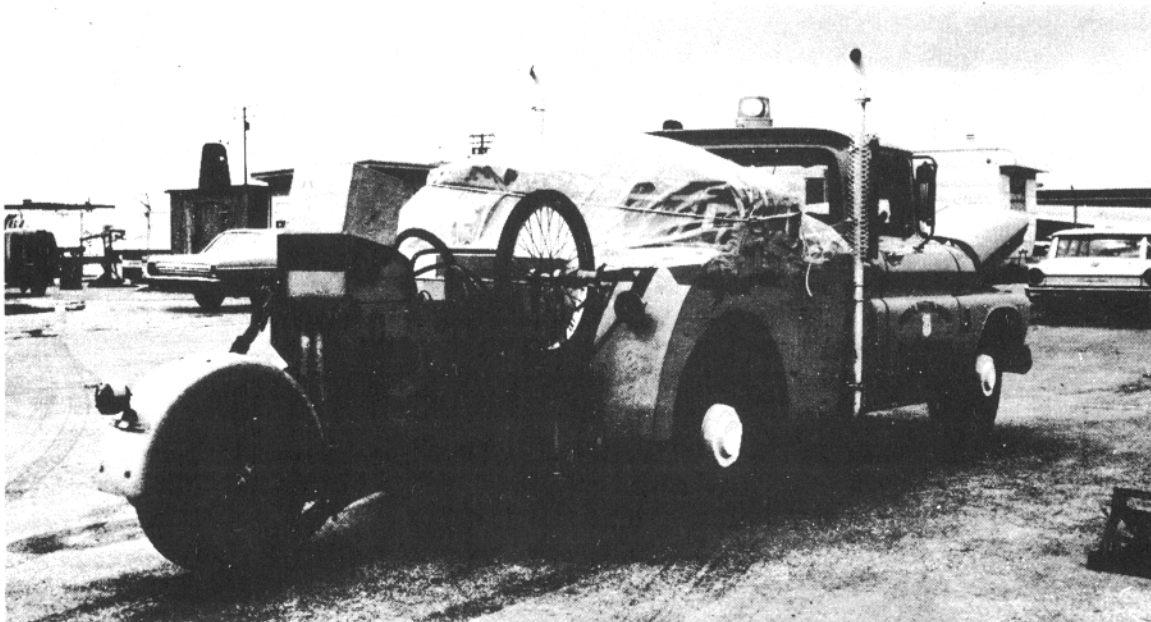


FIGURE 1. FAA VARIABLE SLIP RUNWAY FRICTION TESTER

As designed, the friction tester was equipped to record vehicle speed, test wheel speed, and drag load on an ink pen recorder. The friction tester was also equipped with an 8-channel tape recorder. For these tests, however, additional instrumentation was temporarily installed on the friction tester to obtain the following measurements and record them on a CEC-Type 350, 50-channel oscillograph recorder.

Measurement	Type of Transducer or Derivation of Signal
Vehicle Speed	Weston DC Tachometer
Test Wheel Speed	Magnetic Coil
Slip Velocity	Friction Tester Mounted Computer
Pneumatic Cylinder Pressure	Pressure Transducer
Shock Absorber Load	Strain Gage
Trailer Vertical Acceleration	Accelerometer
Normal Load	Friction Tester Mounted Computer
Drag Load	Thwing-Albert Load Cell
μ	Friction Tester Mounted Computer
Average μ over a 1-second interval	Friction Tester Mounted Computer
Hydraulic System Pressure (2 locations)	Pressure Transducers

TEST AIRCRAFT DESCRIPTION

The test aircraft, shown in Figure 2, was a DC-7 which had been modified to incorporate DC-9 landing gear axles, wheels, brakes, tires, and Hytrol Mark II Anti-Skid System. Test weights varied between 77,007 and 80,365 pounds. Throughout the tests, flaps and ailerons were faired and the elevator column was positioned full forward. New 40 x 14 Type-VII main landing gear tires were installed and inflated to 115 psi. One set of tires was used and was approximately 50-percent worn at the end of testing. Consecutive runs were delayed until brake tie bolt temperatures fell below 100°C to ensure proper and consistent brake performance.

Pertinent aircraft data recorded manually during the runway tests are listed below:

Aircraft Gross Weight, Adjusted for Fuel Consumption Between Tests

Tire Pressure

Tire Tread Depth

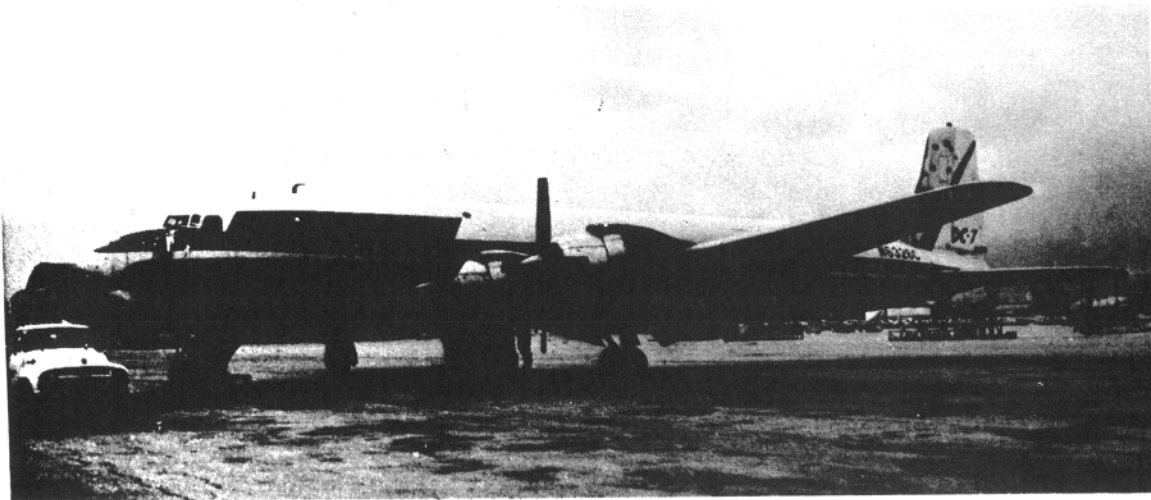


FIGURE 2. DC-7 TEST AIRCRAFT

Data items recorded on a 50-channel, CEC-Type 119 P3 oscillograph and type of transducer used to obtain the measurement are listed below:

Measurement	Type of Transducer or Derivation of Signal
Event Correlation Signal	Manual
Pitch Angular Acceleration	Accelerometer
Roll Angular Acceleration	Accelerometer
Yaw Angular Acceleration	Accelerometer
CG Longitudinal Acceleration	Accelerometer
Nose Wheel RPM	Magnet and Coil
Main Wheel RPM (Left Outboard)	Anti-Skid Signal
Main Wheel RPM (Left Inboard)	Anti-Skid Signal
Main Wheel RPM (Right Outboard)	Anti-Skid Signal
Main Wheel RPM (Left Inboard)	Anti-Skid Signal
Brake System Pressure (Left Pedal)	Pressure Transducer
Brake System Pressure (Right Pedal)	Pressure Transducer
Brake Pressure (Left Outboard)	Pressure Transducer
Brake Pressure (Left Inboard)	Pressure Transducer

Brake Pressure (Right Outboard)	Pressure Transducer
Brake Pressure (Right Inboard)	Pressure Transducer
Anti-Skid Valve Voltage (Left Outboard)	Anti-Skid Signal
Anti-Skid Valve Voltage (Left Inboard)	Anti-Skid Signal
Anti-Skid Valve Voltage (Right Outboard)	Anti-Skid Signal
Anti-Skid Valve Voltage (Right Inboard)	Anti-Skid Signal
Drag Load (Right Outboard)	Strain Gage
Drag Load (Right Inboard)	Strain Gage
Vertical Load (Right Outboard)	Strain Gage
Vertical Load (Right Inboard)	Strain Gage
Brake Torque (Right Outboard)	Strain Gage
Brake Torque (Right Inboard)	Strain Gage

RUNWAY DESCRIPTION

A centrally located 3000-foot section of Runway 12-30 at Long Beach Airport was selected for the correlation tests. This runway, shown in Figure 3, had recently received an asphaltic concrete overlay and a portion of the runway, including the first 2080 feet of the test section, received a second "smoothing" overlay. The resulting surface texture is shown in Figure 4.

A runway vertical profile survey of the test section was conducted. The survey covered 2-foot increment widths on two longitudinal parallel lines, 1.2 feet to each side of the runway centerline. The runway profile was taken for analysis information to account for any irregularities, undulations, or slopes that might affect friction reading during correlation efforts and that might have caused peculiar or erratic anti-skid operation. The readings were taken on either side of the center line to be in the approximate paths on which the main wheel tires of the airplane would travel. Downhill slope measured in the direction of aircraft travel was 0.38 percent. The RMS roughness deviation was 0.0139 feet. A 1-inch dropoff over a 10-foot length was measured where the second "smoothing" overlay was terminated. The runway drainage crown was one percent.

Surface profile charts and the overlay specification are contained in Appendix I.

DESCRIPTION OF TESTS

Friction Tester Developmental Tests

Developmental tests were performed with the friction tester, to determine if data produced by the friction tester were satisfactory to warrant pursuit of the methodology program and, second, to select the test tire and the friction tester mode of operation. These tests and their results are described in Appendix II.

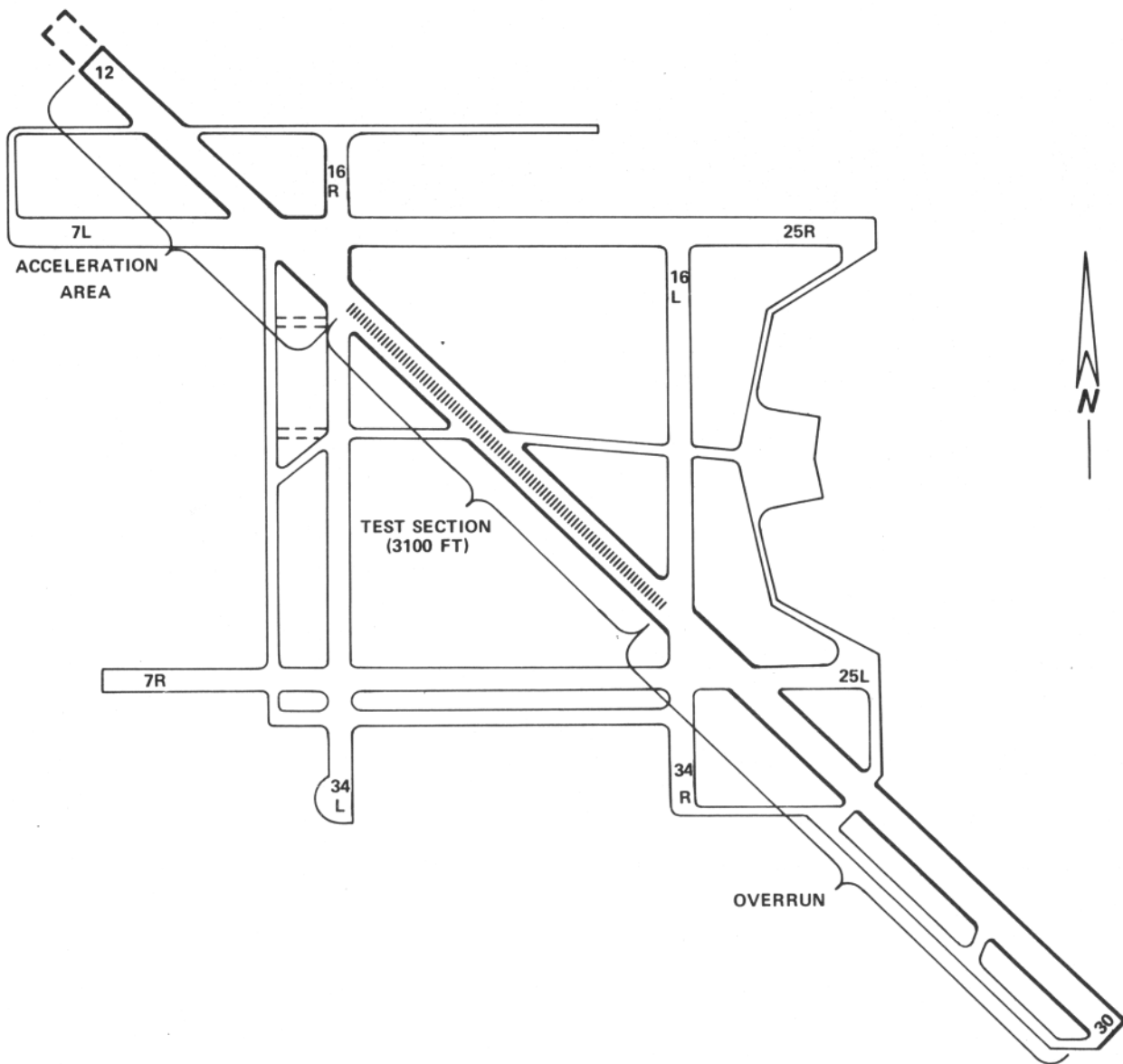


FIGURE 3. LONG BEACH AIRPORT, RUNWAY 12-30.

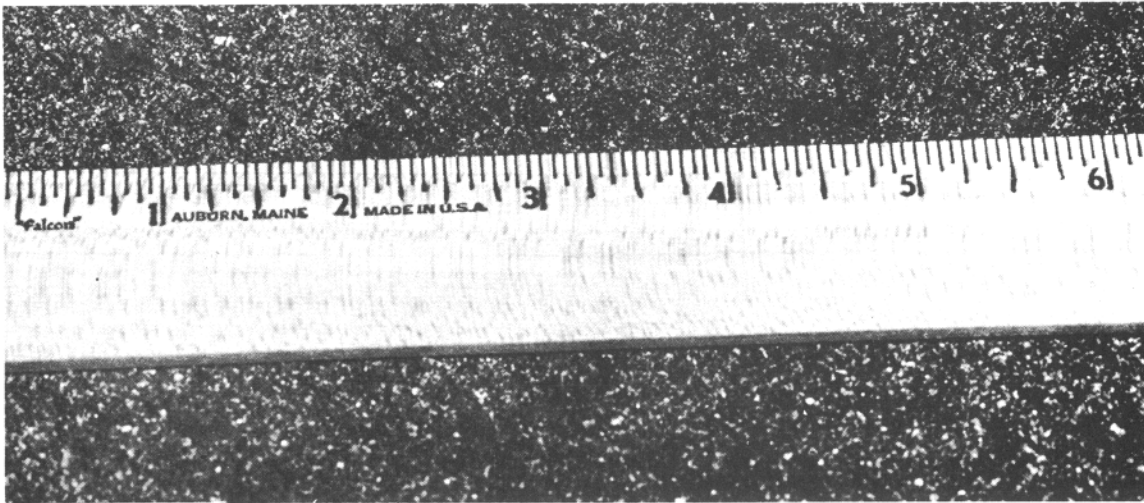


FIGURE 4. RUNWAY SURFACE TEXTURE

Runway Friction Calibration Tests

Runway tests using the friction tester were conducted on Long Beach Airport runway 12-30 to obtain a friction calibration of the 3000-foot test section. Runway friction was measured for the following environmental conditions: dry, friction tester self-wetted, natural damp, and natural rain. The damp tests were performed in the morning after a light rainfall. The natural rain tests were conducted under medium-to-heavy rain conditions. Eighteen dry runs, 18 vehicle wetted runs, 10 natural damp runs, and 12 natural rain runs were performed in alternating directions on the runway, 12 feet to each side of the centerline. The tests were performed using the autocycling system set for a 7-second cycle period and 35-percent maximum slip to ensure that slip was more than adequate to obtain peak friction, and the standard ASTM E-249 ribbed tire inflated to 60 psi and loaded to 600 pounds. Constant friction tester speeds of 30, 60, and 80 mph were used.

Results of the calibration tests are contained in Appendix III.

Friction Tester – Aircraft Correlation Tests

The friction tester – aircraft correlation tests were performed on the runway 12-30 test section at Long Beach Airport. Four dry, eight minimum wet, and six maximum wet tests were performed with the friction measuring vehicles preceding the aircraft into the test area on all tests. One water truck travelling at 15 mph laid down a thin layer of water to simulate minimum wet runway conditions, and two or three water trucks travelling at 8 mph were used to simulate the maximum wet runway conditions. The friction measuring vehicles operated at constant speeds of 30, 60, or 80 mph. The test aircraft accelerated to above 120 knots before entering the test area and, after entering the test section, used full anti-skid braking until completely stopped. None of the runs required more than the 3000-foot test section for a complete stop. Throughout the entire speed spectrum of the aircraft run, data were recorded on the aircraft's oscillograph and with a phototheodolite. All testing was performed in one direction from northwest to southeast.

Two nonbraking runs were also performed on dry pavement to verify aerodynamic constants and engine thrust levels. For these tests, the aircraft was accelerated in the same manner; however, the brakes were not applied while the aircraft was in the test area. Two speed ranges, 108 to 87 and 95 to 69 knots, were covered.

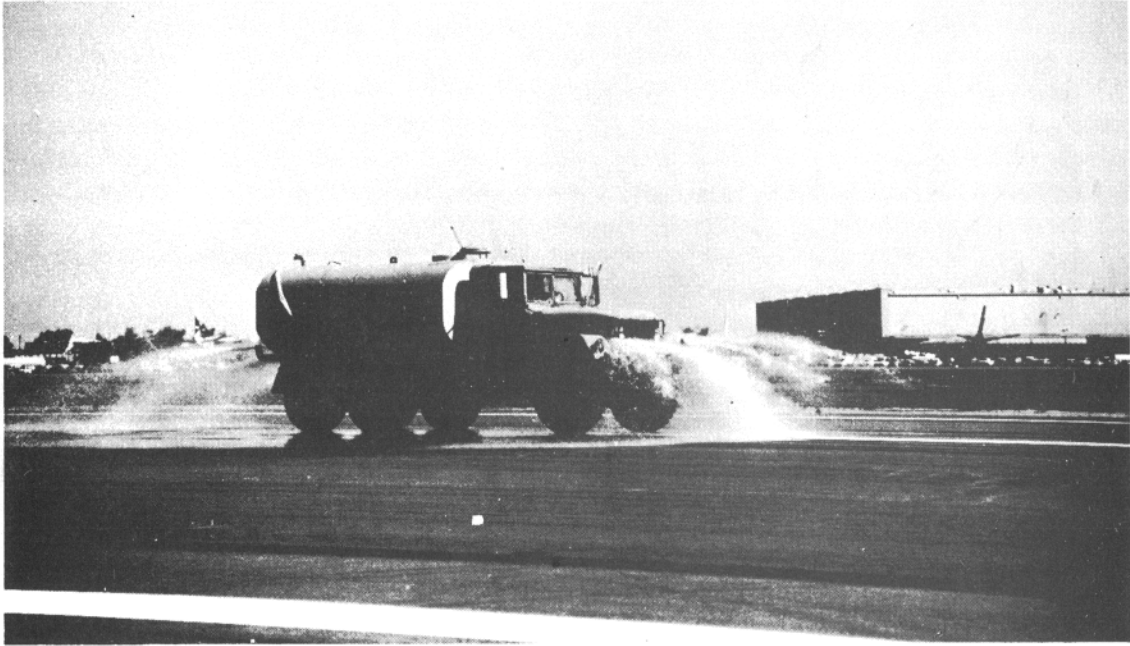


FIGURE 5. RUNWAY WETTING FOR MINIMUM WET CONDITION



FIGURE 6. RUNWAY WETTING FOR MAXIMUM WET CONDITION



FIGURE 7. FAA VARIABLE SLIP RUNWAY FRICTION TESTER

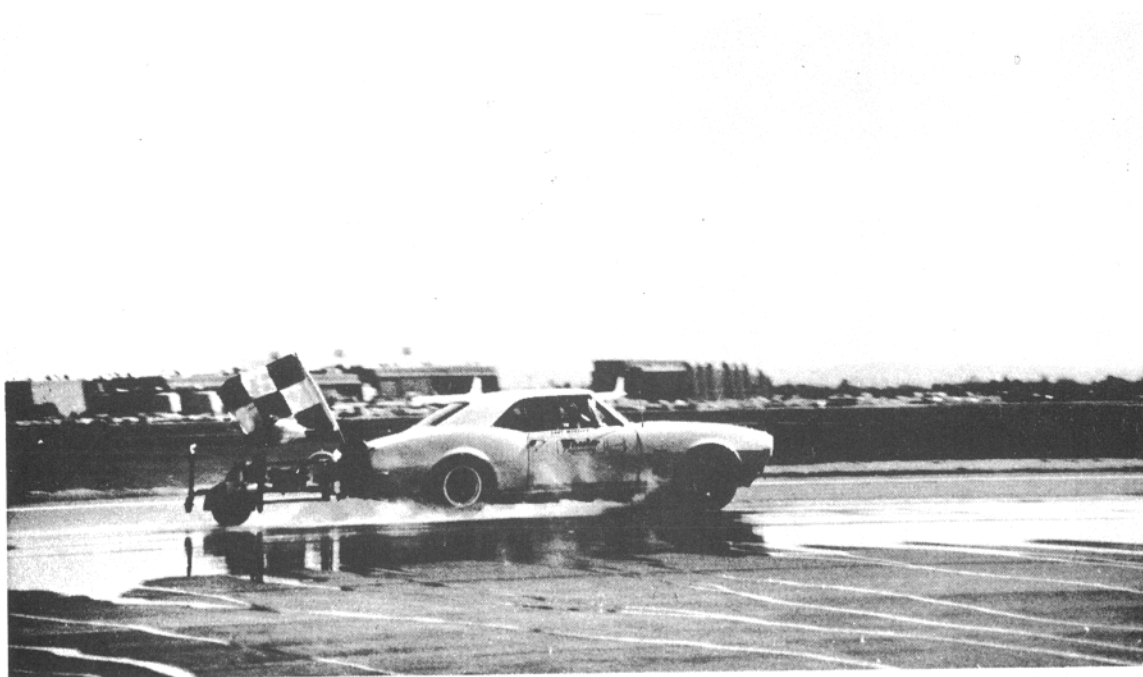


FIGURE 8. MILES LABORATORY TRAILER

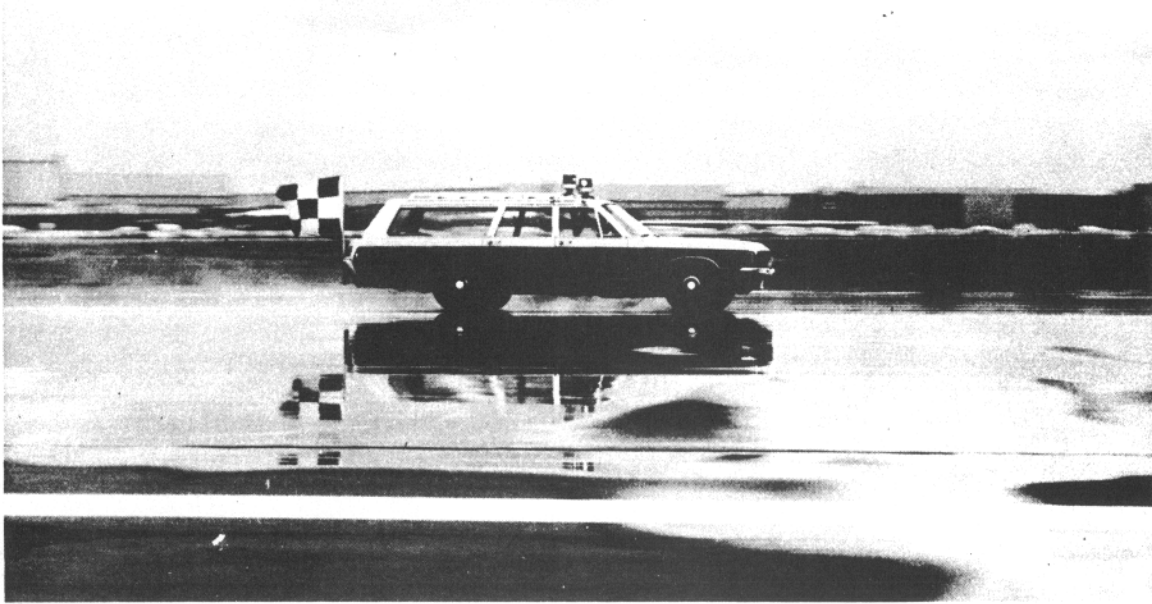


FIGURE 9. FAA STATION WAGON EQUIPPED WITH JAMES BRAKE DECELEROMETER



FIGURE 10. DC-7 TEST AIRCRAFT DURING MAXIMUM WET TESTS



FIGURE 11. RUNWAY WETNESS AFTER A MAXIMUM WET TEST HAD BEEN COMPLETED

DESCRIPTION OF DATA REDUCTION

The data reduced from the friction tester – aircraft correlation tests consisted of –

Friction Tester

- Drag load versus slip velocity.
- Tabulated test condition, tester velocity, maximum drag force, slip velocity, maximum slip velocity, test wheel velocity, air loading cylinder pressure, runway location, and high and low hydraulic pressures.
- Maximum drag load versus runway location.

Test Aircraft

- Plots of μ , drag load, and brake pressure versus aircraft velocity. Read for each right main landing gear wheel just prior to each anti-skid pressure release.
- Plots of μ versus aircraft velocity read every third of a second during braking.
- Schedule of aircraft gross weight, center of gravity position, environmental conditions, and tire wear during each test.

- Reduced size traces of oscillograph records of drag, normal load, and brake torque for each instrumented wheel and brake pressure, anti-skid valve voltage, and wheel-speed voltage for all wheels. Reduced for dry, minimum wet, and maximum wet conditions.
- Phototheodolite coverage showing aircraft velocity, deceleration, and distance versus time.
- Aircraft distance versus velocity squared normalized to 80,000 pounds, no wind, no slope, sea level, and standard day temperature.

DESCRIPTION OF THE COMPUTER SIMULATION

The analog computer simulation of the test aircraft was developed to determine if friction data obtained by the friction tester could be used as input to determine stopping distance of the simulated aircraft, thereby establishing a relationship between measured friction and aircraft stopping distance.

The analog computer simulation of the test aircraft is shown in Figure 12. All equations necessary to describe the aircraft dynamic qualities were programmed into a Douglas Automatic Parameter Scan Analog Computer (DAPSAC). Actual anti-skid and braking system hardware (anti-skid control box, anti-skid control valve, brake, and hydraulic system) were included in the simulation to provide accurate and realistic real time relationships between computed wheel speed and brake pressure. Photographs of the analog simulation are shown in Figures 13, 14, and 15.

A constant 3000-psig hydraulic pressure was made available to the simulation's anti-skid system after verifying that the same pressure was available to the aircraft's anti-skid system throughout the aircraft tests. Hydraulic line lengths, sizes, bends, fittings, manifolds, fuses, and other hydraulic components on the aircraft were duplicated in the simulation. The anti-skid control box and one anti-skid control valve were removed from the aircraft and used in the simulation. A voltage-controlled oscillator converted computed wheel speed into a signal representing wheel speed transducer output. This signal went into the anti-skid control box, whose output controlled brake pressure via the anti-skid control valve. A pressure transducer converted brake pressure to a voltage representing brake pressure, which was used, along with computed wheel speed, by the computer to calculate brake torque.

Brake torque characteristics used in the simulation were a function of both brake pressure and wheel speed, and were determined from dynamometer test data obtained from the manufacturer. From dynamometer stops made at different pressure levels, the relationship between torque and pressure was determined. Torque versus velocity plots for these stops also gave the relationship between torque and wheel speed. Particular care was taken to ensure that the brake torque characteristics were based upon test energy levels similar to those tested.

To provide a realistic randomness to the depth and spacing of the wheel skids, Gaussian (white) noise with a bandwidth of 5 Hz was added to the main gear vertical loads to simulate runway roughness. The amplitude was adjusted to give vertical load excursions approximating that shown on oscillograph records obtained during the aircraft tests.

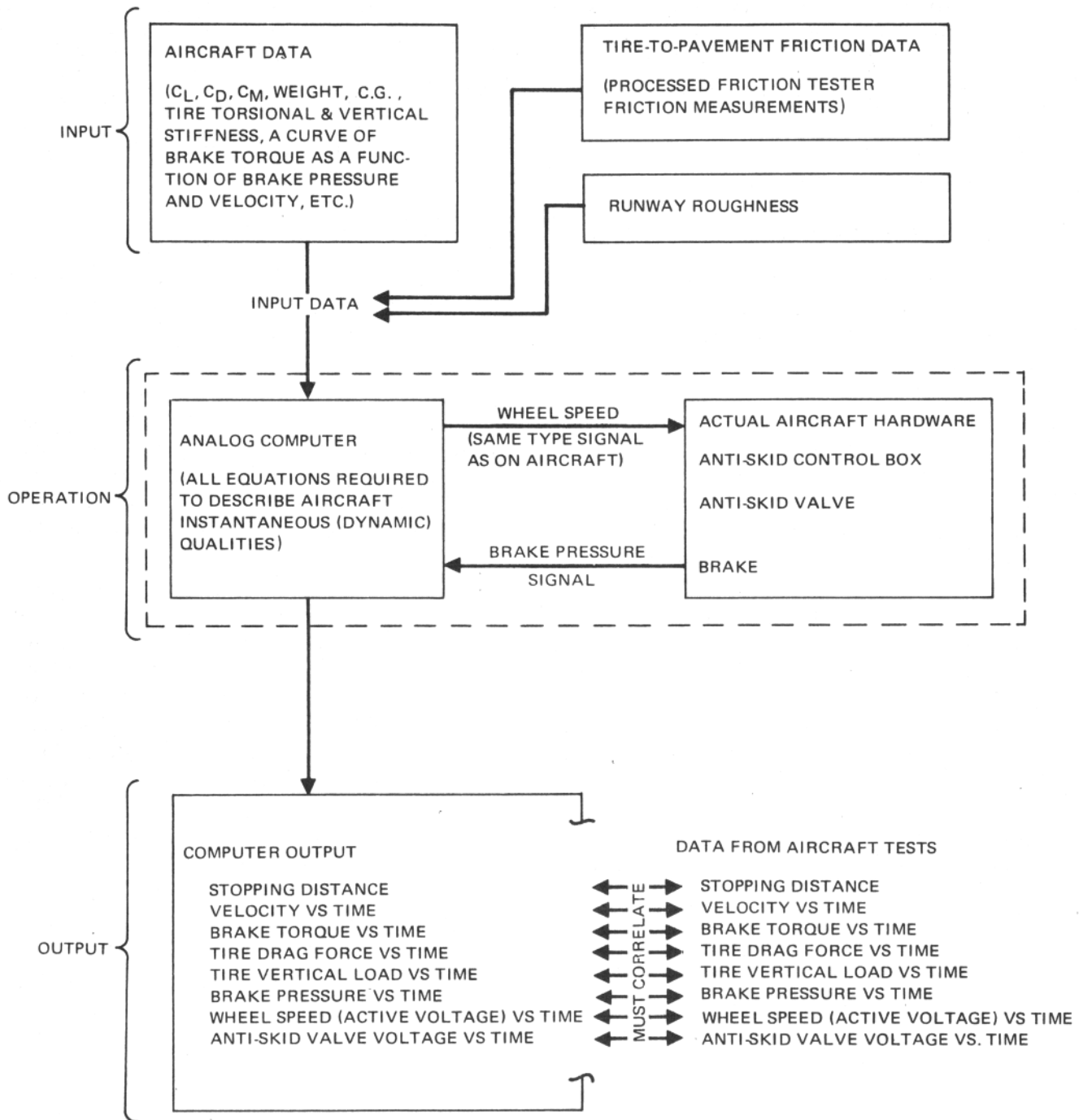


FIGURE 12. ANALOG COMPUTER SIMULATION OF DC-7 TEST AIRCRAFT

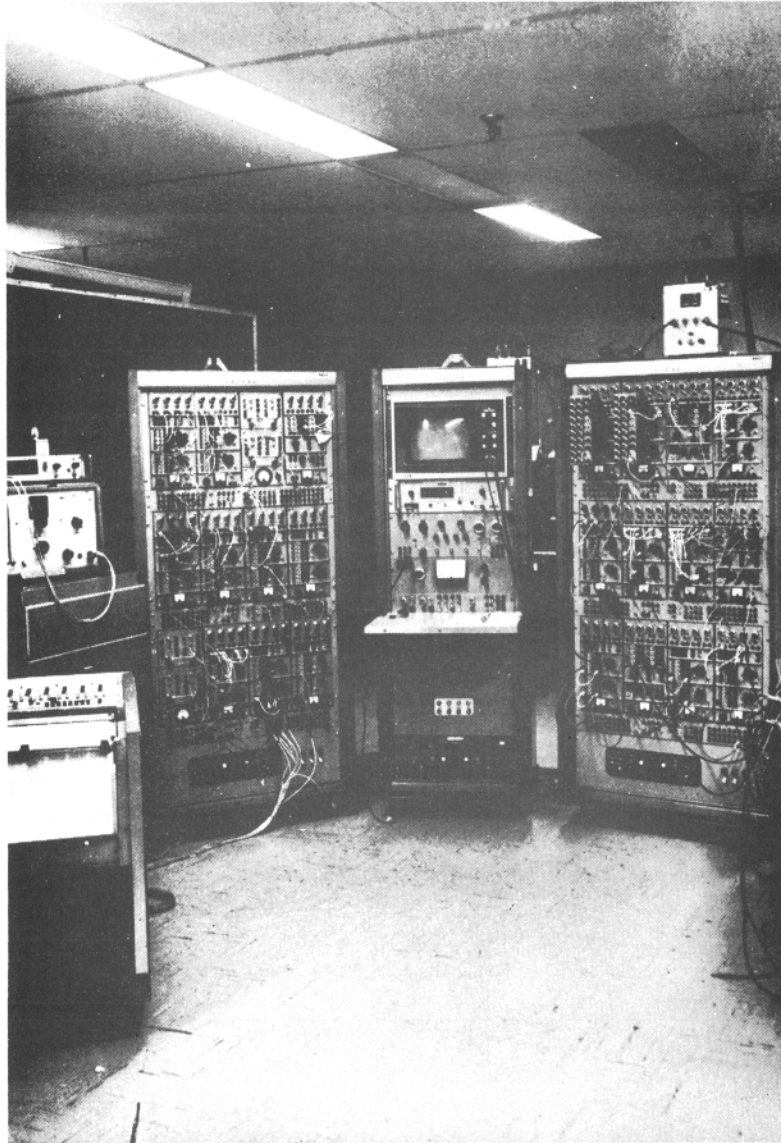


FIGURE 13. DOUGLAS AUTOMATIC PARAMETER SCAN ANALOG COMPUTER (DAPSAC)

The net effect of rolling resistance and propeller thrust was obtained from the aircraft nonbraking test results, combined with aerodynamic drag, and input to the computer as a unit. Tire-to-pavement friction data were input as μ_{MAX} versus velocity and percent of μ_{MAX} versus tread slip velocity.

The simulation was considered complete when the computer output successfully matched the aircraft data generated during the runway tests. Development of the runway friction data relationships used in the analog simulation is described in detail in Appendix V, and the final simulation is documented in Appendix VI.

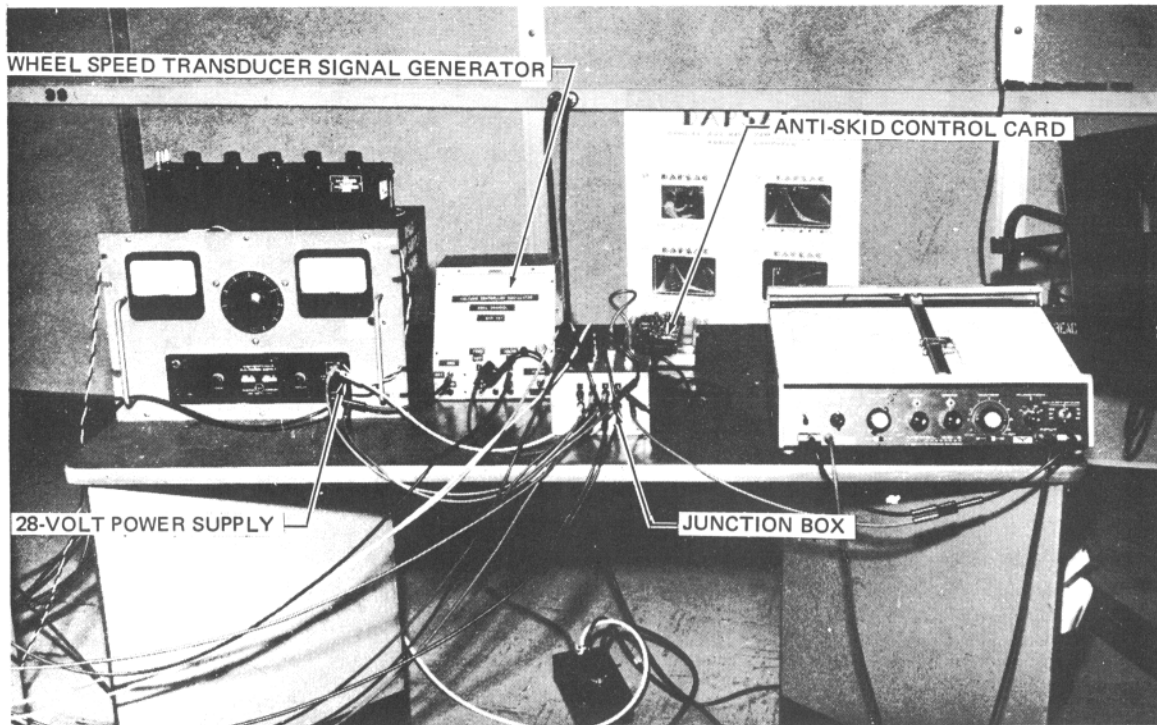


FIGURE 14. ANTI-SKID ADAPTIVE ELECTRONICS AND ANTI-SKID CONTROL CARD

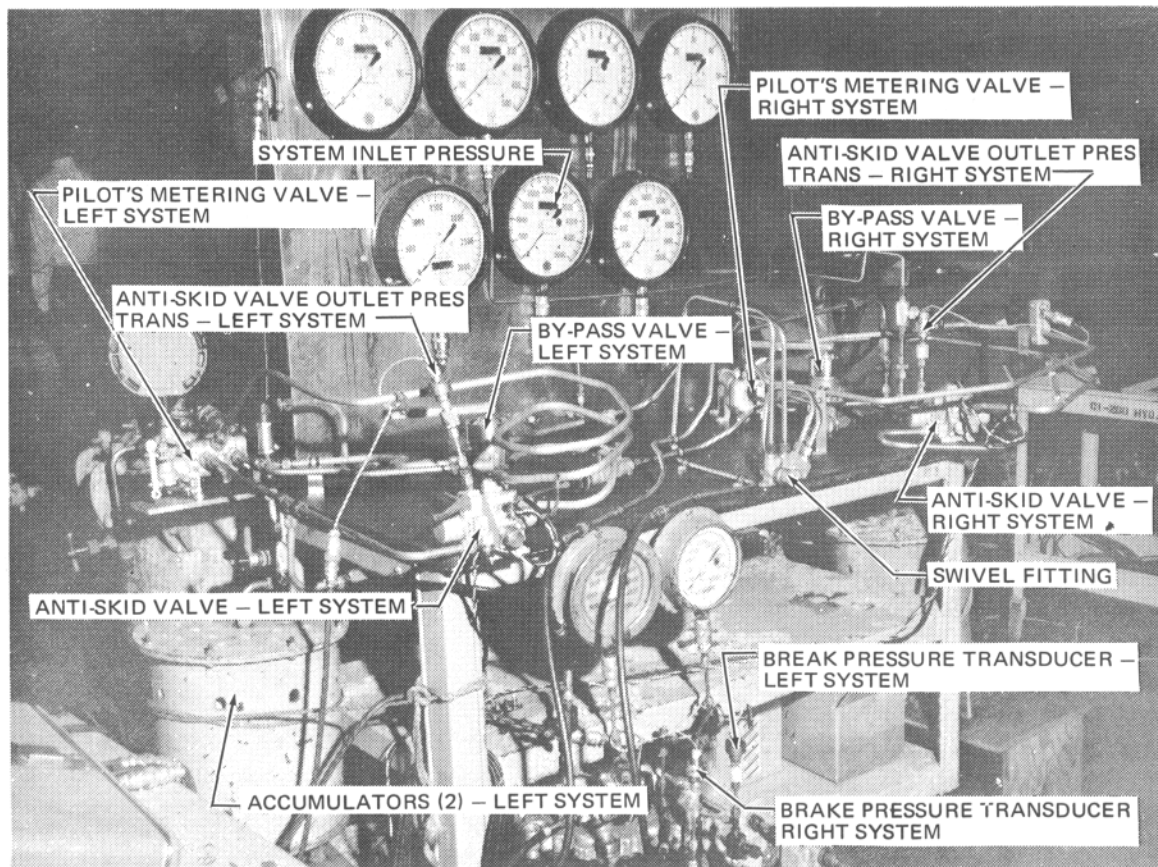


FIGURE 15. SIMULATION HYDRAULIC SYSTEM

DESCRIPTION OF PROCEDURE USED TO DETERMINE A RELATIONSHIP BETWEEN TESTER FRICTION AND AIRCRAFT TIRE FRICTION

The parameter selected to show the relationship between friction coefficient information obtained by the friction tester and that experienced by the aircraft was the maximum friction coefficient, μ_{MAX} . Relating the maximum friction coefficient of the friction tester, $\mu_{MAX T}$, to the similar aircraft parameter, $\mu_{MAX A/C}$, by a ratio kept the relationship simple. This relationship was made a function of velocity presented as a ratio that was normalized to the theoretical hydroplaning velocity.

The procedure is illustrated by the block diagram in Figure 16. To implement the procedure the simulator was used to determine anti-skid system efficiency as a function of velocity and maximum friction coefficient. The efficiency was expressed as effective friction coefficient, μ_{EFF} , versus μ_{MAX} for various aircraft velocities.

The effective friction coefficients of the aircraft during the runway tests, determined from phototheodolite data, were then converted to maximum friction coefficient data using these results. The maximum aircraft coefficient, $\mu_{MAX A/C}$, was then divided by the maximum friction tester coefficient, $\mu_{MAX T}$, for specific velocity ratios, which was the relationship desired.

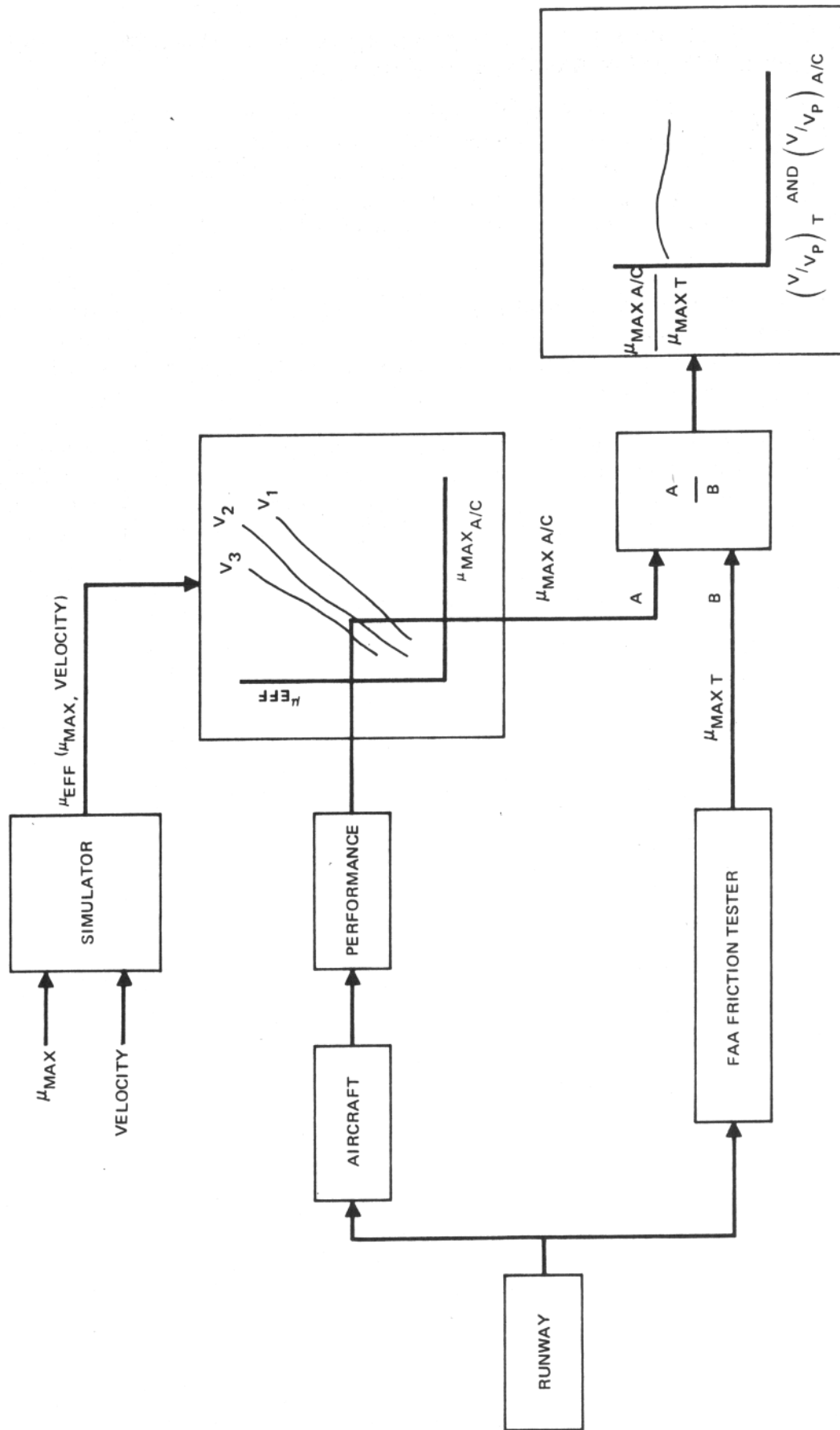


FIGURE 16. CORRELATION METHOD - BLOCK DIAGRAM DESCRIPTION OF PROCEDURE USED TO DETERMINE RELATION BETWEEN AIRCRAFT AND FRICTION TESTER FRICTION COEFFICIENT

RESULTS

1. A basic methodology for predicting aircraft stopping distances on wet runways was developed and was verified for the test aircraft on the test runway. The methodology briefly stated is as follows:

Runway friction available to the braking tires of an aircraft was related to runway friction measured with the FAA Variable Slip Runway Friction Tester. By using this relation and an analog computer simulation of the test aircraft braking on a wet runway, stopping distances were computed for various measured runway friction values and included into a Flight Manual type stopping distance nomogram which presents stopping distance as a function of the FAA friction tester-measured friction.

The following results were necessary to support the methodology.

2. The friction data obtained by the FAA Variable Slip Runway Friction Tester was of sufficient repeatability, validity, and character to establish a correlation between friction measured by the tester and the wet runway stopping performance of the test aircraft.
3. The analog computer simulation of the test aircraft successfully duplicated, in the laboratory, the braking characteristics and stopping performance of the test aircraft on the 3000-foot test section of the runway.
4. Correlation was achieved between the friction tester friction (μ_{MAX_T}) and the test aircraft tire friction ($\mu_{MAX_{A/C}}$). The relationship was that $\mu_{MAX_{A/C}}$ equaled 0.59 times μ_{MAX_T} when the ratio between aircraft and friction tester velocities was equal to the ratio between their respective theoretical hydroplaning velocities.
5. The correlation between friction tester friction and aircraft tire friction was extended to aircraft stopping distance through use of the aircraft simulation, thereby relating measured friction to aircraft stopping performance.
6. A flight-manual-type landing field length nomogram was prepared for relating friction tester friction measurements to the landing distance requirements of the aircraft.

DISCUSSION

This development program has resulted in meaningful observations and data that point out factors which should be considered in applying the methodology to civil transport aircraft operations. Relevant factors to the development, application and limitation of the methodology are discussed in the following paragraphs.

FRICTION TESTER OPERATION

The friction tester mode of operation selected for the correlation tests was automatic cycling with the autocycling system set for a 7-second cycle period and 35-percent maximum slip. Comparative tests performed over short distances showed that constant slip and autocycling resulted in the same measured friction values. The primary reason for selecting the cycling mode is that its intermittent operation resulted in less tire heating. Tire heating was considered a serious obstacle to obtaining repeatable friction measurements. The secondary reasons for selecting the autocycle mode was that it provided a better definition of the shape of the μ -slip curve and that the μ_{MAX} value could always be determined during a single run, eliminating the need for making several runs. Alternate methods would have required either plotting results to determine μ_{MAX} or the other alternative of selecting a constant slip about which μ_{MAX} values generally, but might not always occur. These advantages of the autocycle procedure were considered to outweigh its disadvantages which were that it provided intermittent, rather than continuous, friction measurement and the spindown test wheel inertia force produced a plus 6-pound drag load error at 80 mph when using 7-second, 35-percent autocycle settings. The 7-second cycle period (setting could be varied from 7 to 14 seconds) was selected because it would provide the most μ_{MAX} friction measurements per run. The 35-percent maximum slip was selected to ensure that slip would be more than adequate to produce peak friction during each cycle. (The peak friction is considered to occur from 10 to 20 percent slip ratio.) Also limiting the slip ratio to 35 percent minimized tire heating.

Reviewing friction tester operational procedures used to determine the relationship between measured friction and friction available to the aircraft tire, the shape of the μ -slip curve of the test runway was not part of the determined relationship and therefore not significant for predicting aircraft stopping distance. In selecting a best velocity from the range of 30 to 80 mph for performing measurements, friction measured at 80 mph provided the best delineation (reference Figure III-6) of varying wetness conditions and provided the best correlation when plotted directly against aircraft stopping distance (reference Figure III-7). The autocycle mode is still preferred on the basis that it minimizes tire heating. The maximum slip setting should be at least 30 percent to ensure that peak friction is obtained during each cycle. A minimum cycle period is advantageous to provide the most measurements per run.

Four test tires were evaluated for use on the friction tester. Of the four tires, the standard ASTM E-249 ribbed tire was selected on the basis of better friction consistency, reasonable wet/dry friction ratio, and standardized configuration. A more detailed description of the evaluation and selection of the test tire is contained in Appendix II.

RUNWAY TESTS

Friction values recorded by the FAA friction tester and the noncontractual friction measuring vehicles indicated that the test section surface texture was much superior, both dry and wet, to the average ungrooved runway. Although three to four times as much water was applied to the

test section during the maximum wet tests as during the minimum wet tests (reference Table IV-1), very little difference was evident in either aircraft stopping distance or measured friction. This is believed due to the high friction quality of the runway which was resurfaced shortly before the test program (reference Appendix I). The high friction characteristics of the runway are also considered to be the cause of large differences between truck-wetted and rain-wetted friction as measured by the tester and plotted on Figures III-4, III-5, and III-6. Water depths conducive to hydroplaning were apparently experienced in rain.

A detail description of the runway tests and results is contained in Appendices III and IV.

DISCUSSION OF SIMULATION

The analog computer method used to simulate the DC-7 test aircraft was used extensively in DC-9 anti-skid development work. Perfect agreement between simulator data and aircraft test results can not be expected, since only one wheel is represented in the simulation, whereas the actual aircraft has four, eight or more braked wheels which do not behave in unison but skid randomly and may have different vertical loads, slightly different brake characteristics, etc. Hence the best that can be expected is that the simulation matches the average of the test data for the various braked wheels. This was accomplished in the simulation.

One of the most important parameters in the simulation is the μ -slip curve. The curve used is partly theoretical and partly based on trial and error adjustments in agreements with DC-9 flight test results. Its previous use enabled the simulator to duplicate recorded DC-8 and DC-9 anti-skid operation and in Appendix V it is shown to agree fairly well with data determined from the friction tester runs.

Random vertical load variation representing runway roughness was added to the main gear vertical load to make the simulator output resemble aircraft test data. This addition gave a realistic randomness to the depth and spacing of the wheel skids. The amplitude used was selected so that vertical load variations approximated those shown on test records.

DISCUSSION OF PROCEDURE USED TO DETERMINE A RELATIONSHIP BETWEEN TESTER FRICTION AND AIRCRAFT TIRE FRICTION

The method employed to relate maximum friction coefficients obtained from the friction tester and the aircraft that offered the most valid results was described in the Description Section. The relationship between the aircraft μ_{EFF} and aircraft μ_{MAX} that was obtained from the simulator for various velocities is shown in Figure 17. This curve was obtained by configuring the simulator to operate at a constant specified velocity and various values of μ_{MAX} . Anti-skid efficiency was obtained by integrating the ratio μ_{EFF}/μ_{MAX} over a time period and dividing by the time period. These efficiencies are shown in Figure 18. Over the range of conditions encountered during the aircraft tests, maximum anti-skid efficiency was achieved at 150 ft/sec and lower values of μ_{MAX} . This curve was then replotted as Figure 17 by multiplying the appropriate efficiency by μ_{MAX} to obtain μ_{EFF} .

Aircraft performance data in the form of μ_{EFF} versus aircraft velocity were then combined into three categories according to runway environmental condition. The data were combined into a curve, using the least squares technique, for each runway condition. These data were then converted to μ_{MAX} data with Figure 17 for the velocity ratios for which friction tester data were available. The results are shown in Figure 19. Run 425 was excluded from this data since phototheodolite information was not available for this run.

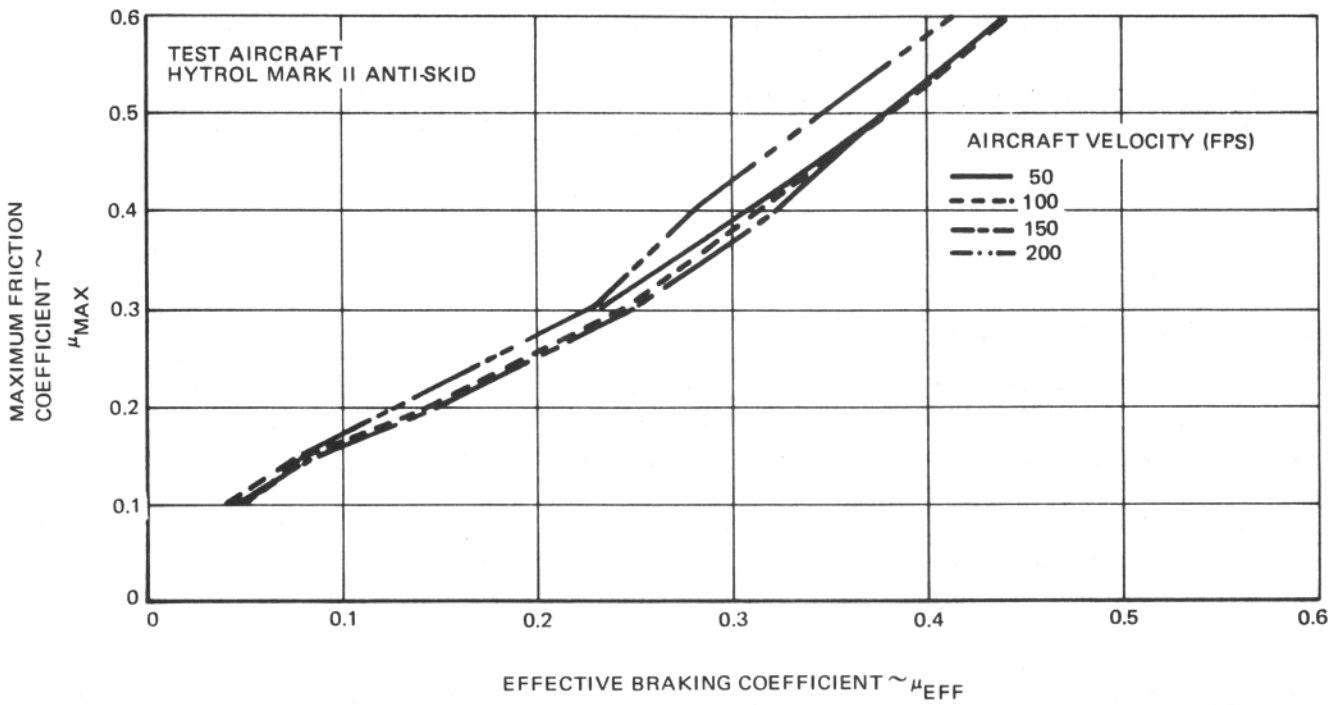


FIGURE 17. ANTI-SKID EFFICIENCY EXPRESSED AS A RELATIONSHIP BETWEEN μ_{MAX} AND μ_{EFF}

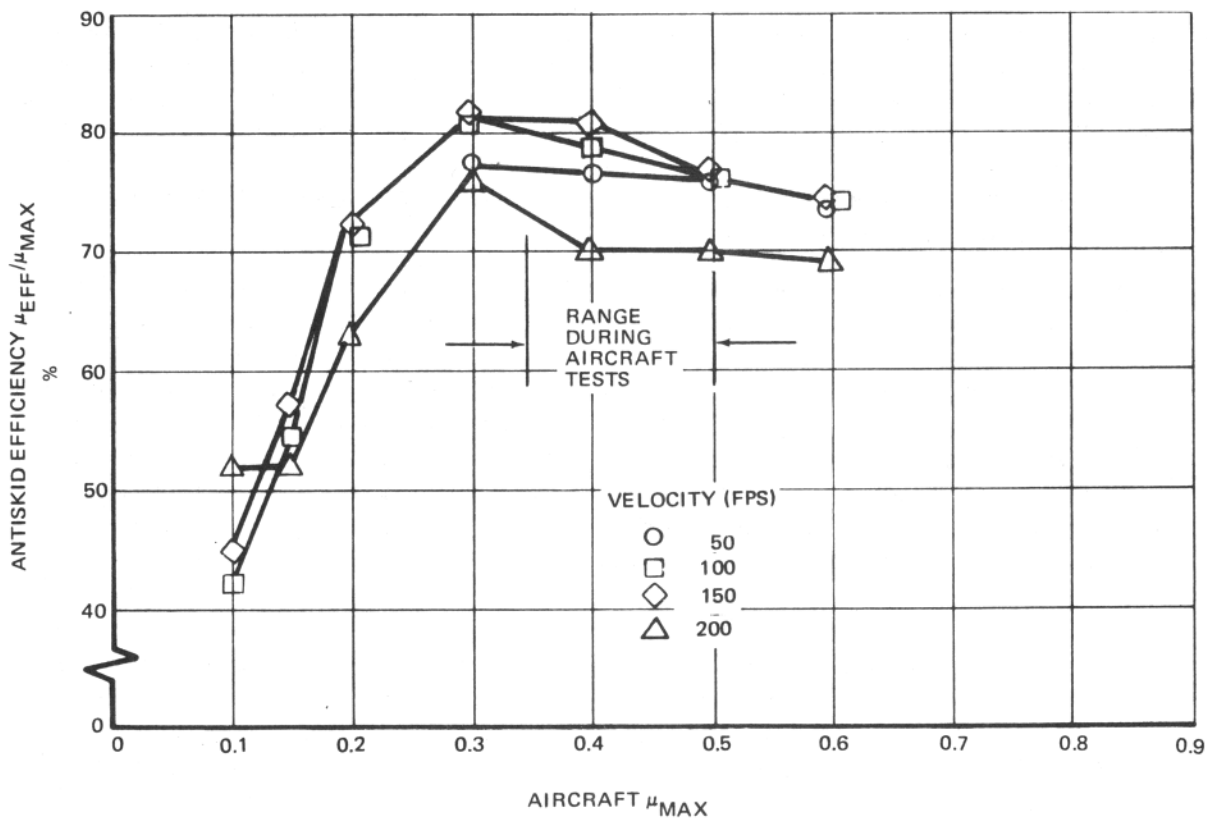
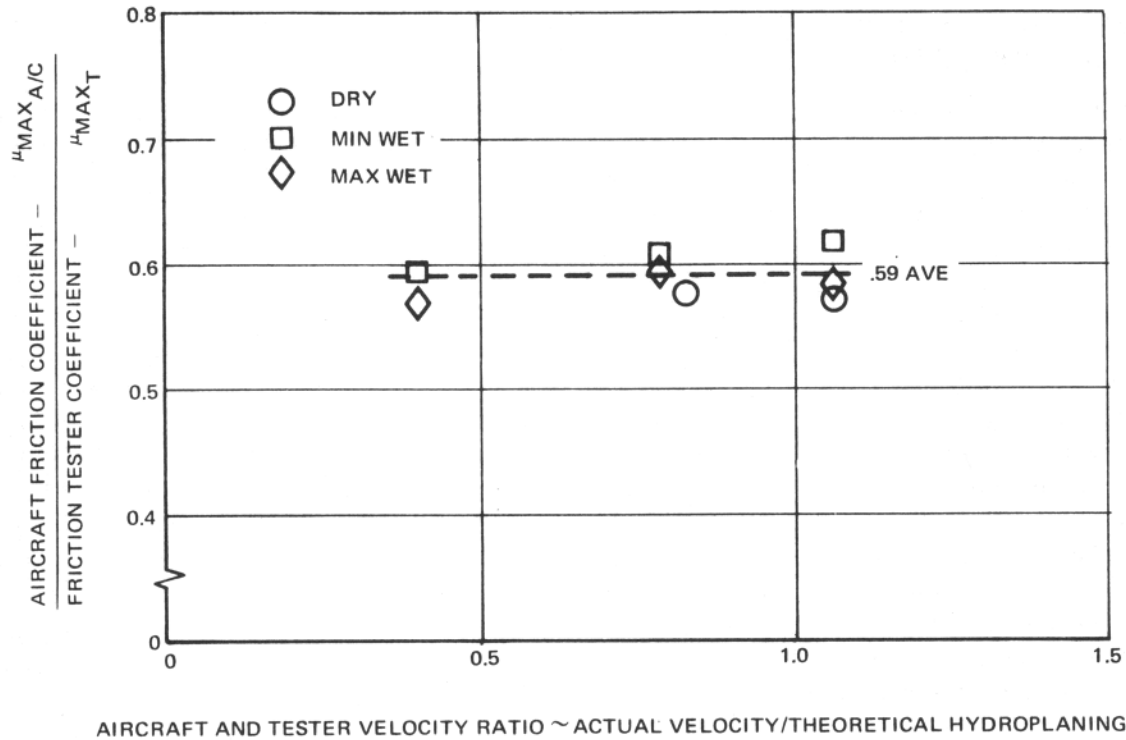


FIGURE 18. ANTI-SKID EFFICIENCY

The results indicated no distinct variation with velocity, so an average of each group adequately represented the relationship. Also, each cluster of data points increased in the order: dry to max wet to min wet. This indicated that the wetness condition was not linearly related to the results. The range of data scatter about each average was approximately ± 5 percent which appeared reasonable for these types of measurements.



$$\text{VELOCITY} \left(\frac{V}{V_{P_T}} \right) \text{ AND } \left(\frac{V}{V_{P_{A/C}}} \right)$$

DC-7 μ_{EFF} DETERMINED BY LEAST SQUARES BEST FIT OF TEST RUNS AS NOTED:

DRY TEST NO. 411, 412, 413, 414

MINIMUM WET TEST NO. 415, 416, 417, 418, 419, 420, 427, 428, 429

MAXIMUM WET TEST NO. 421, 422, 423, 424, 426

μ_{MAX} DETERMINED BY APPLYING ANTI-SKID EFFICIENCY SIMULATOR TO μ_{EFF} DATA (FIGURE 18)

FRICTION TESTER μ_{MAX} DETERMINED BY AVERAGING RESULTS OF TEST RUNS AS NOTED:

DRY TEST NO. 411, 412

MINIMUM WET TEST NO. 415, 416, 417, 418, 419, 420, 427, 428, 429

MAXIMUM WET TEST NO. 421, 422, 423, 424, 425, 426

FIGURE 19. RELATIONSHIP BETWEEN MEASURED FRICTION AND AIRCRAFT TIRE FRICTION

Two additional independent determinations were made to check the validity of the results of Figure 19. These methods and results are described in Appendix VII. One method resulted in an average value of $\mu_{MAX A/C} / \mu_{MAX T}$ of 0.62 and the other resulted in 0.58.

The check indicated that consistent results were achieved for the tests conducted and were independent of velocity. However, results reported in Reference 1 indicated that the relationship between aircraft friction coefficients and tester-measured friction coefficients varied not only with velocity, but also with pavement type. These results are shown in Appendix VII. This variation points out the need to subject the friction tester to a variety of conditions that were not present during the tests.

DISCUSSION OF THE PROCEDURE USED IN PREPARING THE LANDING DISTANCE NOMOGRAM

The procedure used in preparing the flight manual type landing distance nomogram consisted of the five steps shown in Figure 20. The family of friction curves, developed from the Friction Tester data and shown by the Composite Runway Friction Calibration Chart, Figure III-6, were extrapolated for the airplane full velocity range. Additional curves of the same character were also added to represent different friction levels. An expanded family of friction versus velocity curves was thus developed whose locus included a point at 80 mph (117 ft/sec) for μ_{MAXT} values of 0.8, 0.9, 1.0, and 1.1. These curves were then converted into aircraft $\mu_{MAXA/C}$ versus velocity curves by applying the correlation ratios of Figure 19 and then into aircraft μ_{EFF} versus velocity curves by the use of the anti-skid efficiency curves of Figure 18. The μ_{EFF} versus velocity curves, along with the other parameters necessary to define the aircraft, atmospheric conditions, and touchdown velocity, were input to a digital computer program which computed stopping distance. Stopping distances were obtained by inputting a constant weight, 60,000 pounds, and a constant temperature, 59°F, then varying altitude to produce combinations of required touchdown velocities and associated stopping distances, shown in Figure 21. The decision to hold weight and temperature constant and vary altitude was arbitrary, the important factor being that weight, atmospheric density, touchdown velocity and aerodynamic loads were all compatible. The following comparison shows three weight, altitude, and temperature combinations which require a touchdown velocity of 175 ft/sec and the computed stopping distance of each.

Weight (lb)	Altitude (ft)	Temperature (°F)	V _{T.D.} (ft/sec)	Stopping Distance (ft)
97,000	0	59.0	175	2290
60,000	12448	59.0	175	2306
97,000	2000	51.9	175	2292

The landing distance nomogram, Figure 22, was prepared by incorporating the information contained in the stopping distance chart, Figure 21, plus the air run distances (horizontal distance from the 50-foot barrier to touchdown) and the necessary charts for determining touchdown velocity. Air run distance and touchdown velocity, 1.2 times power off stall speed, were previously determined from DC-7 certification tests. The landing distances are demonstration type distances obtained by best effort stopping, and no attempt was made to include operational safety factors. The stopping distances also apply only to the Long Beach Airport runway 12-30 and to the aircraft tire wear condition, new to 50 percent worn, during the runway tests.

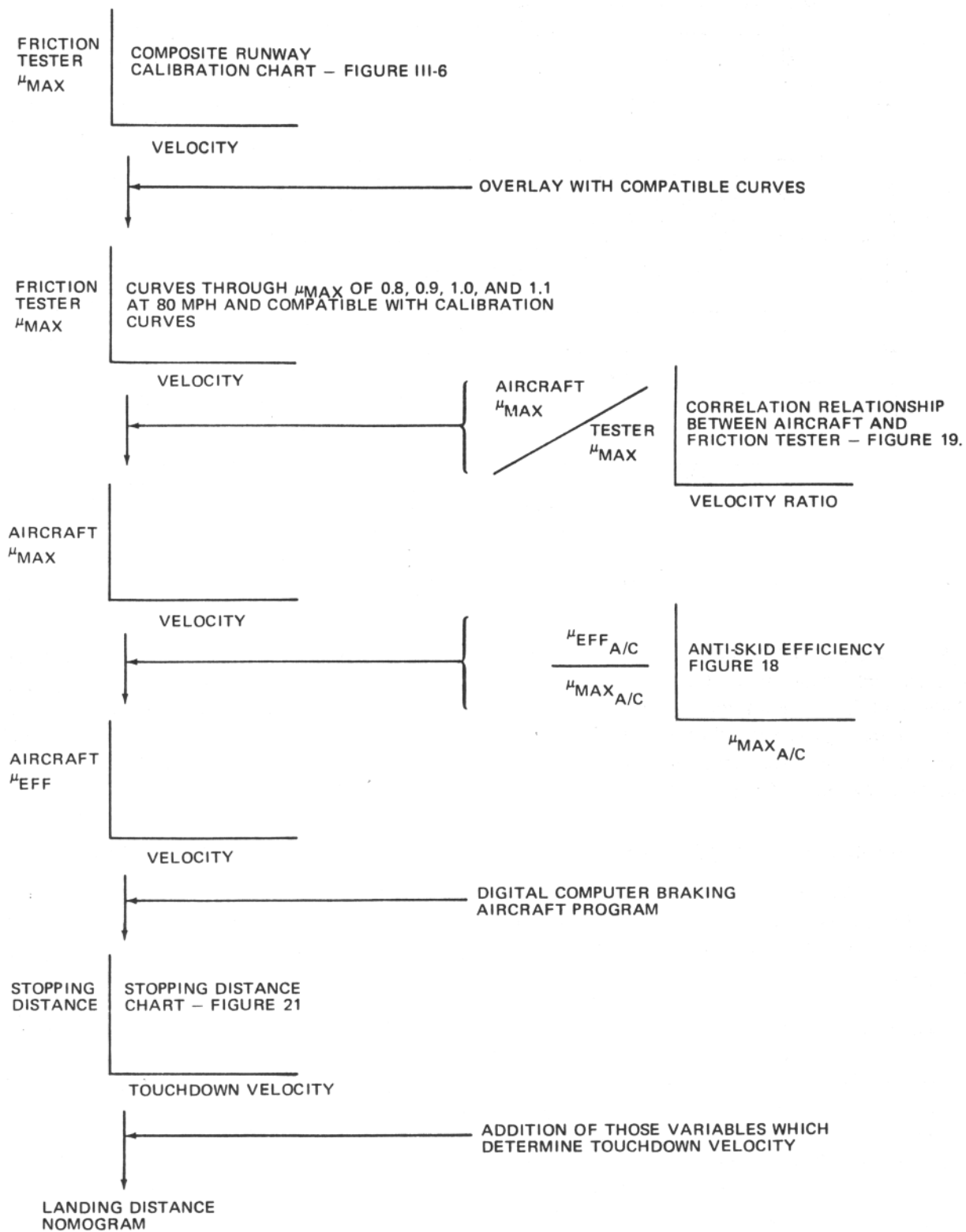


FIGURE 20. NOMOGRAM PREPARATION PROCEDURE

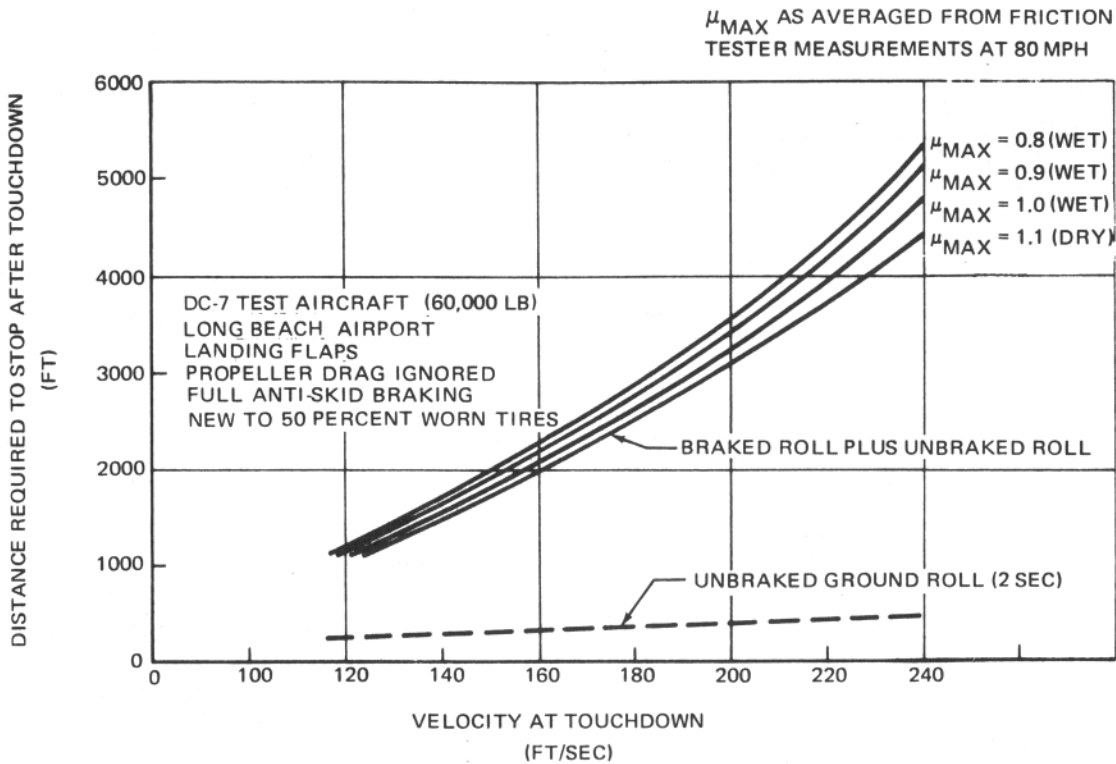


FIGURE 21. STOPPING DISTANCE CHART

As an equally valid alternative, stopping distance data for the nomogram could have been determined using the analog computer aircraft simulator instead of the digital computer program. This would have eliminated the need for preparing the aircraft μ_{EFF} versus velocity curves since aircraft μ_{MAX} versus velocity curves would have been used for analog input. The advantage of the digital computer program was that it enabled more rapid computation of the cases needed for preparation of the nomogram.

DISCUSSION OF THE DEVELOPMENT AND APPLICATION OF THE BASIC METHODOLOGY

The development, verification testing, and correlation analysis conducted in this program substantiates the methodology concept. The use of the anti-skid real time hardware in the simulation is believed essential. Figure 19 shows the normalized constant of 0.59 for $\mu_{MAX A/C} / \mu_{MAX T}$.

Since only one runway was used to develop the friction/aircraft correlation method, additional testing should be accomplished on other runways to ensure the 0.59 factor (Friction Ratio versus Velocity Ratio - Figure 19) developed on the test runway will hold for other runways. This work should be done on worn and new, rough and smooth concrete and asphalt runways. After this verification is accomplished, operational nomograms applicable for any civil transport aircraft can be prepared. This effort will fall into two categories: (a) establishment of friction tester-aircraft correlation for a specific transport aircraft and (b) nomogram preparation for these transport aircraft. This can be accomplished as follows:

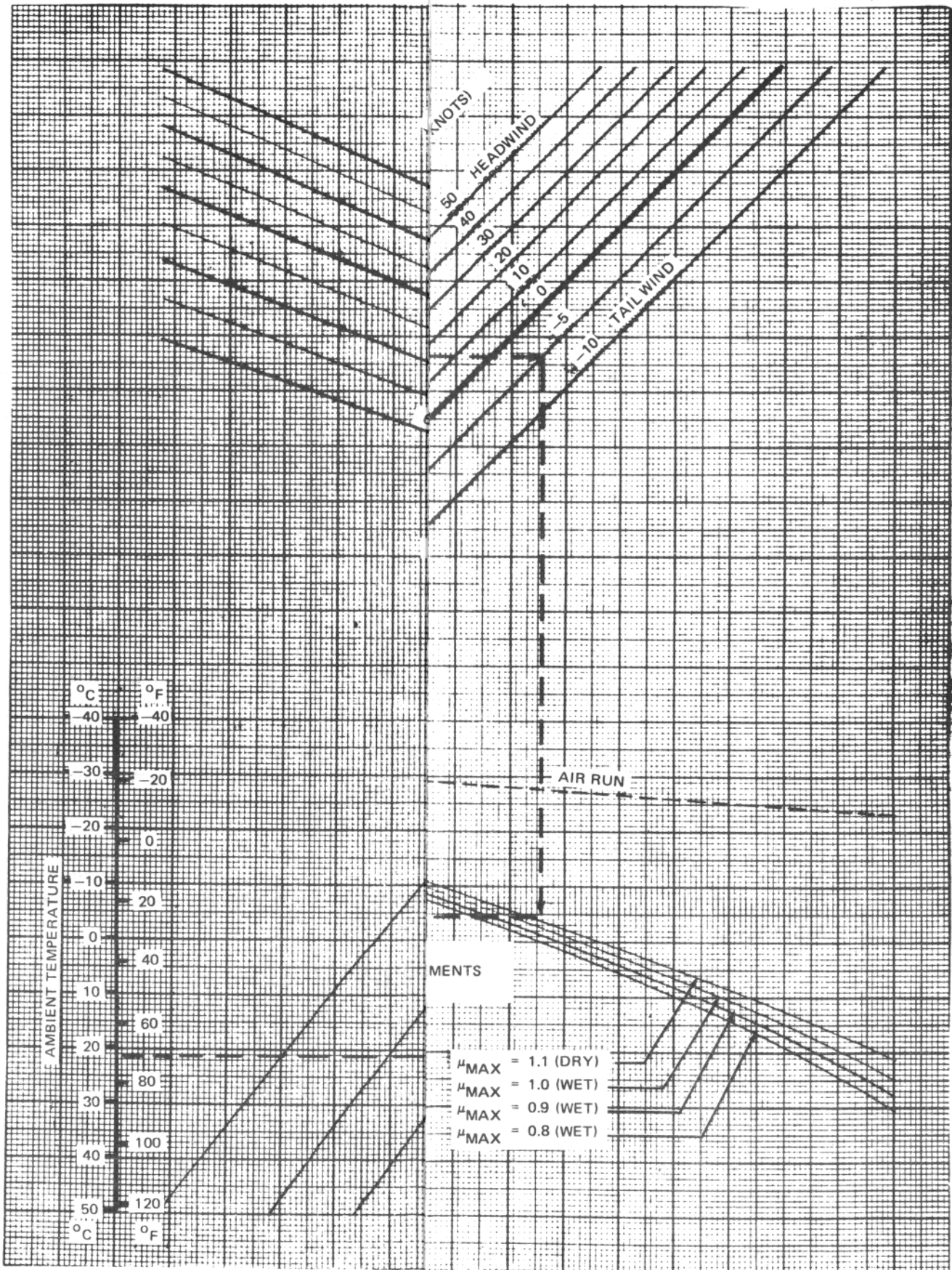


FIGURE 22. LANDING DISTANCE NOMOGRAM

1. Correlation

For each transport aircraft selected, and a typical transport-operations runway, conduct friction tester-aircraft correlation tests for both wet and dry conditions. The aircraft anti-skid signals in addition to phototheodolite data should be recorded. The test aircraft should have 80-percent worn tires because tests conducted with varying degrees of tire wear will result in undesirable variables.

During the aircraft-friction tester tests, additional friction tester measurements should be performed to prepare a μ_{MAX} versus velocity runway calibration chart for the runway. This curve is used in preparation of the nomograms and correlation work.

An analog simulation of the aircraft should be constructed as defined in Appendix VI. The simulator should incorporate the anti-skid and braking system hardware as indicated. The recorded data from previous aircraft tests will be used to verify simulation accuracy.

Sufficient simulator work should be conducted to obtain correlation between friction-tester-measured friction and aircraft runout distances. The μ_{MAX} tester versus velocity data should be put into the simulator with the 0.59 ratio and V_p ratio (obtaining $\mu_{MAX A/C}$ vs velocity). If test and simulator distances disagree, data obtained from the aircraft should be reviewed to obtain proper brake-pressure relationship to provide agreement. Traces from both aircraft and simulator should agree in character to ensure the simulator will predict aircraft runout for other type runways also.

2. Nomogram Preparation

A nomogram may be required for a specific runway. However, it is more probable that runways will be classified into wet friction categories such that a nomogram would be required only for a class. The following paragraphs discuss the development techniques for each type.

Type I – Nomogram for a Particular Runway – Calibration runs using the friction tester at 30, 60, and 80 mph on the runway for both dry and “tester-wetted” surface conditions will provide a “ $\mu_{MAX T}$ versus velocity runway calibration chart for each runway.” The procedure then used is that shown in Figure 20. The calibration chart must then be overlaid with curves which pass through $\mu_{MAX T}$ values at 80 mph of 0.1, 0.2, . . . 0.9, 1.0 and duplicate the μ versus velocity character of the calibration curves. The correlation relationship must then be used to convert the “overlay $\mu_{MAX T}$ versus velocity” curves into “ $\mu_{MAX A/C}$ versus velocity” curves labeling each curve as to the $\mu_{MAX T}$ value at 80 mph that it represents. These curves can then be input to the simulator to obtain corresponding curves of “stopping distance versus touchdown velocity” for inclusion into the nomogram. (Alternative – The simulator can be used to develop curves of “ $\mu_{EFF A/C}$ versus $\mu_{MAX A/C}$ for combinations of aircraft velocity and weight. These curves and a digital computer braking aircraft program can be used to solve for the “stopping distance versus touchdown velocity” curves.) The nomogram can then be prepared by adding the effects of pressure altitude, ambient temperature, weight, and tailwind on touchdown velocity.

Type II – Nomogram for Friction Classified Runways – (Friction classification as to measured $\mu_{MAX T}$ friction level at 80 mph and slope of the $\mu_{MAX T}$ versus velocity curve as it passes through 80 mph.)

Classification procedure is contingent upon statistical runway friction data which is not now available; however, it is anticipated that a class letter-number (e.g., A1, C2, B7) system could be

used wherein the number would designate the μ_{MAXT} value at 80 mph and the class letter would designate the slope of the μ_{MAXT} versus velocity curve at 80 mph (e.g., Class A, no slope; Class B, $\mu/\text{velocity} = 0.02/10$ mph; Class C, $\mu/\text{velocity} = 0.04/10$ mph). Based on the classification procedure, standard classification charts (see Figure 23) would be prepared. The nomograms for each model aircraft would be prepared in a manner identical to preparation of the Type I nomogram except the standard classification charts replace the "overlay μ_{MAXT} versus velocity" curves negating the need for individual nomograms for each intended runway. Three nomograms, or sub-nomograms, would be required for each model aircraft, one for each class letter.

In addition to the aircraft's nomogram, calibration runs using the friction tester at 30, 60, and 80 mph must be performed on each intended runway for both dry and "tester-wetted" surface conditions to obtain a " μ_{MAXT} versus velocity" runway calibration chart. The calibration chart must then be overlaid with curves which pass through μ_{MAXT} values at 80 mph of 0.1, 0.2, . . . 0.9, 1.0 and duplicate the μ versus velocity character of the calibration curves enabling each μ_{MAXT} value at 80 mph to be assigned a class letter reflecting its slope (e.g., μ_{MAXT} of 0.4 might be assigned to Class C).

Nomogram Usage During Inclement Weather Conditions

The runway friction level or classification would be determined by performing one friction tester run over the full length of the runway at 80 mph. Values of μ_{MAXT} would be read and the friction level or classification established by averaging readings. Runs would be repeated at frequencies deemed necessary by the instability of weather conditions and experience.

As the aircraft is in approach, the nomogram would be entered with runway friction level or classification, airport pressure altitude, ambient temperature, and wind velocity, and predicted stopping distance determined for comparison against available field length to establish a "go-no-go" decision. The nomogram could be read by either the aircraft flight engineer or the airport controller provided that the necessary information is transferred by radio between airport and aircraft.

ADDITIONAL CONSIDERATIONS

Runway Surfaces – The methodology was verified on one runway surface which had high, nearly constant friction throughout the 3000-foot test length and with one test aircraft. Additional tests are needed to determine the degree of correlation which can be obtained for other aircraft and other runway surfaces, including runways with two or more sections of different surfacing. It is anticipated that adequate correlation will be obtained for other aircraft and for all surfaces since the methodology is based on rational concepts rather than empirical data.

Rain Conditions – The results of the few friction tests performed during actual rain conditions indicate that rainfall and the resulting loss of friction, which may be due to partial hydroplaning conditions, are highly variable with both time and runway location. Statistical rainfall-friction-time data should be accumulated to study possible loss in runway friction which may occur during the time elapse between friction measurement and aircraft landing.

Flooded Runway – The ability to determine hydroplaning conditions should be investigated. No work was done in this program to evaluate the ability of the tester to predict airplane hydroplaning or the extent thereof. Adequate correlation should be obtained if the friction conditions or hydroplaning drag can be measured with sufficient accuracy.

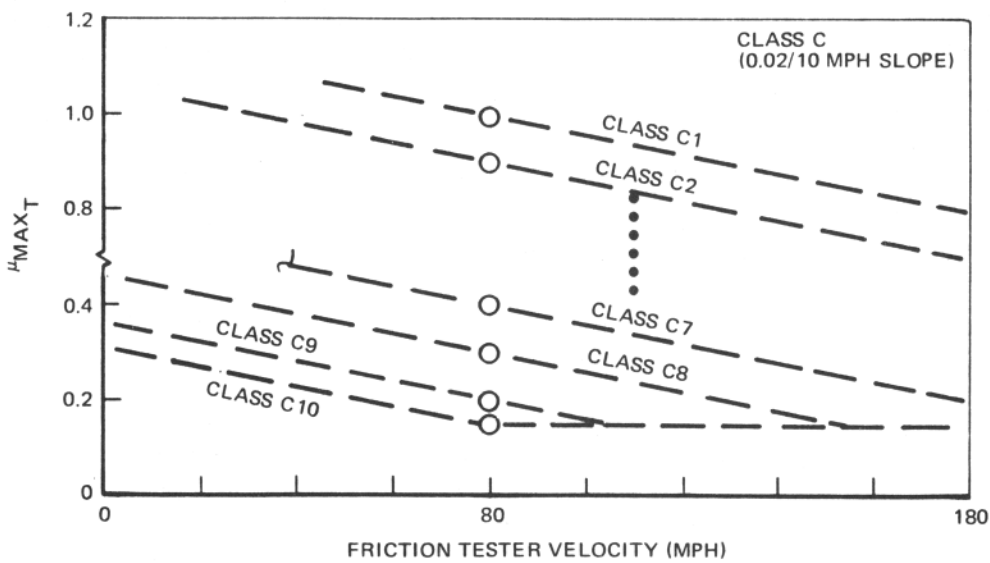
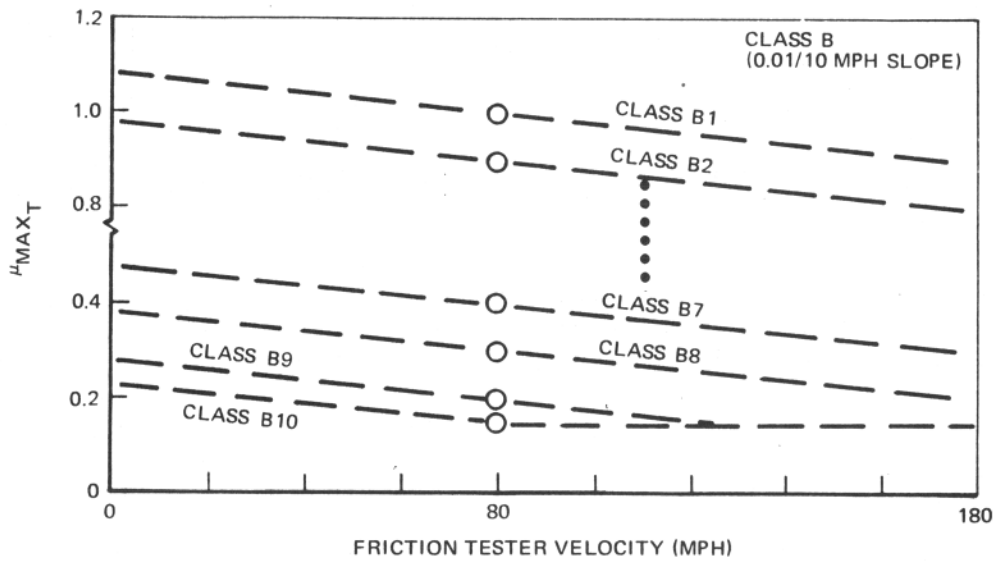
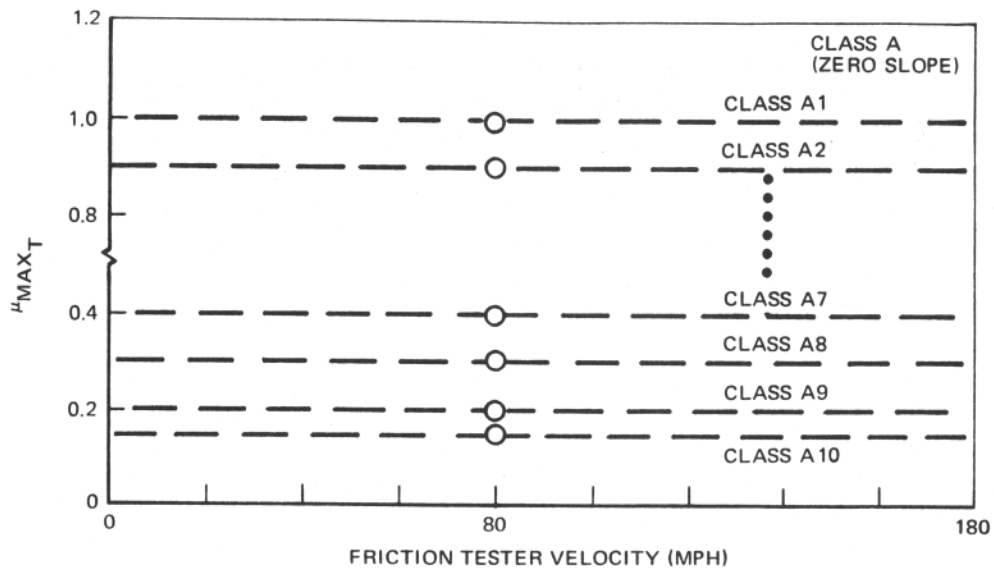


FIGURE 23. POSSIBLE RUNWAY FRICTION CLASSIFICATION CHARTS

Ice, Snow and Slush – Landing surfaces covered with ice, snow or slush were not included in the development of the methodology. It is believed, however, that the ice or frozen slush condition would cause the greatest problem for the friction tester since the effect of the slush on the tester tire may be much greater than on the aircraft tire. As a result the normally predicted ratio of tester friction to aircraft friction will not hold.

Tandem Landing Gear – The leading tire of a tandem landing gear tends to clear water from in front of the trailing wheel and it is likely a different μ_{MAX} ratio to V_p ratio may exist for the tandem wheel arrangement than the side by side twin arrangement tested. This condition should not create a problem, however, since the proper ratio can be determined during correlation work.

CONCLUSIONS

The following are general and specific conclusions drawn from the subject program:

1. The FAA Variable Slip Runway Friction Tester used in a cycling mode with a standard ASTM E-249 ribbed tire has adequately delineated with repeatability a wide range of friction from dry pavement to varying degrees of wetness at Long Beach Airport.
2. Correlation exists between friction measured by the friction tester and friction available to the tires of the test aircraft when normalized with respect to theoretical hydroplaning velocities. The relationship is that $\mu_{MAX_{A/C}}$ equals 0.59 times μ_{MAX_T} when the ratio between aircraft and friction tester velocities was equal to the ratio between their respective theoretical hydroplaning velocities.
3. The use of analog simulation of an aircraft using real time anti-skid and braking system hardware is a practical method of predicting aircraft stopping distance on a wet runway using friction tester data obtained from the particular wet runway.
4. Nomograms can be constructed relating the stopping distance of an aircraft with runway friction as measured by the FAA Variable Slip Runway Friction Tester.
5. The methodology was verified for one runway, which had high friction values, and one test aircraft. Substantiation of the methodology for other types of surfaces and other aircraft requires additional testing.

REFERENCES

1. Pavement Grooving and Traction Studies, NASA SP-5073, 1969.
2. T.J.W. Leland and G.R. Taylor, An Investigation of the Influence of Aircraft Tire-Tread Wear on Wet-Runway Braking, NASA TN D-2770, April 1965.
3. J.J. Shrager, Vehicular Measurements of Effective Runway Friction, Final Report, Project No. 308-3X, Federal Aviation Agency, May 1962.
4. R.H. Sawyer and J.J. Kolnick, Tire-To-Surface Friction – Coefficient Measurements with a C-123B Airplane on Various Runway Surfaces, NASA TR R-20, 1959.
5. R.F. Smiley and W.B. Horne, Mechanical Properties of Pneumatic Tires with Special Reference to Modern Aircraft Tires, NASA TR-R-64, 1960.
6. F.J. Lynch, W.E. Meyer and H.W. Kummer, A Technique for Measuring the Slip Resistance of Airport Runway Surfaces, Paper No. 97 presented at the Fifth Pacific Area National Meeting of the American Society for Testing and Materials, November 1965.
7. W.E. Meyer, H.W. Kummer and F.J. Lynch, Design and Development of an Airport Runway Surface Traction Measuring Device, Final Report, Project No. 510-003-OIE, Report No. ADS-55, Federal Aviation Agency, January 1966.

APPENDIX I

LONG BEACH AIRPORT RUNWAY PROFILE SURVEY AND SURFACING SPECIFICATION

RUNWAY PROFILE SURVEY

A runway vertical profile survey of the 3000 foot test section was performed at two foot intervals along two lines twelve feet to each side of the runway centerline. The results of this survey are shown in Figure I-1. Downhill slope measured in the direction of aircraft travel, southeast, was 0.38 percent. The RMS roughness deviation was 0.0139 feet.

RUNWAY SURFACING SPECIFICATION

The Long Beach Airport runway 12-30 received an overlay in August of 1968 and a second "smoothing" overlay in November of 1968. Specification of the surface course was to reference (1), Item F-401 "Bituminous Surface Course" with the following deviations:

401-1.1 DESCRIPTION

Add the following: For this project the terms "Bituminous Surface" and "Asphalt Concrete" (or the abbreviation "A.C.") shall be considered identical in meaning. "Item P-410 ASPHALT CONCRETE SURFACE COURSE" of the Standard Specification, is hereby deleted, and "Asphalt Concrete" shall relate only to this item P-401, insofar as specifications for same are concerned.

The asphalt cement shall have a penetration of 85-100.

401-2.1 AGGREGATE

Add the following paragraph after the eighth paragraph: Sand Equivalent when sampled after all processing, except addition of filler and asphalt binder (Calif. No. 217) shall be 50 (minimum).

401-3.1 COMPOSITION OF MIXTURE

Add the following to the first paragraph: Pavement mixture shall conform with Column B of Table I with the exception that unless otherwise directed by the Engineer, resurface less than 1-1/2 inches in thickness and feathered edges shall be constructed of a mixture conforming to Column C of Table I.

401-4.6 SPREADING AND LAYING

Delete the fourth (final) paragraph of subsection (a) "Preparation for Placing" and substitute the following paragraph:

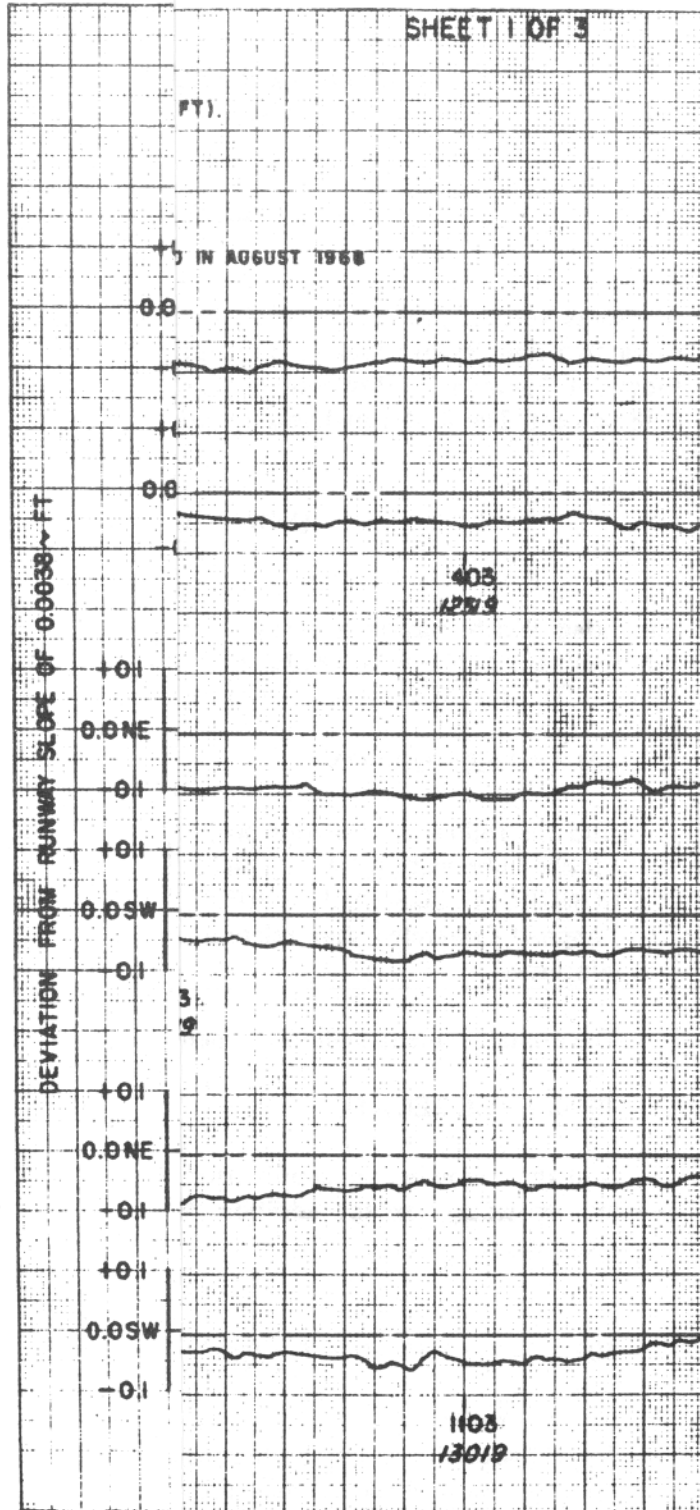


FIGURE I-1. RUNWAY 12-30, PROFILE SURVEY,
LONG BEACH AIRPORT (SHEET 1 OF 3)

SHEET 2 OF 3

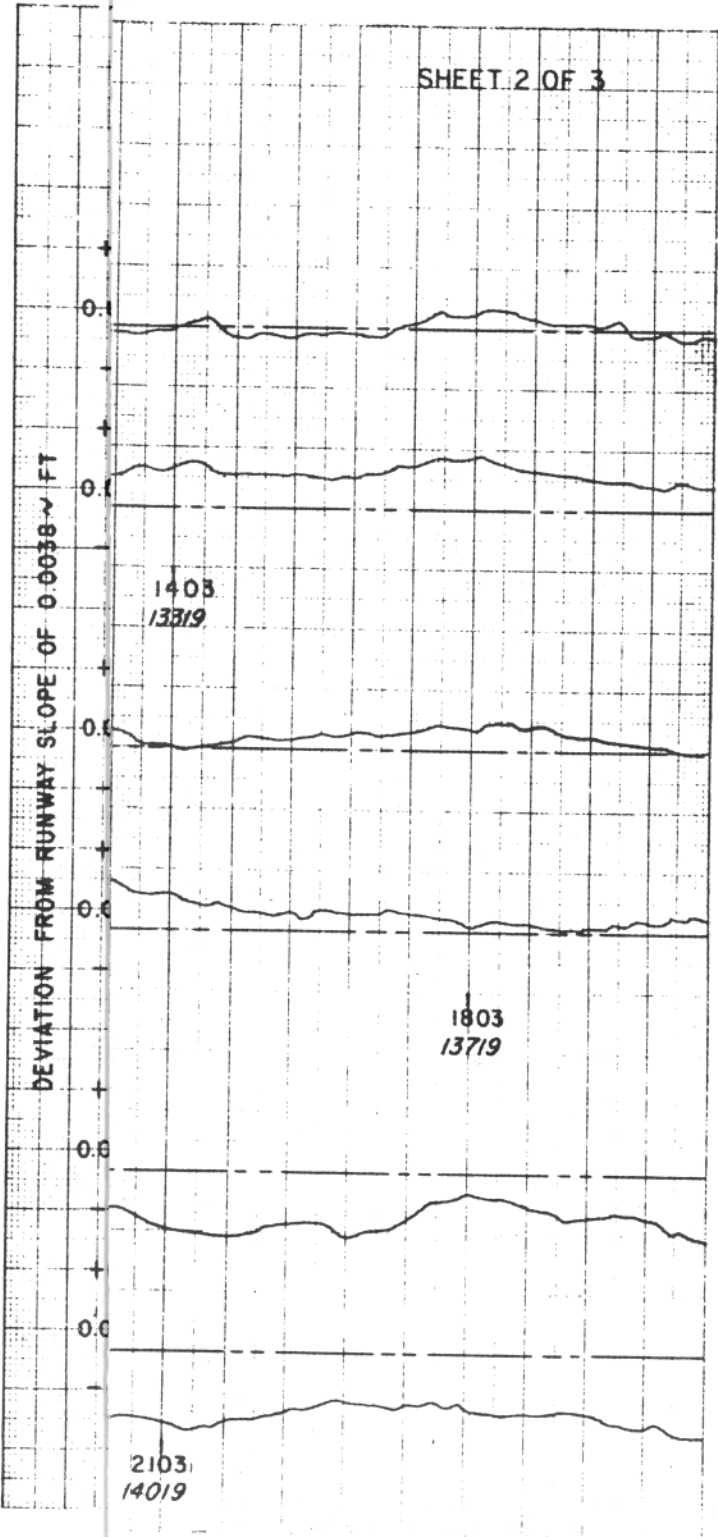
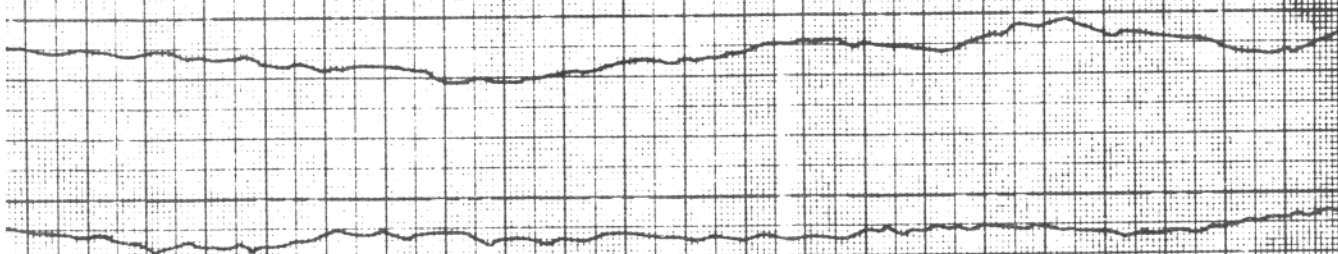


FIG I-1. RUNWAY 12-30, PROFILE SURVEY,
LONG BEACH AIRPORT (SHEET 2 OF 3)



WEST AREA DISTANCE - FT
STATION NO. - FT

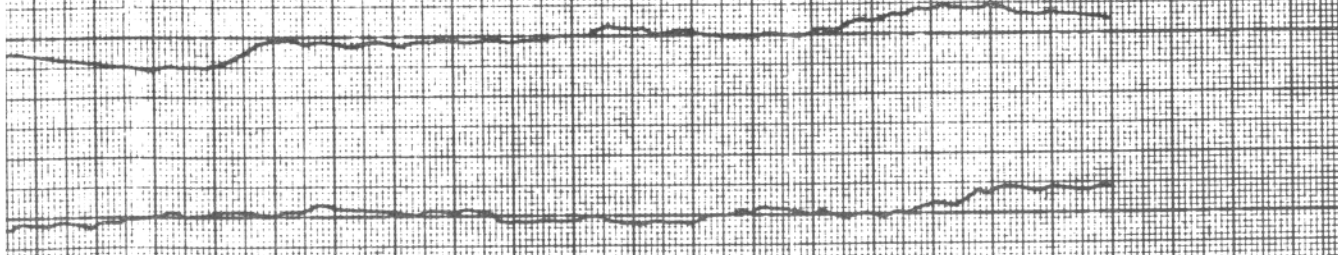
2405
14319

2505
14419



FT 2705
14519

2805
14719



WEST AREA DISTANCE - FT
STATION NO. - FT

3105
15019

3205
15119

Asphalt concrete resurface shall be constructed on pre-treated existing surfaces in two layers whenever the finished thickness of new material is required to be 2-1/2 inches or more. Whenever the finished thickness of new resurface material is to be less than 2-1/2 inches, construction in one layer is permissible provided the required compaction and surface smoothness are achieved.

P-401-1.3 ASPHALT JOB MIX FORMULA

Three-Quarter Inch Maximum Surface Course

Combined Aggregate Grading (25 percent 3/4 in.; 14 percent 1/2 in.; 15 percent 3/8 in.; 44 percent sand; 12 percent rock dust)

Sieve Size	Percent Passing					Total
	3/4 In.	1/2 In.	3/8 In.	Sand	Rock Dust	
3/4 In.	14.4	14.0	15.0	44	12	99.4
1/2 In.	7.6	13.5	15.0	44	12	92.2
3/8 In.	1.8	6.3	14.7	44	12	78.8
No. 4	0.3	0.7	6.3	41.4	11.9	60.8
No. 10				33.0	9.3	42.3
No. 40				15.4	4.7	20.1
No. 80				6.6	2.8	9.4
No. 200				2.2	1.4	3.6

Sand-Silt Ratio: Sand 38.7 percent; Silt 3.6 percent; Ratio 10.7 to 1

Percentage of asphalt:

Percent (decimal) of rock in mix	0.577
Percent (decimal) of sand in mix	0.387
Percent (decimal) of silt in mix	0.036

Estimated value of C: 1.0

$$P = (0.577 \times 4 + 0.387 \times 7 + 0.036 \times 12)(1.0) = 5.45 \text{ percent}$$

Temperature at time mixture is discharged: 310°F.

One-Half Inch Maximum Surface Course

Combined Aggregate Grading (20 percent 1/2 in.; 20 percent 3/8 in.; 10 percent sand; 50 percent rock dust)

Percent Passing

Sieve Size	1/2 In.	3/8 In.	Sand	Rock Dust	Total
1/2 In.	19.4	20	10	50	99.4
3/8 In.	9.0	19.6	10	50	88.6
No. 4	1.0	8.4	9.4	49.5	68.3
No. 10			7.5	39.0	46.5
No. 40			3.5	19.7	23.2
No. 80			1.5	11.5	13.0
No. 200			0.5	6.0	6.5

Sand-Silt Ratio: Sand 40.0 percent: Silt 6.5 percent; Ratio 6.1 to 1

Percentage of asphalt:

Percent (decimal) of rock in mix	0.535
Percent (decimal) of sand in mix	0.400
Percent (decimal) of silt in mix	0.065

Estimated value of C: 1.0

$$P = (0.535 \times 4 + 0.400 \times 7 + 0.065 \times 12)(1.0) = 5.72 \text{ percent}$$

Type of asphalt: 85/100

Temperature at time mixture is discharged: 310°F.

SIEVE ANALYSIS

Three-Quarter Inch Maximum Surface Course

Sieve Size	Percent Passing
1 In.	100.0
3/4 In.	98.2
1/2 In.	85.7
3/8 In.	75.6
No. 4	60.4
No. 10	44.1
No. 40	21.1
No. 80	9.8
No. 200	5.0
Penetration (85/100) Asphalt Cement	98 Degrees 6.00 Percent

One-Half Inch Maximum Surface Course

Sieve Size	Percent Passing
1/2 In.	100.0
3/8 In.	99.8
No. 4	78.7
No. 10	59.5
No. 40	26.8
No. 80	10.1
No. 200	4.2
Penetration	87 Degrees
Asphalt Cement (85/100)	6.0 Percent

REFERENCES

1. Standard Specifications for Construction of Airports, Federal Aviation Agency, June 1959.

APPENDIX II

FAA VARIABLE SLIP RUNWAY FRICTION TESTER DEVELOPMENTAL TESTS

FRICTION TESTER EVALUATION TESTS

The friction tester evaluation program consisted of the installation of additional data recording instrumentation on the friction tester experimental tests, and an engineering evaluation to determine if the data produced by the friction tester were satisfactory, in type, suitability, and validity, to warrant continuation of the overall program. The results of these tests are contained in McDonnell Douglas Corporation Report No. DAC 66925, dated 28 February 1968, available from the FAA, NA-543, NAFEC, Atlantic City, N.J. 08405.

These tests were directed toward familiarizing Douglas personnel with the friction tester's operation and providing data for use in evaluating repeatability and conformance to accepted tire friction theories.

The friction tester evaluation program resulted in the recommendation that the correlation program be continued after performing mechanical modifications to improve the reliability of the friction tester and after performing tire tread evaluation tests.

The evaluation also resulted in the selection of the autocycle mode of operation over the constant slip alternative. Autocycling was considered to offer the following advantages:

- Better definition of the shape of the μ -slip curve.
- The μ_{MAX} value can always be determined during a single vehicle run, eliminating the need for making several runs which would require plotting results to determine μ_{MAX} or the other alternative of selecting a constant slip about which μ_{MAX} values generally, but might not always, occur.
- The μ_{MAX} value is determined in a manner more similar to the operation of the aircraft anti-skid system; however, during evaluation tests the use of constant slip versus autocycle gave the same μ_{MAX} values but at different slip ratios.
- The intermittent operation results in less tire heating. Tire heating is a potential obstacle to obtaining repeatable friction measurements.

INVESTIGATION TESTS

Tests of the friction tester under dry runway conditions and wet runway conditions, using the friction tester's integral watering (self-wetting) system, were performed at Long Beach Airport. Investigations were conducted in the following areas:

1. Selection of the test tire tread configuration to be used during the friction tester-aircraft correlation tests.
2. Effects of repeated autocycling upon the ability to obtain repeatable friction measurements.

- Relationships between measured ambient temperatures, pavement temperatures, humidities, and measured friction values.

Test Tire Selection

Two of each of four test tire tread configurations shown in Figure II-1 were evaluated to determine which configuration was best suited for use on the friction tester. The tires are 7.50 x 14 4-ply tubeless tires conforming to ASTM designation E-249 using rayon fabric and oil extended styrene butadiene rubber.

Tests were performed to provide data for use in evaluating the tires' capability to provide consistent friction data, friction data independent of tread wear, and sufficient spread between wet and dry friction data. An inflation pressure of 60 psi was selected for the one-inch and two-inch tread width tires to ensure that the shoulders would remain clear of the pavement surface while testing. An inflation pressure of 60 psi was also selected for the full width bald and ribbed tires as a compromise between avoiding unrealistically low contact pressures and avoiding an uneven wear pattern across the footprint. The tests were performed on taxiway F to ensure undisturbed testing. The available accelerate-test-stop distance limited the friction tester velocity to 60 mph. All tests were performed in one direction only, and friction was consistently measured within a small pavement section.

Three series of tests were performed with tires trimmed to simulate tread wear between series. Preliminary runs were performed with each tire to impart an actual wear pattern to the contact surface prior to friction tests. Tread depth measurements were taken after each test run except for the bald tire which lacked adequate reference. Equivalent tread depth for the bald tires was based upon the depth of rubber removed during cutting. Figures II-2 through II-6 show the results of these tests.

Table II-1 summarizes the selection parameters of each tire. The one- and two-inch tread width tires were rejected because of limited separation between wet and dry friction values, inconsistency of wet friction measurements, high wear rates, and nonstandard configuration. The standard ASTM E-249 ribbed tire was selected over the bald tire, which conforms to the same standard with the exception of ribs, because it obtained friction measurements which were slightly more consistent, and because its higher bearing pressure and lower rib width/length ratio reduced, to a degree, the differences between friction tester and aircraft.

**TABLE II-1
TEST TIRE SELECTION PARAMETERS**

PARAMETER	DEFINITION	AIRCRAFT TIRE (OPTIMUM)	TREAD CONFIGURATION			
			1 IN.	2 IN.	RIBBED	BALD
BEARING PRESSURE	LOAD/NET CONTACT AREA	150 PSI	126 PSI	60 PSI	53 PSI	38 PSI
DRY μ_{MAX} SCATTER	(MAXIMUM-MINIMUM)/AVERAGE	-	10%	9.6%	10%	11%
WET μ_{MAX} SCATTER	(MAXIMUM-MINIMUM)/AVERAGE	-	20%	15%	12%	14%
WET TO DRY RATIO	AVERAGE WET μ_{MAX} /AVERAGE DRY μ_{MAX}	75%	90%	80%	77%	77%
RIB W/L RATIO	RIB WIDTH/RIB LENGTH	0.07	0.20	0.36	0.20	1.0

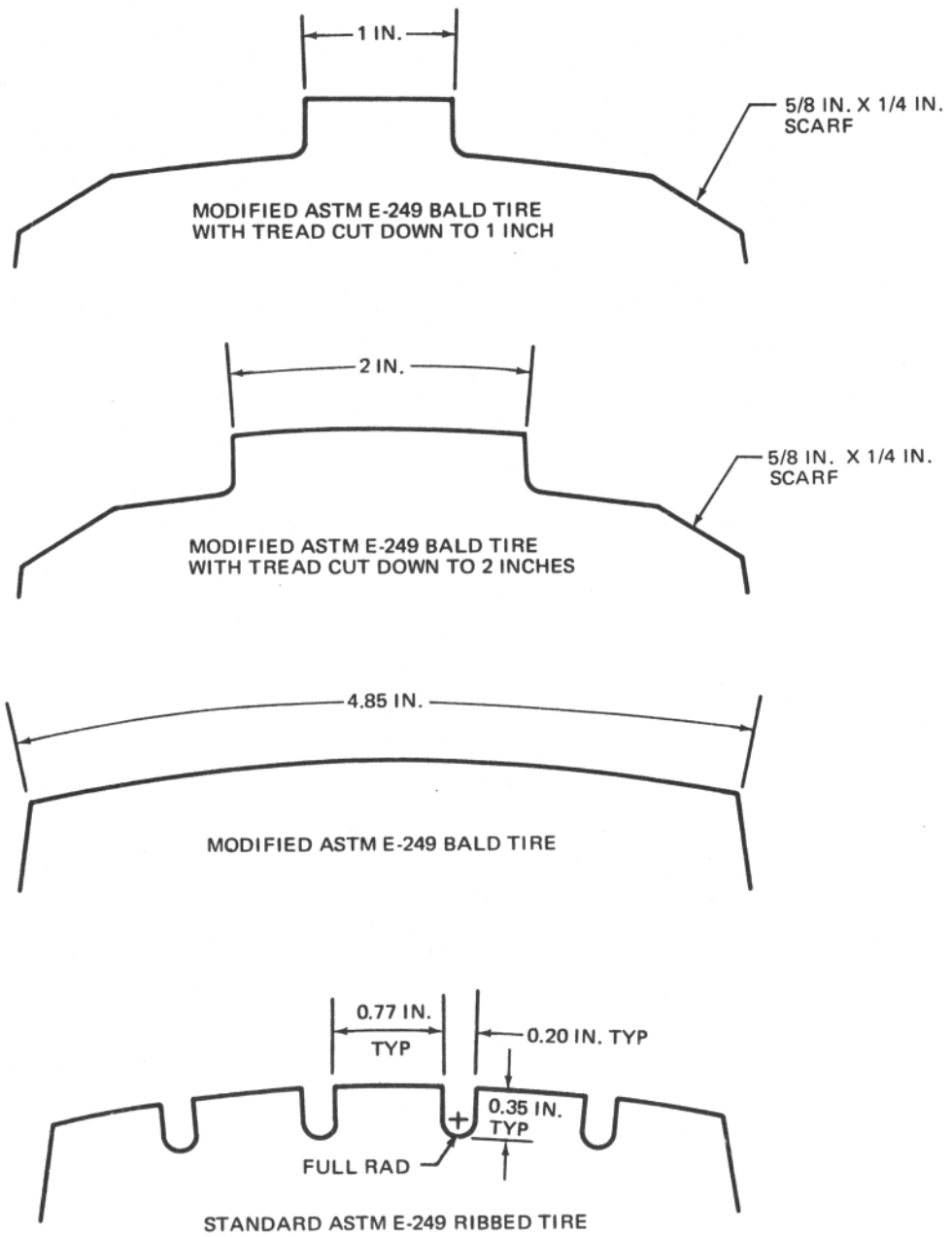


FIGURE II-1. TEST TIRE TREAD CONFIGURATIONS

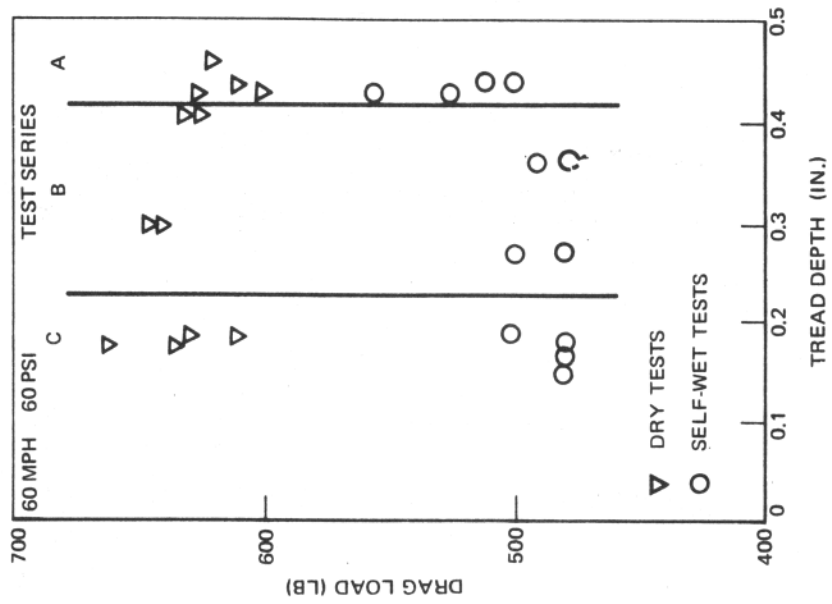


FIGURE II-3. DRAG LOAD VS TREAD WEAR - TWO INCH RIB TIRE

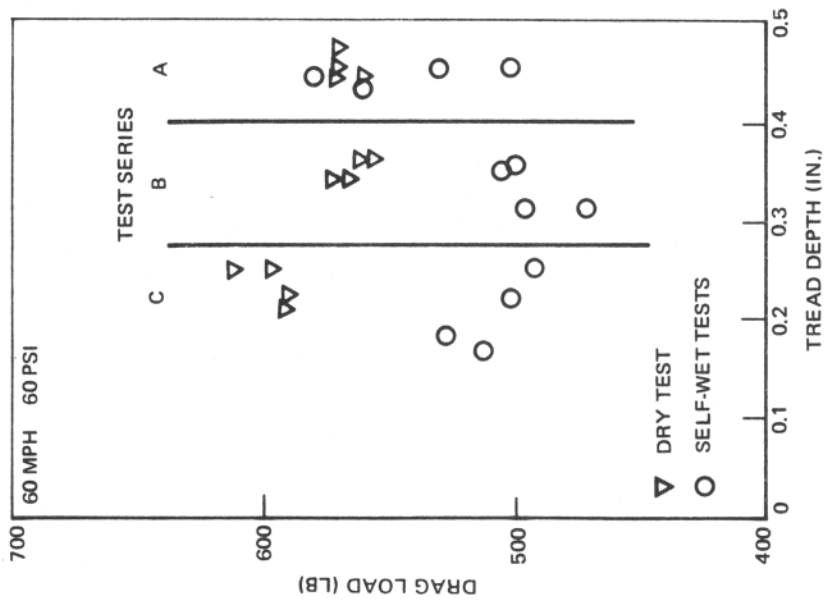


FIGURE II-2. DRAG LOAD VS TREAD WEAR - ONE INCH RIB TIRE

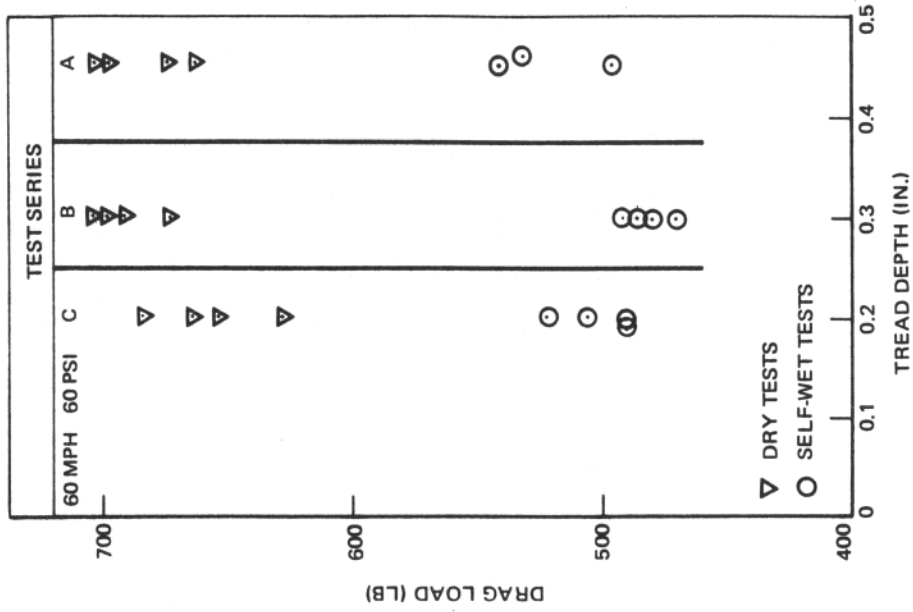


FIGURE II-5. DRAG LOAD VS TREAD WEAR - MODIFIED ASTM E-249 BALD TIRE

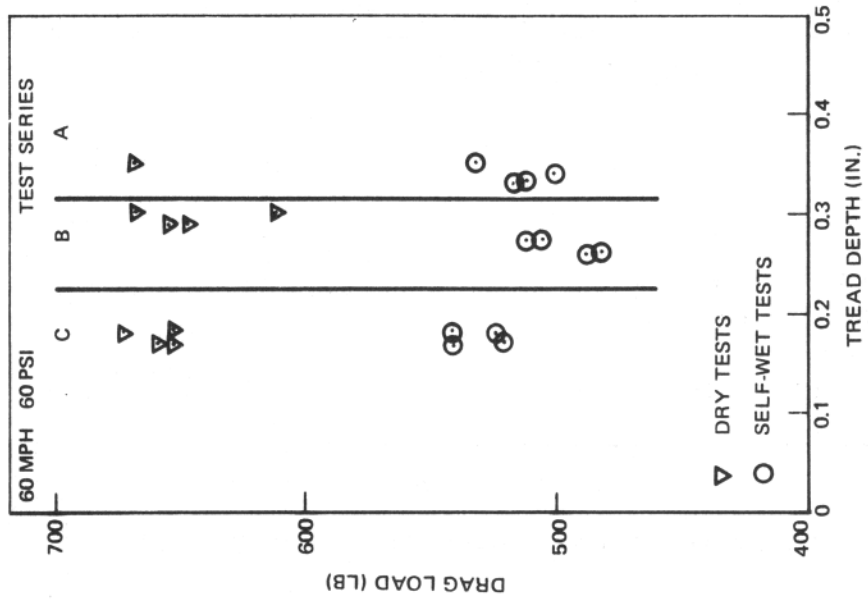


FIGURE II-4. DRAG LOAD VS TREAD WEAR - STANDARD ASTM E-249 RIBBED TIRE

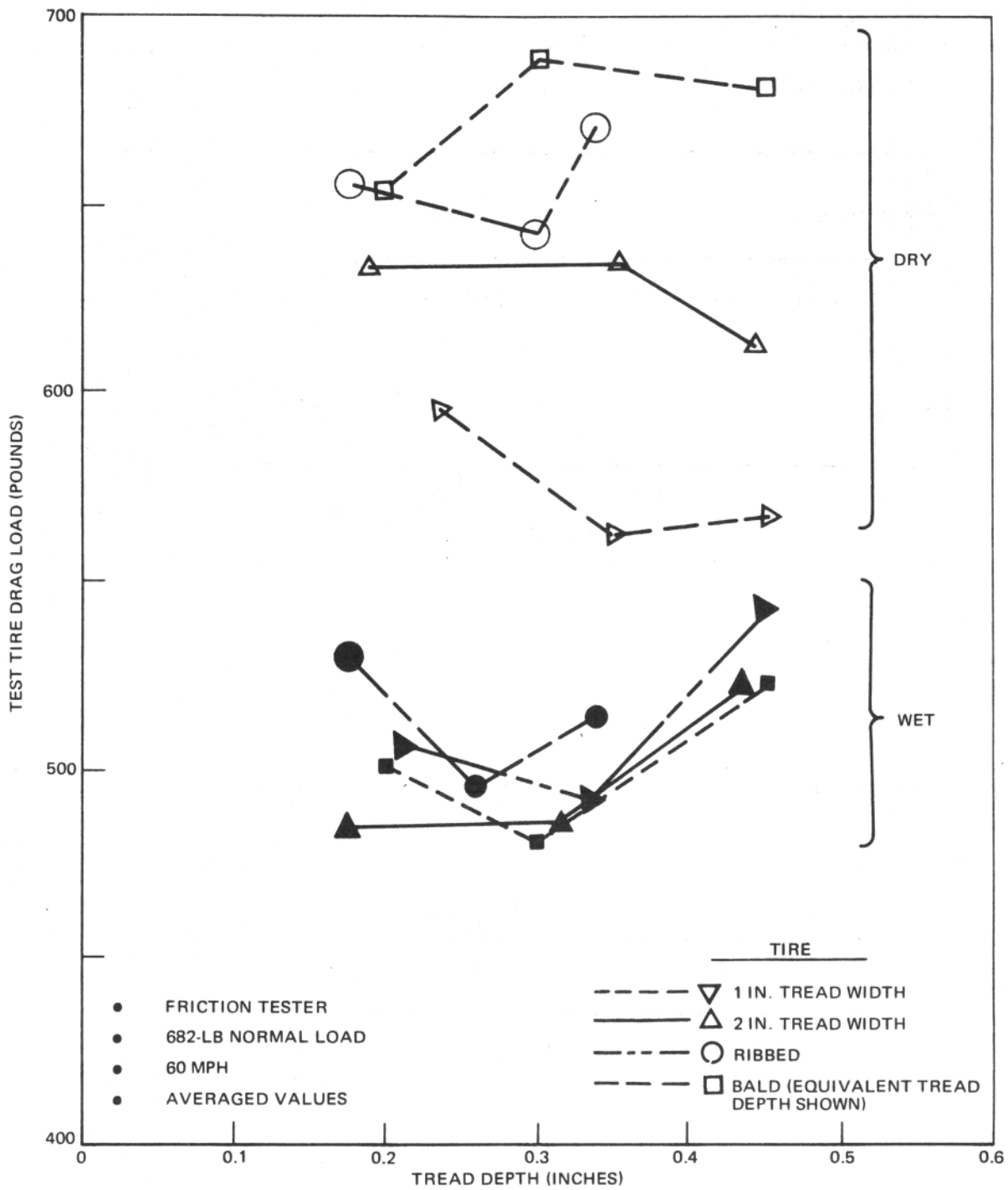


FIGURE II-6. TEST TIRE DRAG LOAD VS TREAD DEPTH

Investigation of the Effect of Repeated Autocycling

This investigation determined that satisfactory repeatable friction measurements could be obtained during repeated autocycling, alleviating the concern that tire heating might interfere with repeatability. Figure II-7 shows the results obtained by the standard ASTM E-249 ribbed tire during repeated cycling on dry pavement.

Investigation of the Effect of Environmental Temperature and Humidity on Friction Measurements

No trend could be distinguished upon investigation of the singular or collective effect of air temperature, surface temperature, and relative humidity upon friction values or slip velocity. Surface temperature ranged from 80 to 130°F, ambient temperatures ranged from 68 to 96°F, and relative humidity varied from 10 to 60 percent. Measurements were recorded during each run.

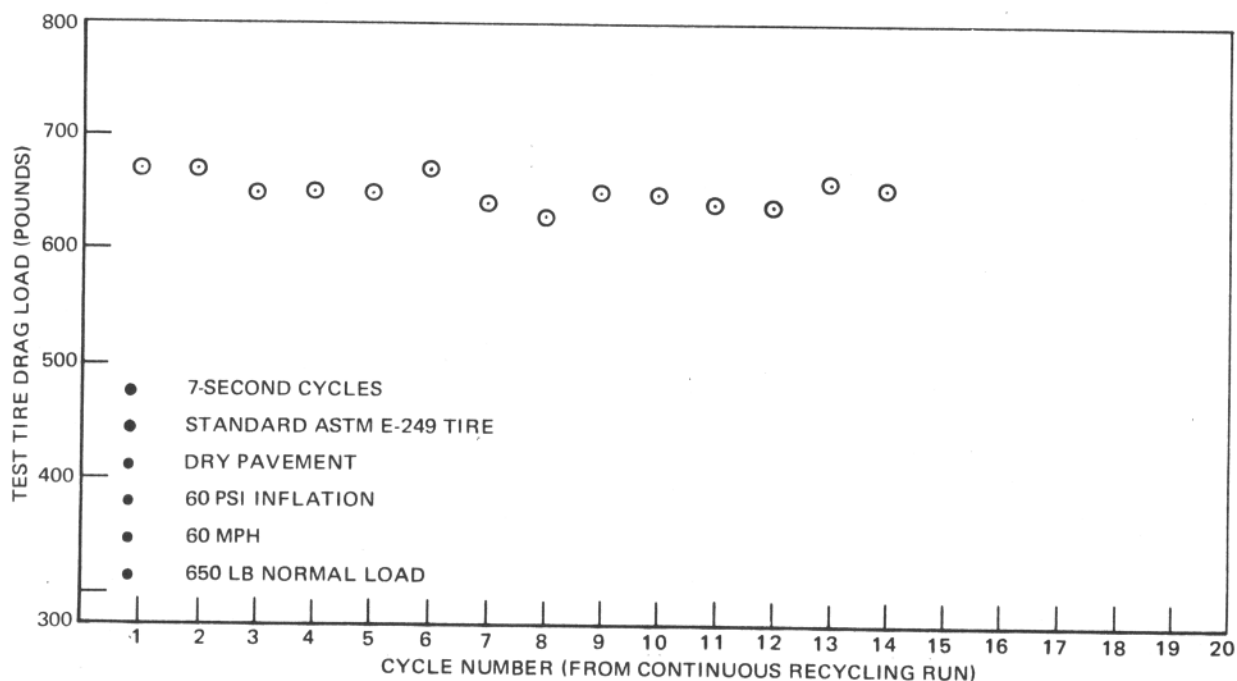


FIGURE II-7. EFFECT OF REPEATED AUTO-CYCLING

APPENDIX III

RUNWAY CALIBRATION AND CORRELATION TESTS

The calibration and correlation tests were performed to establish a correlation data base which could be used to determine a relationship between friction data produced by the FAA Variable Slip Runway Friction Tester and test aircraft stopping performance.

The objective of the calibration tests performed by the friction tester only was to obtain friction information about the test section, particularly the friction-velocity relationship under various wetness conditions and the significance of measurement location and direction. The objective of the correlation tests was to obtain near-simultaneous friction tester and aircraft stopping performance data on the dry and wet runway, and to obtain aircraft braking characteristics data for use in programming and checking the aircraft simulation.

RUNWAY FRICTION CALIBRATION

Friction calibration runs were conducted with the FAA friction tester on the Runway 12-30 3000-foot test section approximately 2 months before the friction tester/aircraft correlation tests. Eighteen dry runs, 18 tester self-wetted runs, 10 natural damp runs and 12 natural rain runs were performed in alternating directions on the runway, 12 feet to each side of the runway centerline. The natural damp tests were performed in the morning after a light rainfall. The natural rain tests were conducted under medium-to-heavy rain conditions. The tests were performed using the autocycling system set for a 7-second cycle period and 35-percent maximum slip, and the standard ASTM E-249 ribbed tire inflated to 60 psi and loaded to 600 pounds. Constant friction tester speeds of 30, 60, and 80 mph were used.

Friction measurements obtained during the calibration runs are shown as a function of runway locations in Figures III-1 through III-4. Four-to-five friction readings were obtained during each 80 mph run. Slower runs produced more readings since the time in the test section was longer. The difference in friction values between tests with the friction tester traveling in opposite directions on the runway was less than one percent. Natural rain tests (Figure III-4) did show lower friction values over the first half of the test section during the 80 mph tests; however, this variation was the result of changes in rainfall pattern during the tests, as evidenced by the fact that the 60 and 80 mph traces crossed over.

The calibration results were averaged over the length of the test section and plotted as a function of velocity in Figure III-5. The self-wet friction measurements, in the comparison shown in Figure III-5 with dry, natural damp, and natural rain, indicate that the 0.020-inch water depth provided by the friction tester self-wetting system is probably representative of a light rainfall.

FRICTION TESTER-AIRCRAFT CORRELATION TESTS

Four dry, 8 minimum wet, and 6 maximum wet correlation runs were performed on the Runway 12-30 test section with the friction tester preceding the test aircraft on all tests. One water truck traveling at 15 mph laid down a thin layer of water to simulate minimum wet runway conditions, and 2 or 3 water trucks traveling at 8 mph were used to simulate maximum wet runway conditions. The friction tester operated at constant speeds of 30, 60, or 80 mph. The test aircraft accelerated to above 120 knots before entering the test area and, after entering, used full anti-skid braking until stopped. None of the runs required more than the 3000-foot test section for a complete stop.

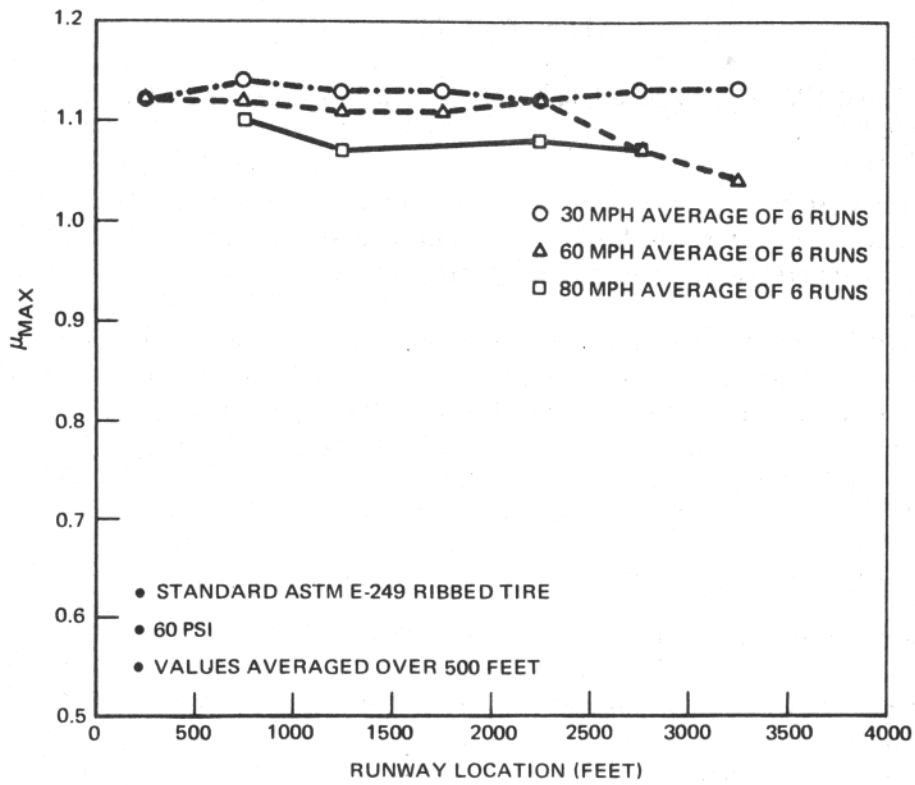


FIGURE III-1. μ_{MAX} VS RUNWAY LOCATION ~ DRY PAVEMENT

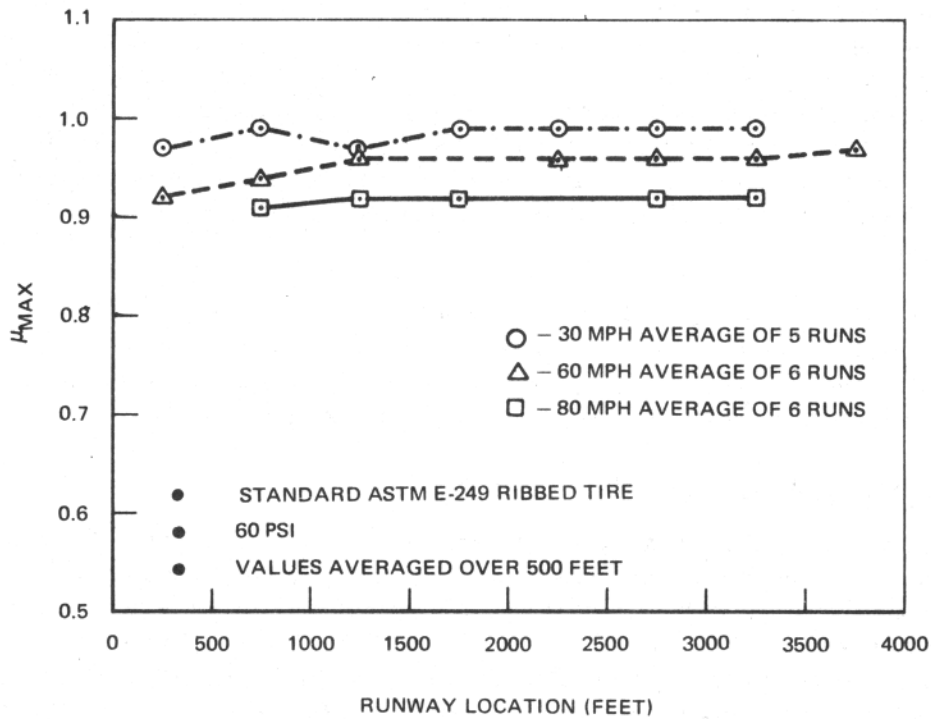


FIGURE III-2. μ_{MAX} VS RUNWAY LOCATION ~ SELF-WET

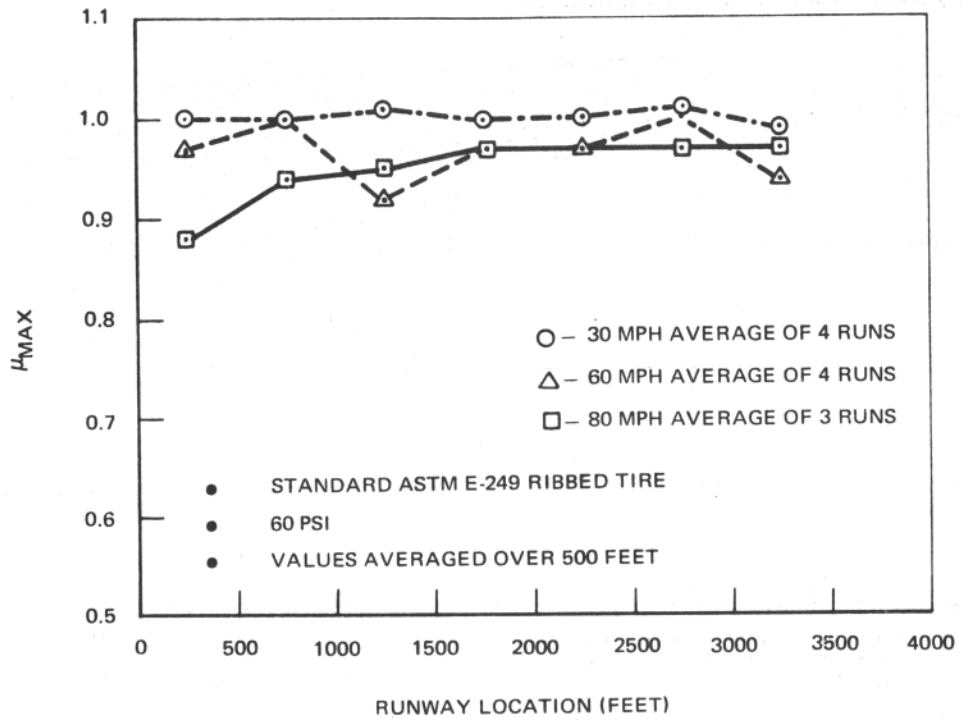


FIGURE III-3. μ_{MAX} VS RUNWAY LOCATION ~ NATURAL DAMP

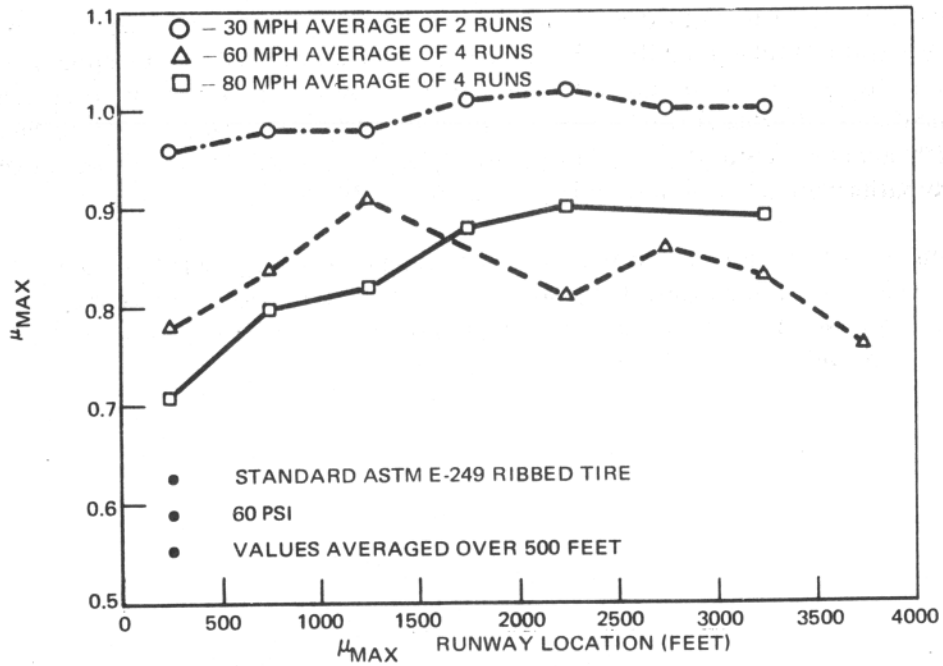


FIGURE III-4. μ_{MAX} VS RUNWAY LOCATION ~ NATURAL RAIN

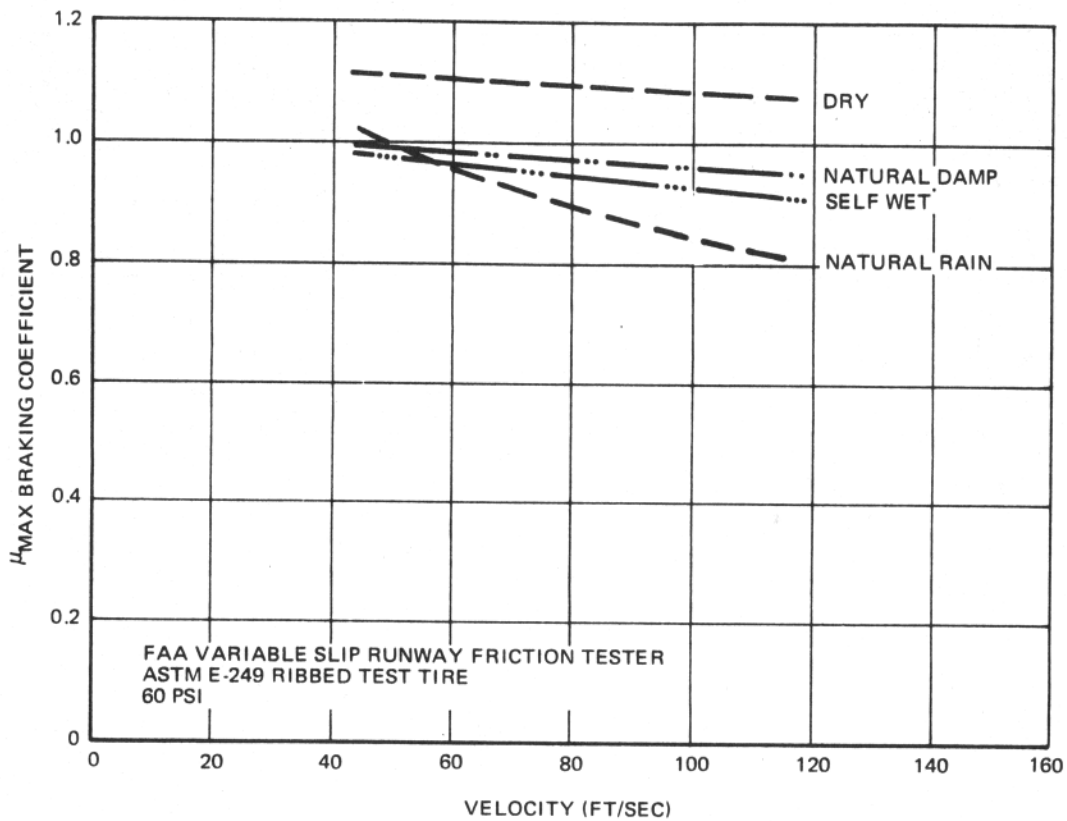


FIGURE III-5. RUNWAY CALIBRATION RESULTS $\sim \mu_{MAX}$ VS VELOCITY

Throughout the entire speed spectrum of the aircraft run, data were recorded on the aircraft's oscillograph and with a phototheodolite. Since friction was shown to be independent of direction during the calibration tests, all aircraft runs were performed in one direction from northwest to southeast. Immediately after each run, water depth was measured near the center of the 3000-foot test section with a water depth gage. A minimum of ten measurements in the region of the main landing gear tire paths were taken in obtaining an average depth.

Two nonbraking runs were also performed on dry pavement to verify aerodynamic constants and engine thrust levels. For these tests, the aircraft was accelerated in the same manner; however, brakes were not applied while the aircraft was in the test area. Two speed ranges, 108 to 87 and 95 to 69 knots, were covered.

The following environmental conditions were recorded during each test:

Measurement	Source
Atmospheric Pressure Altitude	Airport Control Tower
Ambient Temperature	Thermometer
Wind Direction and Velocity	50-Foot Height Airport Control Tower 6-Foot Height Wind Indicator
Humidity	Dry- and Wet-Bulb Thermometer Readings
Pavement Surface Temperature	Thermocouple
Water Depth	Water Depth Gage
Volume of Water Used	Water Truck Volume Estimates

Results of the friction tester/aircraft correlation tests are summarized in Table III-1. Aircraft stopping distances were normalized to eliminate variations in weight, brake application velocity, and wind just before each run. Average normalized dry stopping distance was 1750 feet. Average normalized stopping distance for minimum wet and maximum wet were 1897 and 1923 feet, respectively, with individual distances overlapping. The variation from shortest to longest was 60 feet during dry tests, 115 feet during minimum wet tests, and 170 feet during maximum wet tests.

Friction measurements obtained during the correlation tests were added to those of the calibration tests to provide a larger data base for the Composite Runway Friction Calibration Chart, Figure III-6. The only significant difference between the minimum and maximum wet friction values occurred at 30 mph; however, only two tests were conducted at this speed, one under each wetness condition. Since there was little difference at the other speeds, the two 30-mph values were averaged and an average minimum-maximum wet curve was drawn.

Stopping distance of those aircraft runs during which a friction tester velocity of 80 mph was used is plotted against the friction tester friction measurement in Figure III-7 and also as wet/dry ratios in Figure III-8. The data obtained at 80 mph show good correlation with the aircraft, whereas data obtained at lower speeds were erratic.

Figures III-9 and III-10 show friction measured by the friction tester during the wet correlation tests as a function of location. These figures show a general decrease in friction as the friction tester neared the end of the test section. This trend was not evident during the calibration tests, and it is considered to be the result of the water truck/s wetting procedure which, due to their slow 8 to 15 mph speeds, allowed more time for water runoff at the beginning of the test section than at the end. This dependence upon direction of water truck travel has been experienced during previous aircraft tests.

TABLE III-1
CORRELATION TEST SUMMARY CHART

Aircraft Test No.	Runway Condition	Aircraft Results				Friction Tester Results			Runway Condition	
		V.B.O. ft/sec	Stop Distance	Dist from 190 ft/sec	Normalized Distance ¹	Norm Dist ÷ Ave Dry Distance	Vehicle Speed (mph)	Ave μ -max	Water Depth Measurement (inches)	Gallons of Water Sprayed
411	Dry	202	2025	1725	1720	0.98	60	1.12	0	0
412	Dry	200	2040	1760	1740	0.99	80	1.11	0	0
413	Dry	200	2060	1820	1780	1.02	—	—	0	0
414	Dry	197	1970	1770	1760	1.01	—	—	0	0
Ave					1750	1.00			0	0
415	Min Wet	205	2430	1900	1860	1.06	60	0.94	0.005	3500
416	Min Wet	206	2410	1905	1890	1.08	80	0.86	0.005	2000
417	Min Wet	206	2405	1895	1860	1.06	60	0.89	0.003	1800
418	Min Wet	204	2385	2000	1955	1.12	80	0.77	0.006	1800
419	Min Wet	204	2435	1955	1920	1.10	60	0.84	0.005	1800
420	Min Wet	207	2500	1965	1935	1.11	30	0.94	0.004	1800
427	Min Wet	200	2260	1930	1840	1.05	60	0.86	0.003	1500
428	Min Wet	196	2105	1915	1905	1.09	80	0.88	0.005	3500
429	Min Wet	186	1865	1905	1910	1.09	60	0.92	Damp	1800
Ave					1897	1.08			0.004	2170
421	Max Wet	201	2240	1840	1820	1.04	60	0.91	0.010	6000
422	Max Wet	205	2495	1975	1940	1.11	80	0.80	0.010	7000
423	Max Wet	200	2285	1910	1890	1.08	30	1.00	0.010	10500
424	Max Wet	206	2540	2010	1975	1.13	60	0.87	0.020	10500
425	Max Wet	NO	PHOTOSCOPE		DATA		80	0.90	0.015	10500
426	Max Wet	202	2440	2040	1990	1.14	60	0.88	0.009	11000
Ave					1923	1.10			0.012	9250

¹Normalized to 80,000 lb., Sea Level Standard Day, No Runway Slope, No wind, and 190 ft/sec at brake application.

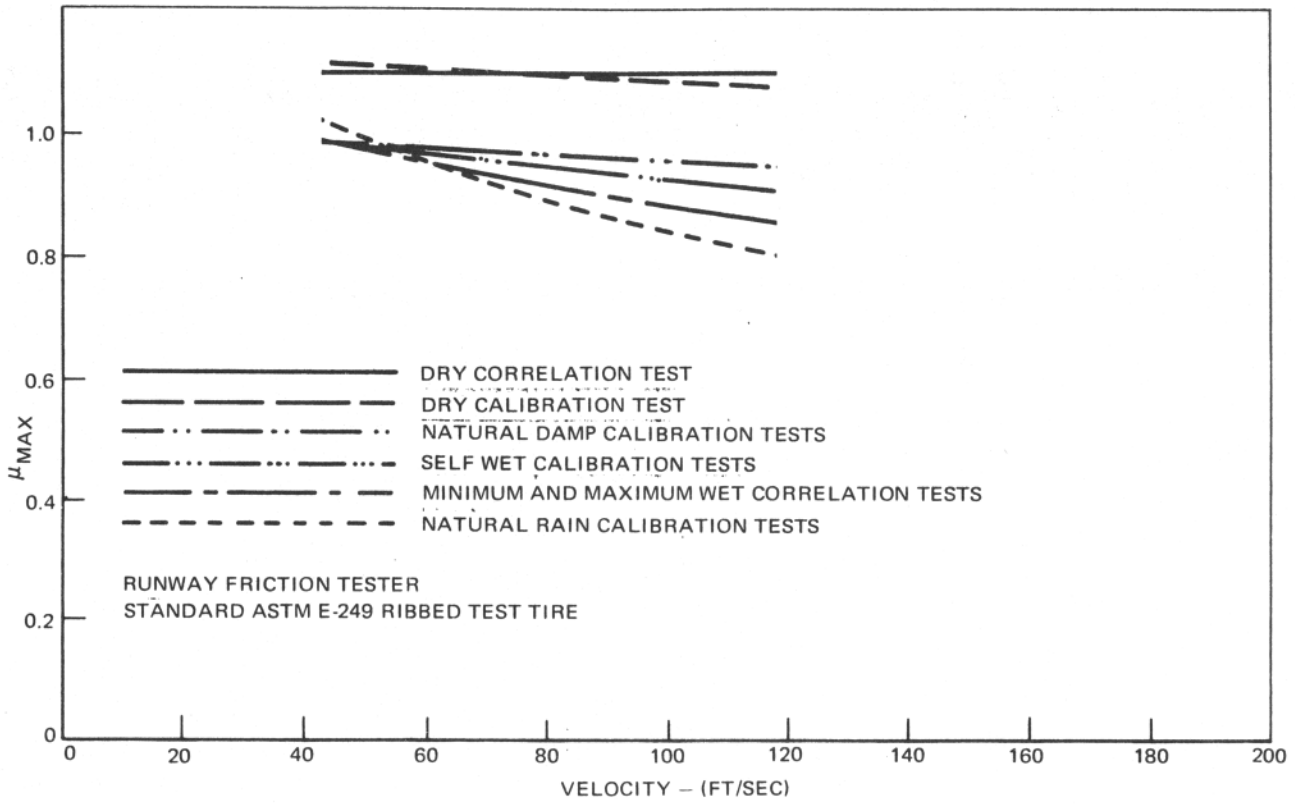


FIGURE III-6. COMPOSITE RUNWAY FRICTION CALIBRATION CHART

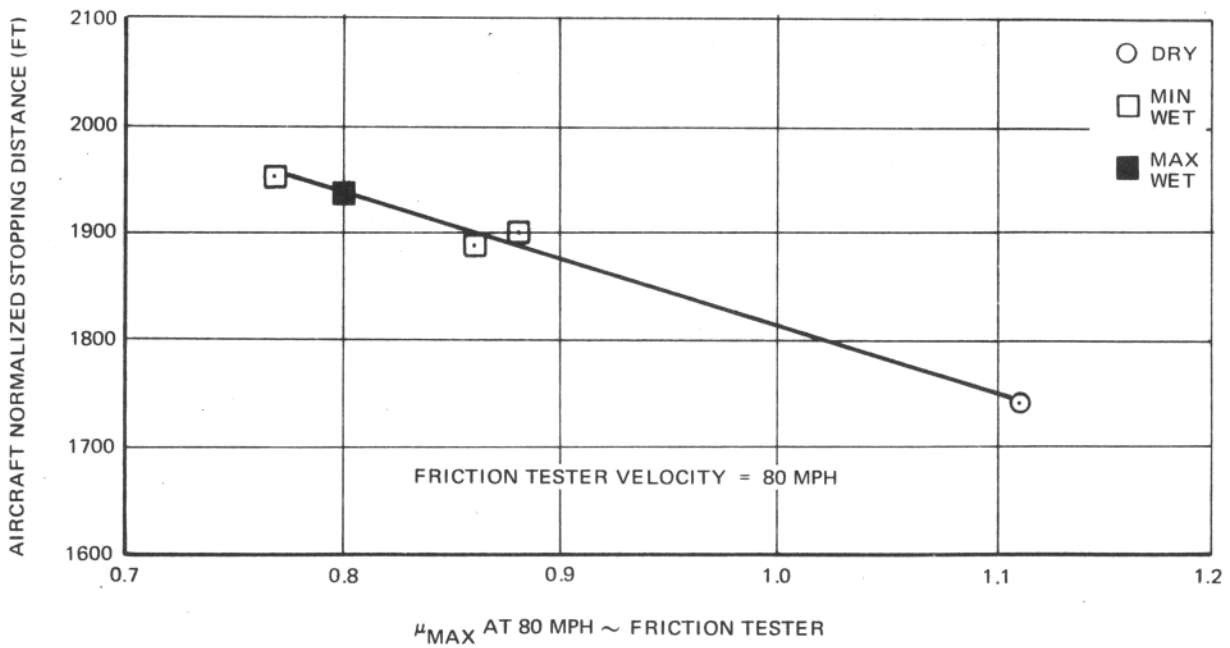


FIGURE III-7 STOPPING DISTANCE VERSUS MEASURED FRICTION

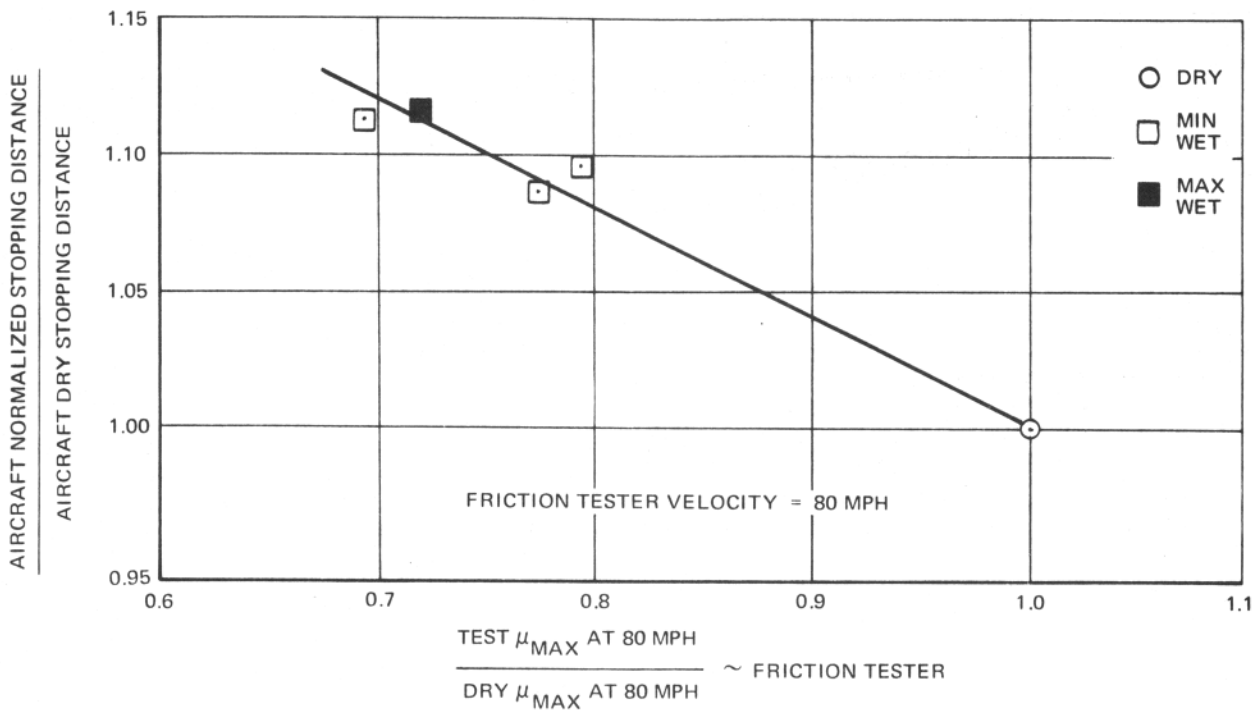


FIGURE III-8. STOPPING DISTANCE RATIO VERSUS MEASURED FRICTION RATIO

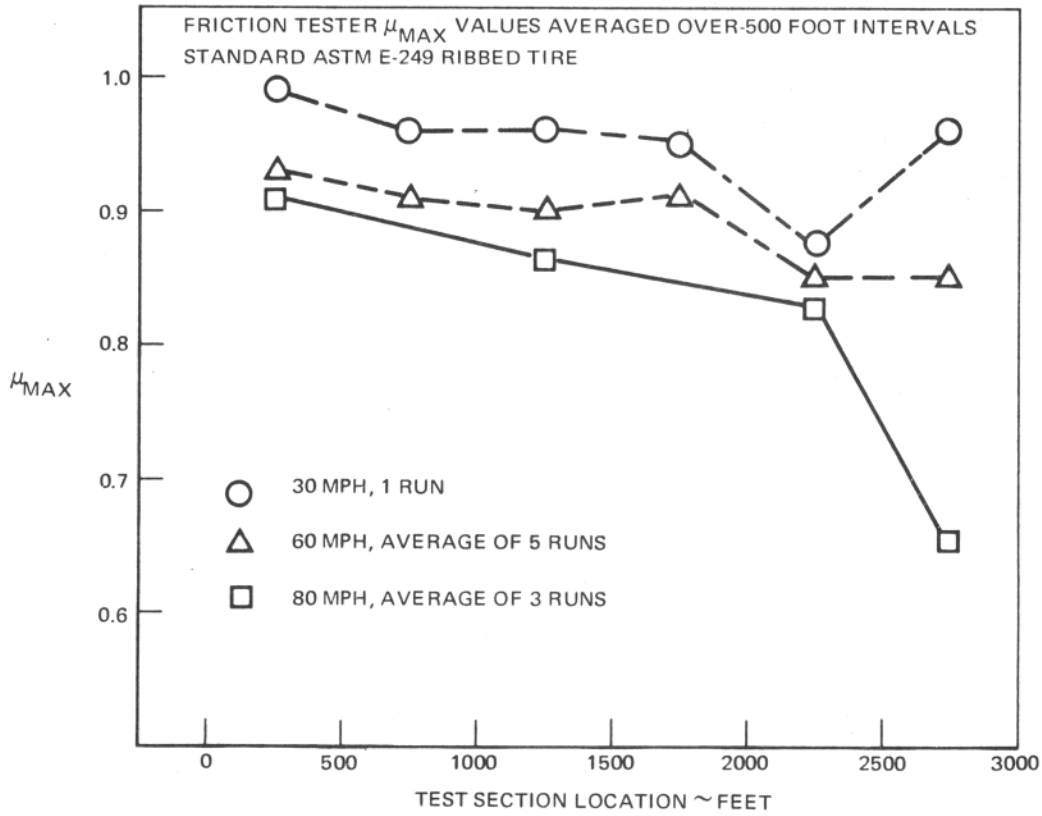


FIGURE III-9. μ_{MAX} VS RUNWAY LOCATION ~ MINIMUM WET CORRELATION TESTS

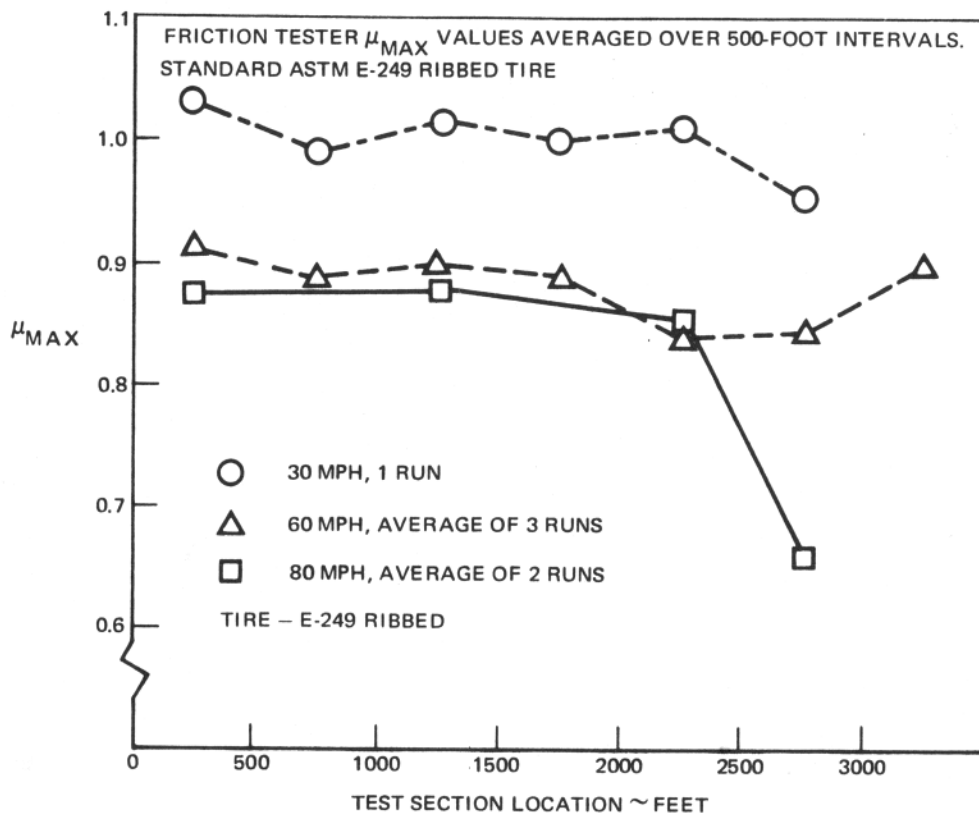


FIGURE III-10. μ_{MAX} VS RUNWAY LOCATION ~ MAXIMUM WET CORRELATION TESTS

Although four times as much water was sprayed onto the runway during the maximum wet tests (9300 gallons average) than during the minimum wet tests (2200 gallons average) and three times as much water depth was measured after the completion of each maximum wet test (0.012 inch average) than after each minimum wet test (0.004 inch average), little difference was evident in either aircraft stopping distance or friction measured by the friction tester. This insensitivity to water depth combined with the relatively high friction values recorded by the friction tester, as well as the noncontractual test vehicles described in Appendix IV, indicate that the test section surface texture was much superior to the average ungrooved runway.

APPENDIX IV

NONCONTRACTUAL FRICTION MEASURING VEHICLES INCLUDED IN RUNWAY TEST PROGRAM

In addition to the FAA Variable Slip Runway Friction Tester, friction measurements were also obtained during the correlation tests by a McDonnell Douglas owned Miles Road Research Laboratory Trailer and by FAA owned and operated James Brake Decelerometer and FAA Fixed Slip Runway Friction Tester (a modified Swedish Skiddometer).

The Miles Trailer, shown in Figure IV-1, measures the braking torque of a locked wheel and is designed for speeds up to 120 miles per hour. The 8.00 x 4 6-ply grooved test tire is inflated to 20 psi and supports a 317-pound load. Braking is accomplished by actuating a vacuum servo system. Brake torque is transformed into pressure by a hydraulic pressure capsule restraint and the pressure is transmitted to a Bourdon tube which controls a recording pen. The trailer is not intended for use on dry pavement.

The James Braking Decelerometer (JBD), shown in Figure IV-2, measures the highest deceleration experienced by a vehicle during tire skid brake application. During the correlation tests, the JBD was used in a specially equipped FAA station wagon with only the rear wheels (racing slicks) braked and in a conventional 1969 sedan with four wheel (street tires) braking.

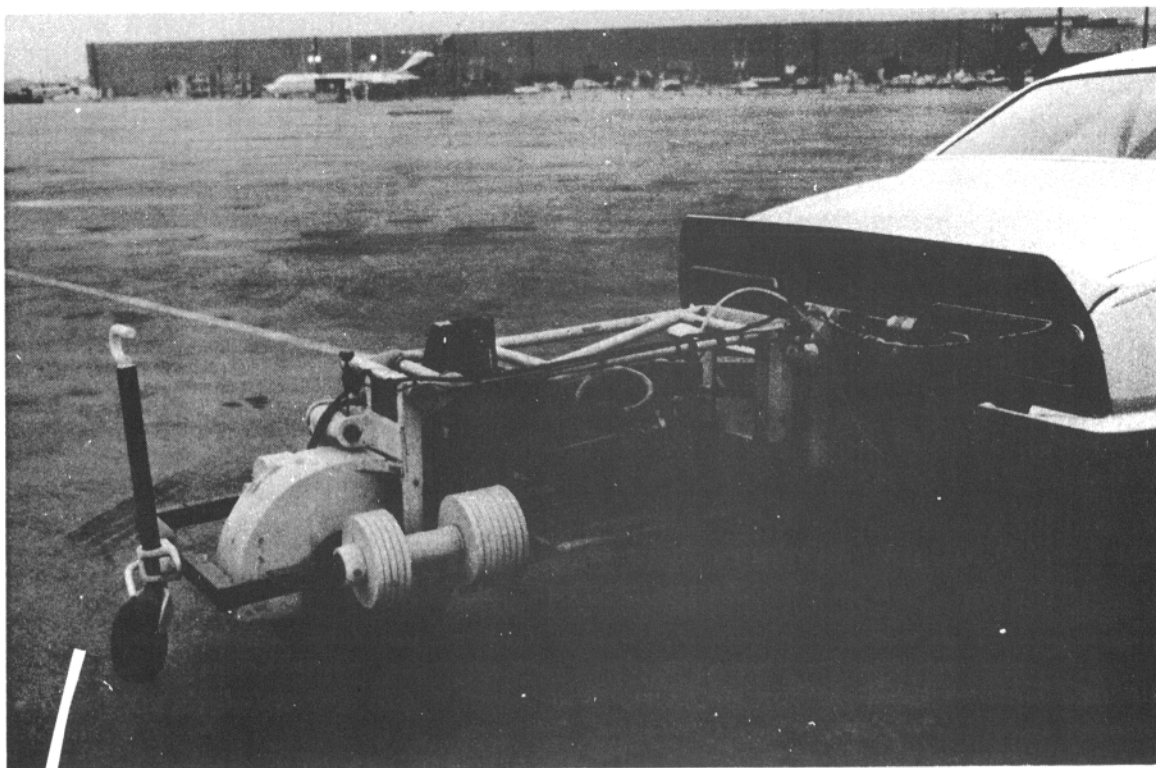


FIGURE IV-1. MILES ROAD RESEARCH LABORATORY TRAILER

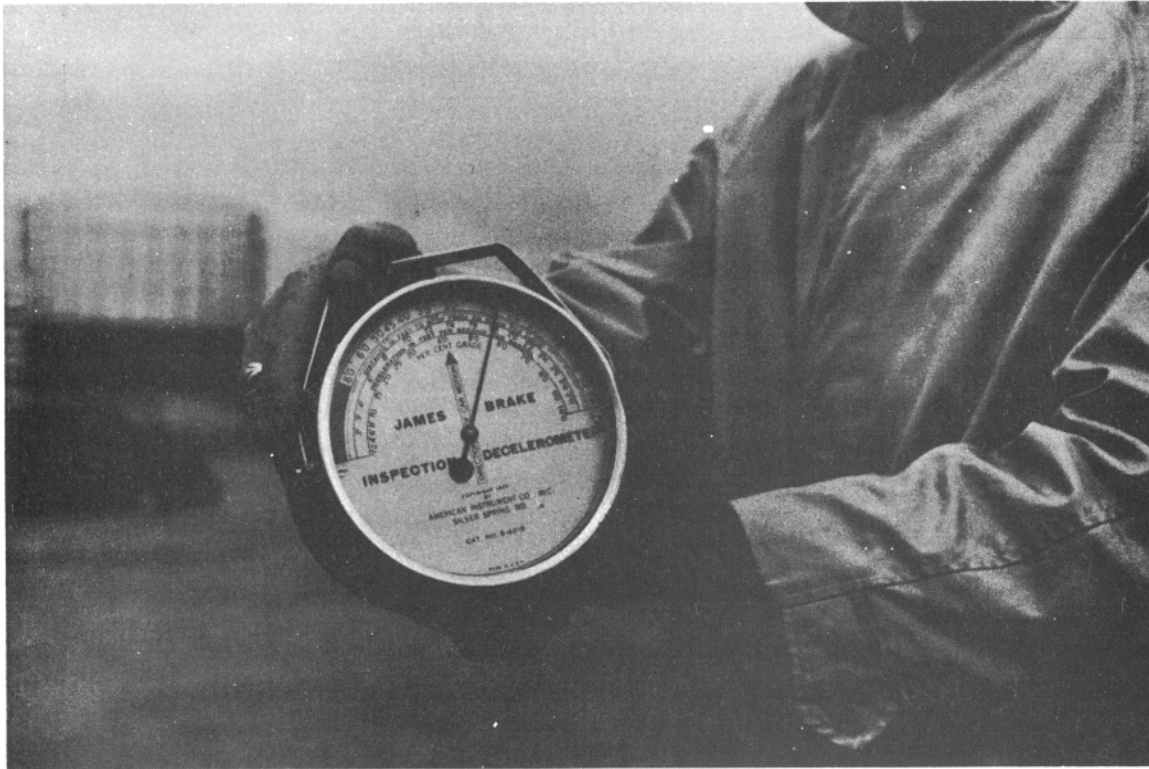


FIGURE IV-2. JAMES BRAKE DECELEROMETER

The FAA Fixed Slip Runway Friction Tester, shown in Figure IV-3, is a three wheel fixed slip trailer. The test wheel, centrally located, is connected through engaging clutches and universal joints to the outer wheels. The tire diameters are such that test tire operates at a constant slip ratio of approximately 13 percent. The normal load on the test tire is 1080 pounds. The tire used was a modified ASTM E-249 bald tire. The FAA Fixed Slip Runway Friction Tester was used only on dry pavement, for these series of correlation tests as clutch synchronization problems made the trailer unstable on wet pavement.

Friction measurements obtained during the aircraft correlation tests by these vehicles are summarized in Table IV-1 and Figure IV-4.

Some hydroplaning in puddles was experienced by the Miles Trailer during 60 and 80 mph runs. Hydroplaning friction values were discarded by eliminating those values which were less than one-half of the run average.

Figures IV-5 through IV-7 show normalized aircraft stopping distance plotted against friction measurements of the Miles Trailer and the James Brake Decelerometer. A definite trend can be seen in Figure IV-7 between deceleration of the rear wheel braked station wagon and aircraft stopping distance.

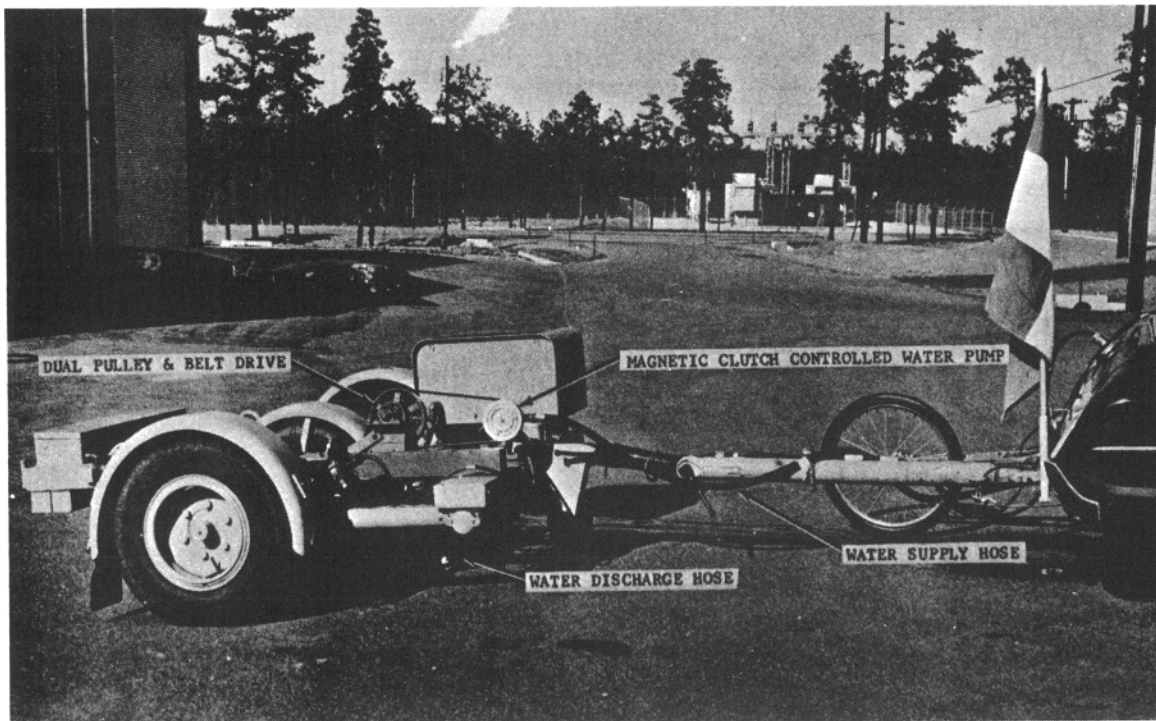


FIGURE IV-3. FAA'S FIXED SLIP RUNWAY FRICTION TESTER

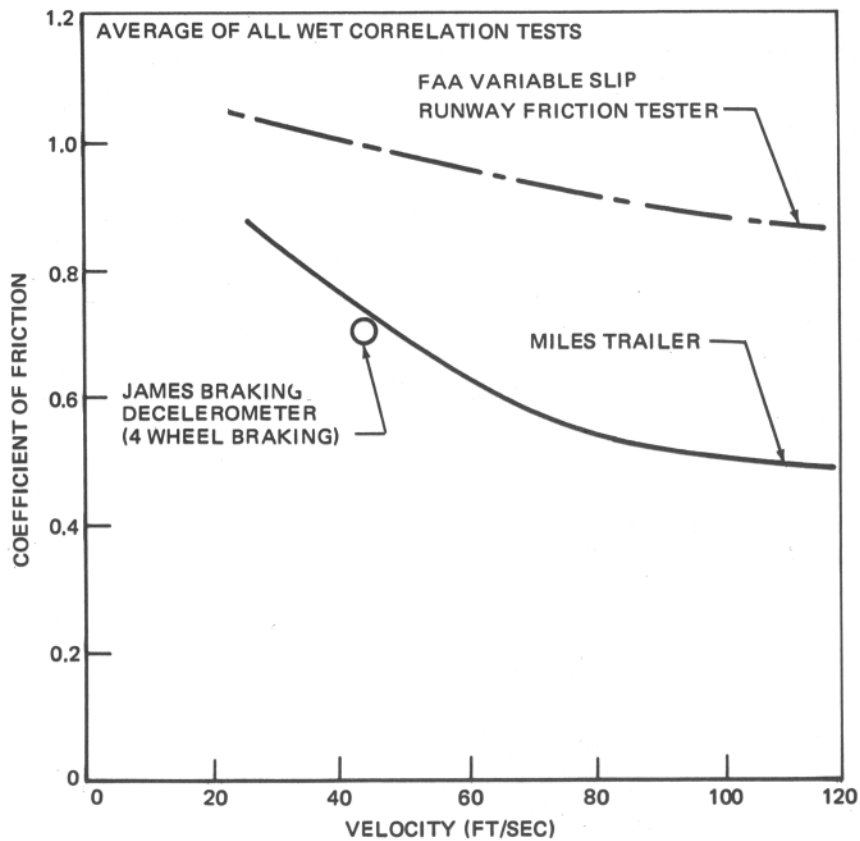


FIGURE IV-4. FRICTION VEHICLE MEASUREMENTS VS VELOCITY

TABLE IV-1
CORRELATION MEASUREMENTS-MILES TRAILER, JBD, AND FAA FIXED SLIP RUNWAY FRICTION TESTER

AIRCRAFT TEST NO.	RUNWAY CONDITION	AIRCRAFT NORMALIZED STOP DIST (1) (FT)	MILES TRAILER		FAA FIXED SLIP RUNWAY FRICTION TESTER		JAMES BRAKE DECELEROMETER										
			VEHICLE SPEED (MPH)	μ	VEHICLE SPEED (MPH)	μ	4 WHEELS BRAKED			REAR WHEELS BRAKED							
							VEHICLE SPEED (MPH)	DECELERATION (FT/SEC ²)	EQUIV-ALENT μ	VEHICLE SPEED (MPH)	DECELERATION (FT/SEC ²)	EQUIV-ALENT μ (3)					
411	Dry	1720			0.80	60										0.93	
412	Dry	1740			0.83	80										1.02	
413	Dry	1780															
414	Dry	1760															
AVERAGE		1750															
415	MIN WET	1860															0.84
416	MIN WET	1890															0.76
417	MIN WET	1860	60	0.55													0.80
418	MIN WET	1955	80	0.49 (2)													0.66
419	MIN WET	1920	60	0.50													0.79
420	MIN WET	1935	30	0.77													0.80
427	MIN WET	1840	60	0.54													0.83
428	MIN WET	1905	80	0.51 (2)													
429	MIN WET	1910	60	0.53													
AVERAGE		1897															
421	MAX WET	1820	60	0.50													0.52
422	MAX WET	1940	80	0.50 (2)													0.73
423	MAX WET	1890	30	0.70													0.70
424	MAX WET	1975	60	0.45													0.84
425	MAX WET	1990	80	0.44													0.68
426	MAX WET	1923	60	0.54 (2)													
AVERAGE																	

NOTES: (1) NORMALIZED TO 80,000 LB, SEA LEVEL STANDARD DAY, NO RUNWAY SLOPE, NO WIND, 190 FT/SEC AT BRAKE APPLICATION.

(2) HYDROPLANING OCCURRED. HYDROPLANING VALUES WERE NOT INCLUDED IN AVERAGE SHOWN.

(3) ASSUMING ONE-HALF OF THE AUTOMOBILE WEIGHT WAS SUPPORTED BY THE REAR WHEELS DURING BRAKING.

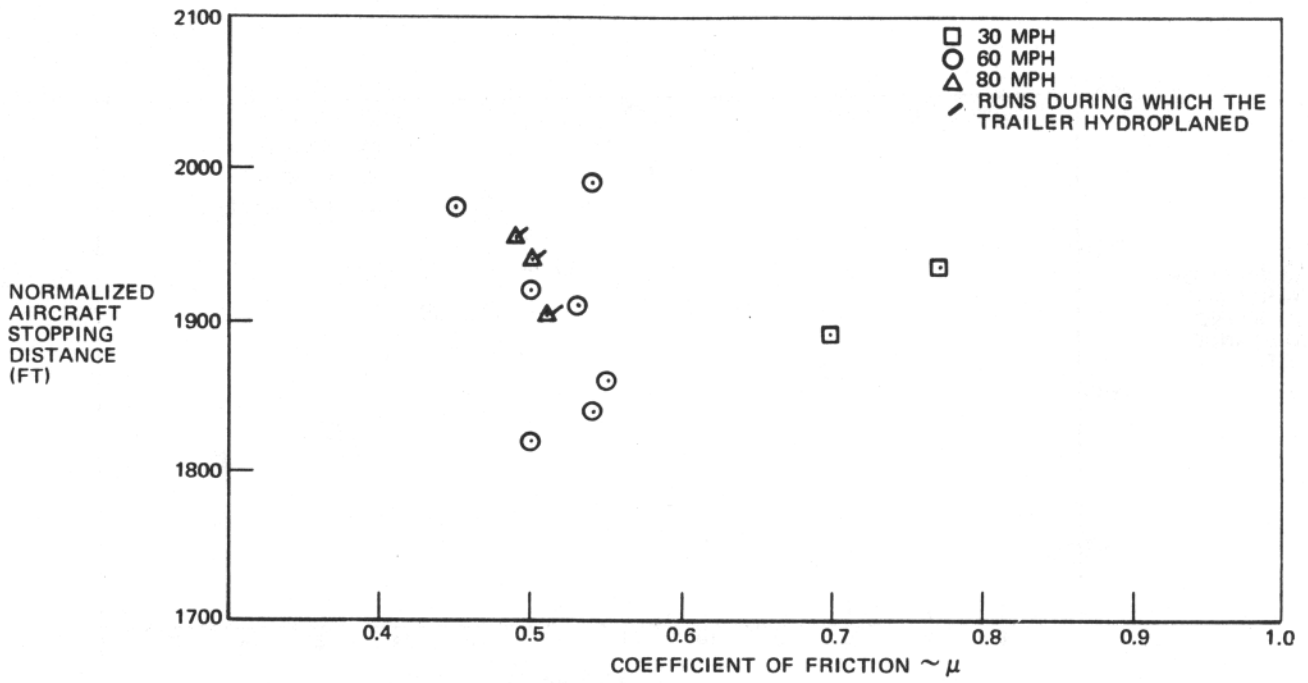


FIGURE IV-5. STOPPING DISTANCE VS MEASURED FRICTION - MILES TRAILER

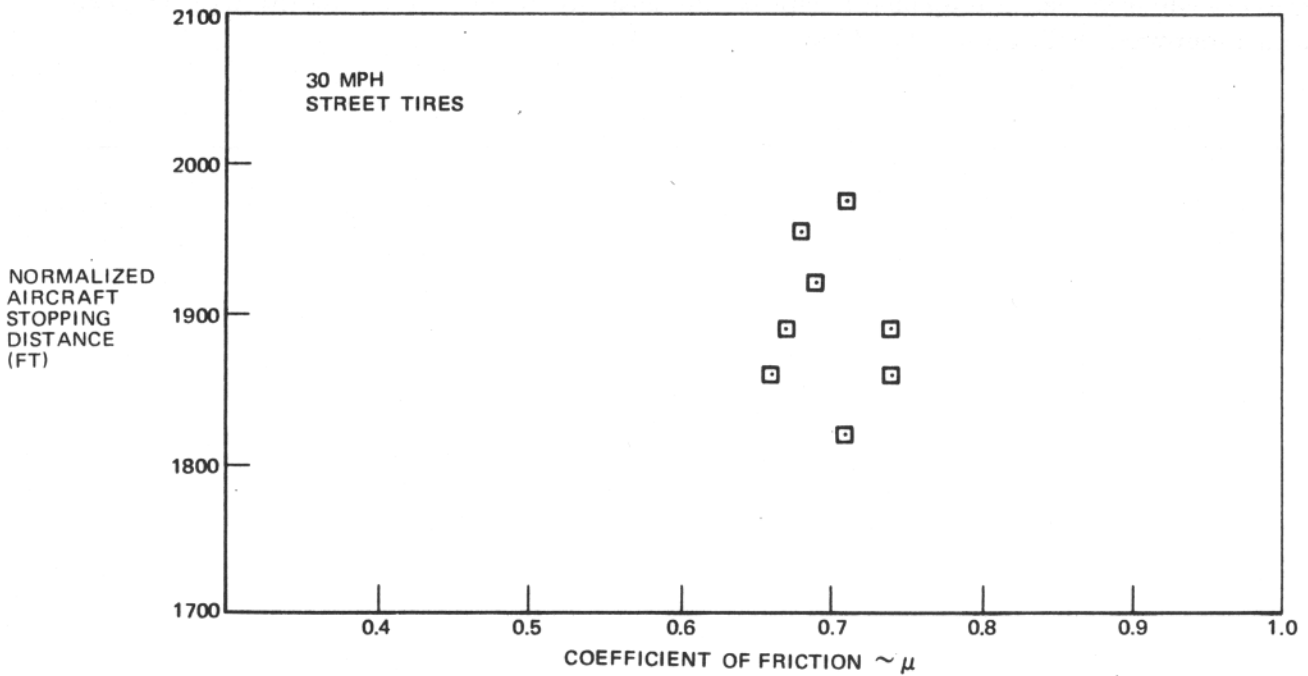


FIGURE IV-6. STOPPING DISTANCE VS MEASURED FRICTION \sim JBD WITH FOUR WHEEL BRAKING

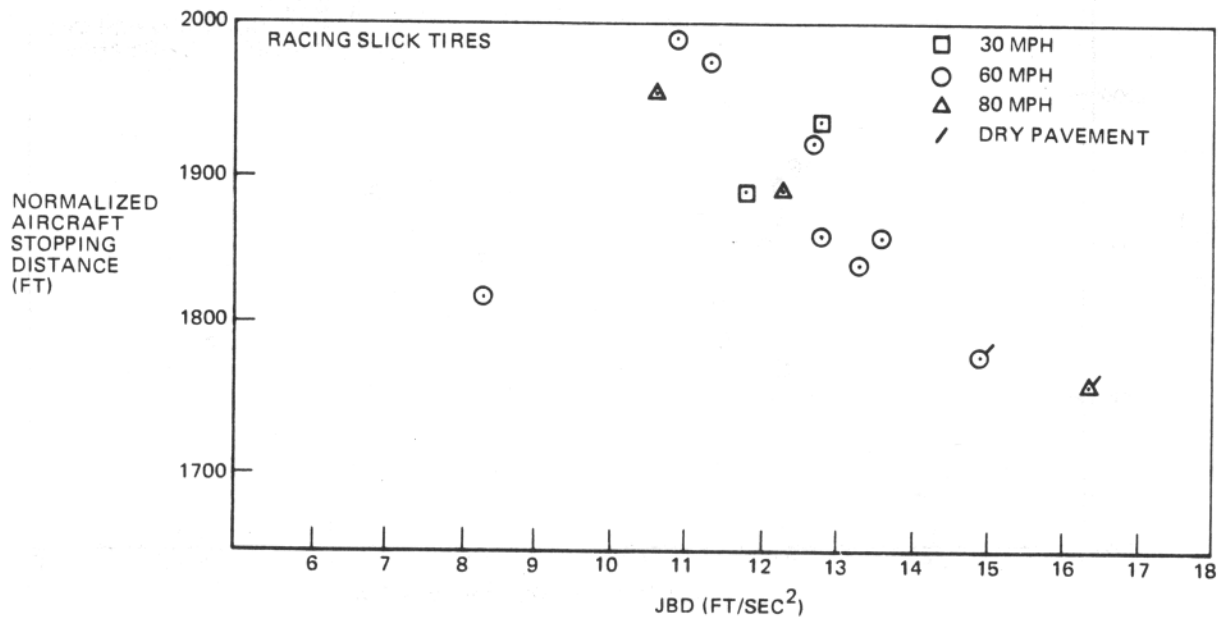


FIGURE IV-7. STOPPING DISTANCE VS JBD READING ~ REAR WHEEL BRAKING

In conclusion it may be stated that the various runway friction testers included in the runway test program did not correlate satisfactorily. However, the relationship of JBD data obtained with a rear-wheel-braked vehicle at 80 mph to airplane stop distance was superior to the JBD data obtained with a four-wheel braked vehicle at 30 mph.

APPENDIX V

DEVELOPMENT OF THE FRICTION RELATIONSHIPS USED IN THE ANALOG SIMULATION

INTRODUCTION

The tire-runway friction data required in the simulation of an aircraft anti-skid braking system consists of two functions:

1. The friction coefficient, μ versus slip velocity relationship.
2. The maximum friction coefficient, μ_{MAX} versus velocity relationship.

These relationships can be obtained from the FAA friction tester data. However, correlation between the anti-skid simulator and DC-7 test data is poor when the friction relationships obtained from the friction tester are used directly. This appendix discusses the μ versus slip velocity and μ_{MAX} versus velocity functions used on the simulator to achieve correlation between simulator output and DC-7 flight test records.

DISCUSSION OF THE FRICTION COEFFICIENT-SLIP VELOCITY RELATIONSHIP

In the computer simulation, the tire-runway friction coefficient was mechanized as a function of tire tread slip velocity. This slip velocity was formed by differencing the hub speed with a velocity calculated from the effective rolling radius [calculated from Eq. 76a of Reference (1)] and tire rotation velocity.

$$\dot{X}_4 = V_H - \left(r_o - \frac{F_z}{3K_z} + \frac{F_x}{K_x} \right) \dot{\theta}_4$$

A study was made to determine the shape of the curve that would result in simulator anti-skid performance that best correlated with anti-skid test data. The shape of Figure V-1 was the result of this study. It was found that the initial slope of the curve between 0 and 1.0, which is primarily dependent upon tire elasticity calculated by the elasticity equations of Reference 1, did not affect the dynamic performance as much as the slope of the second segment of the curve. This backslope, which determines the frequency and depth of skids, was developed to duplicate anti-skid operational characteristics recorded during the aircraft tests. When the second segment slope is too steep, the simulator skids were deeper and less frequent than the aircraft test skids. When the slope was too gentle, the anti-skid operation was more efficient than the aircraft test anti-skid operation.

The function used in the computer may be transformed into a function that can be compared to experimental data obtained during this program. When experimental tests are conducted, slip velocity, V_s , is calculated as follows:

$$V_s = V_H - r_{eff} \cdot \dot{\theta}_3$$

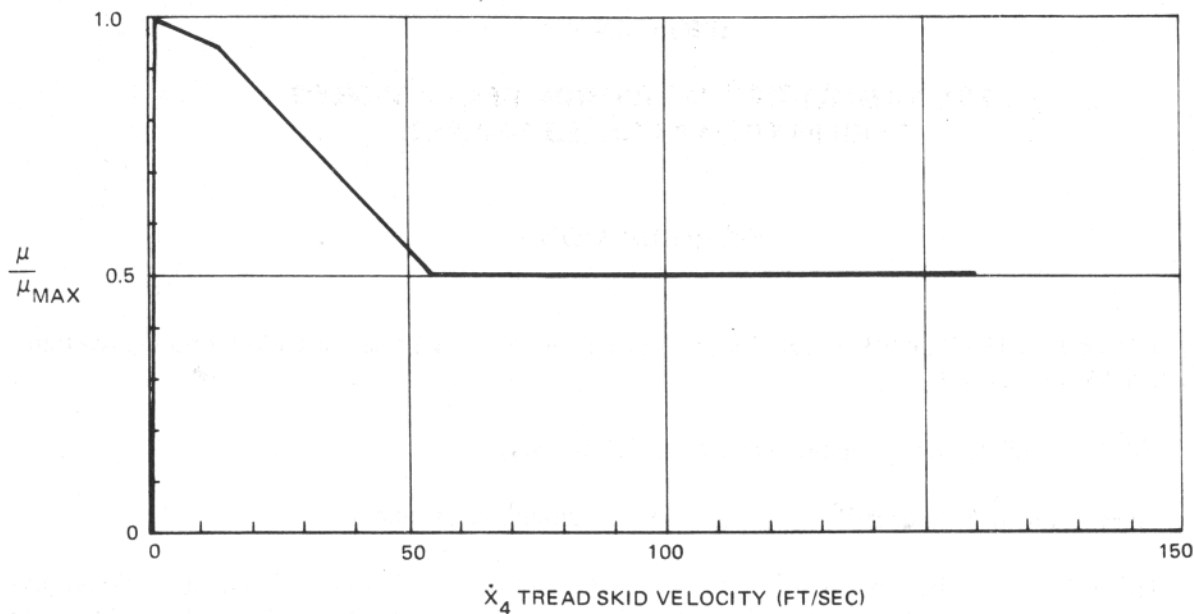


FIGURE V-1. RELATIONSHIP BETWEEN μ AND TIRE TREAD SKID VELOCITY

The actual tread slip velocity may be transformed into an equivalent wheel slip velocity by the equation

$$V_S = \frac{\dot{X}_4 + \left[\frac{\mu F_z}{K_x \left(r_o - \frac{F_z}{3K_z} \right)} \right] V_H}{1 + \left[\frac{\mu F_z}{K_x \left(r_o - \frac{F_z}{3K_z} \right)} \right]}$$

The curve is presented in this manner in Figure V-2. A curve estimated from aircraft data during a transient condition is also shown for comparison. However, the velocity for this latter curve was obtained from the anti-skid wheel speed signal which exhibits a dynamic lag behind true wheel speeds. Also shown in Figure V-2 for comparison is a curve obtained from the friction tester data. There is fair correlation between the simulator and the data, but poor correlation between these and the aircraft data. This poor correlation may be due to the dynamic response of the anti-skid wheel speed measuring system.

There are two characteristics of these friction coefficient-slip velocity curves that are easily determined and may be compared for a more objective judgment of the degree of correlation. The first characteristic is the value of slip velocity at which the normalized friction coefficient is unity. This data is presented in Figure V-3. A line representing a constant slip ratio of approximately 13 percent may be faired through the traction vehicle data. However, for the aircraft data a line of constant slip velocity of 10.4 fps or a line of constant slip ratio of approximately 7 percent could be faired through the data with equal uncertainty. The curve transformed from the simulator decreases

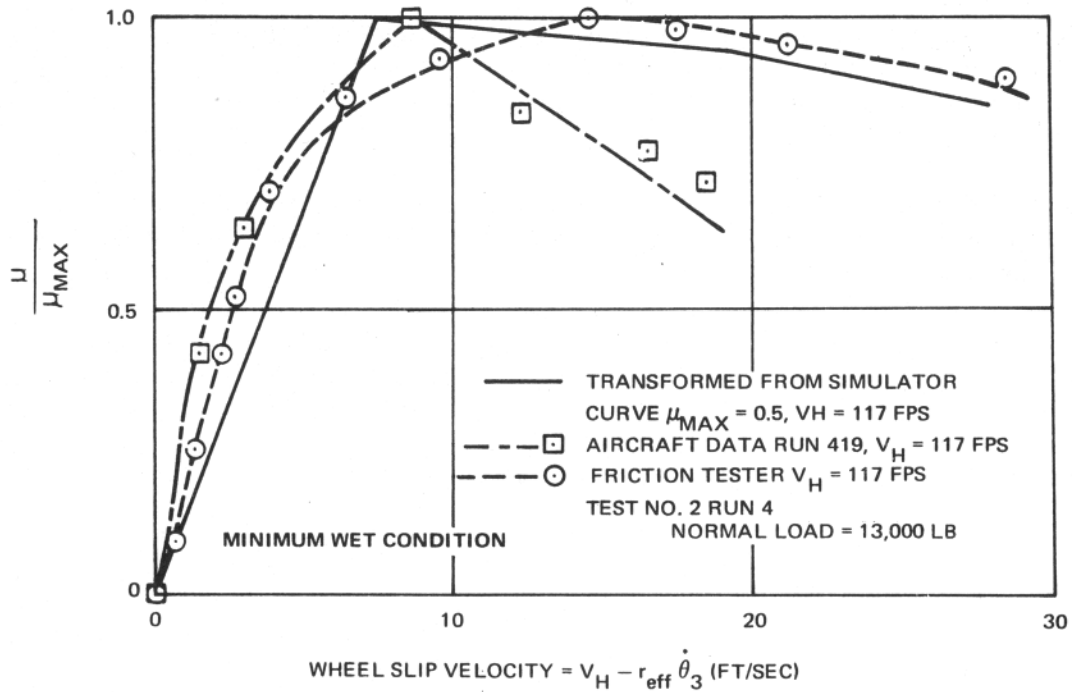


FIGURE V-2. NORMALIZED FRICTION COEFFICIENT AS A FUNCTION OF HUB SLIP VELOCITY

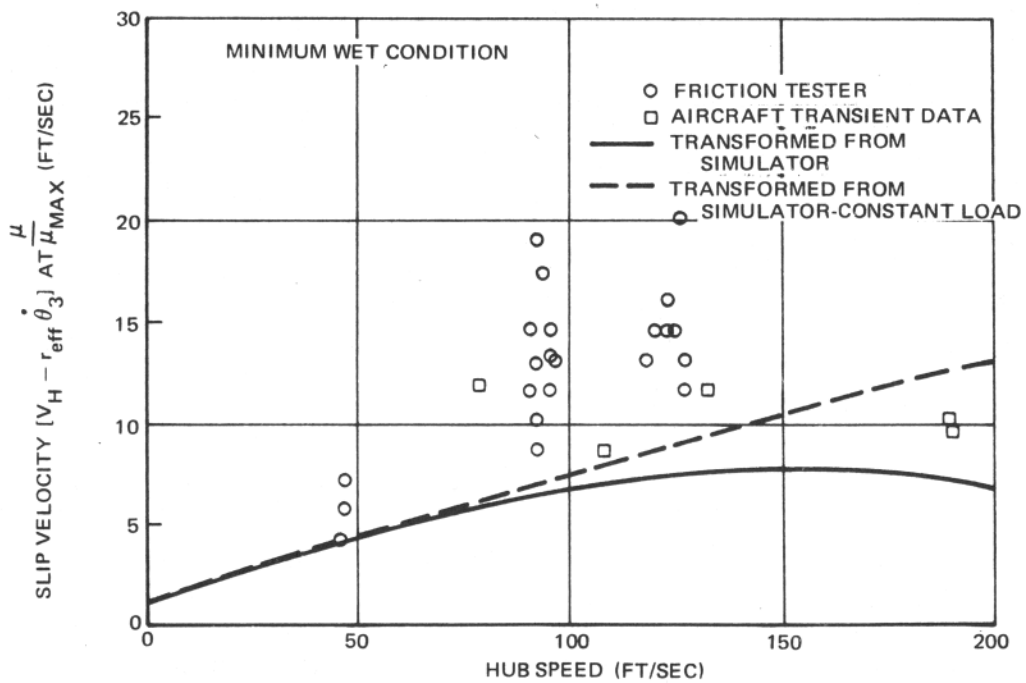


FIGURE V-3. SLIP VELOCITY AT PEAK OF μ -SLIP CURVE

at high speeds because the normal load on the tire is decreased due to aerodynamic lift. If the load were constant, as shown in the figure, a curve results that approximates a constant slip ratio, as does the data from the friction tester. As was noted previously, this initial slope did not appear to affect simulator performance as much as the slope of the curve beyond the peak. This slope is the second characteristic that can be determined and is plotted in Figure V-4. The simulator and friction tester slopes compare quite closely and neither compares well with the aircraft's slope.

To further investigate the effects of the shape of the μ -slip curve, some auxiliary computer simulation runs were conducted. For these tests, the computer mechanization was modified to give the tire-runway friction coefficient as a function of hub slip velocity. The curves from the aircraft and friction tester shown in Figure V-4 were mechanized directly. The wheel speed and valve command signals for two runs with these functions are given in Figure V-5. The results from the aircraft curve show deep skids as would be expected. The results from the friction tester curve yield more efficient operation than the flight test data. Evidently the efficiency is sensitive to the small differences between the curves near the peak and the friction tester tire may not accurately duplicate the aircraft tire function phenomenon in this region.

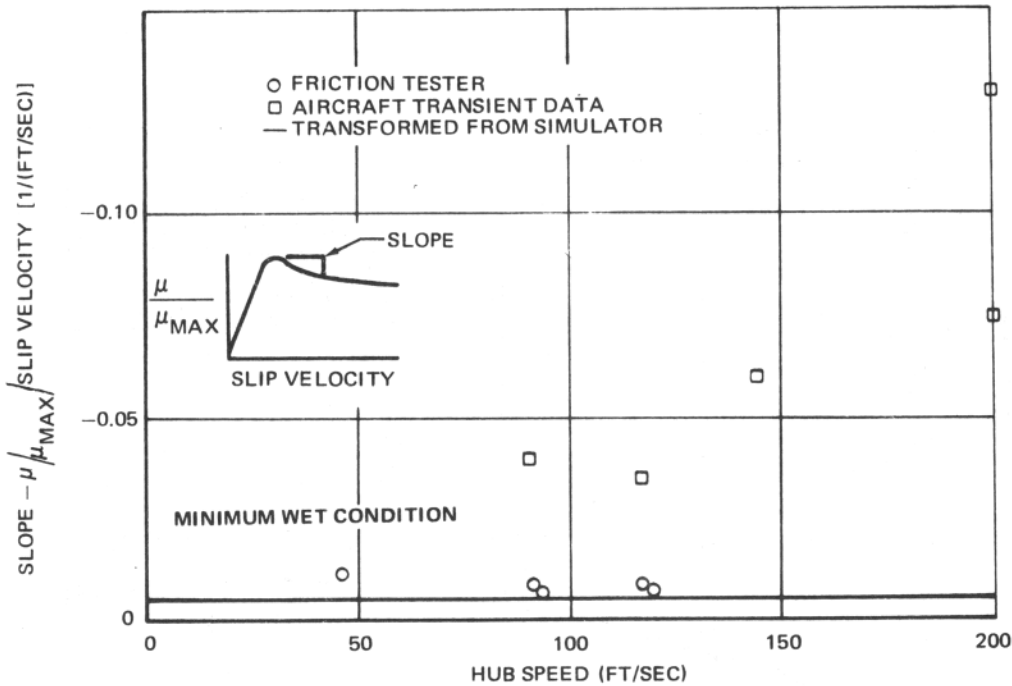


FIGURE V-4. SLOPE OF BACK SIDE OF μ -SLIP CURVE

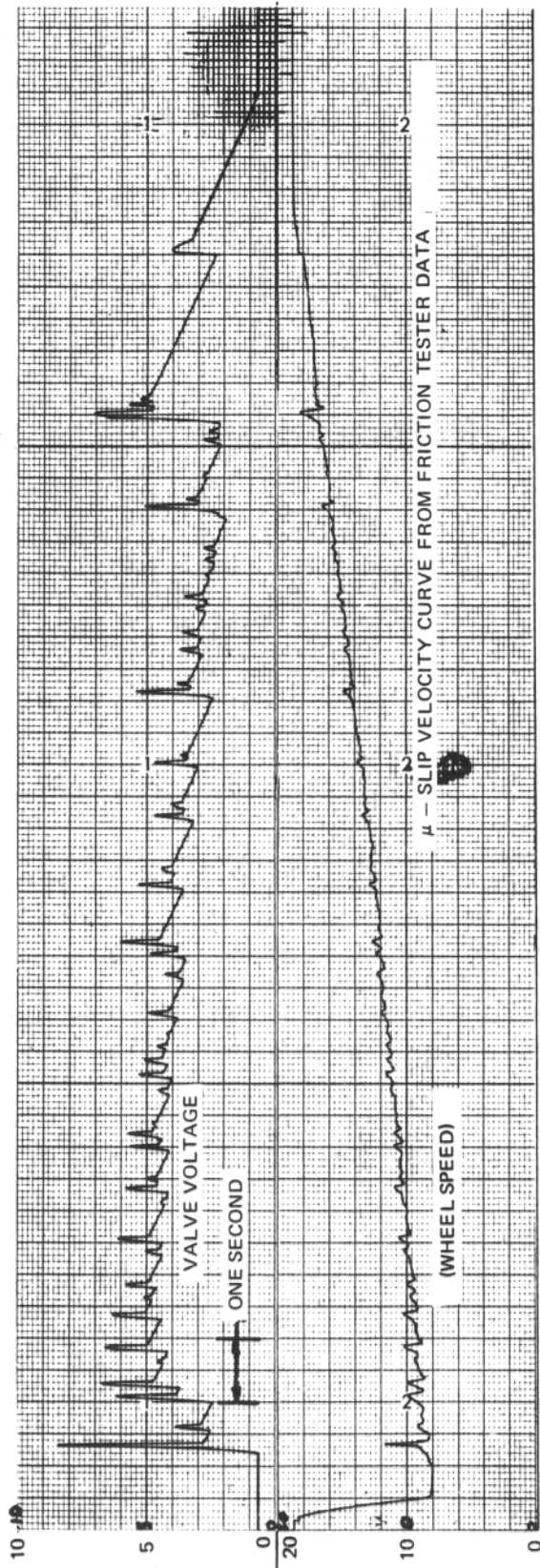
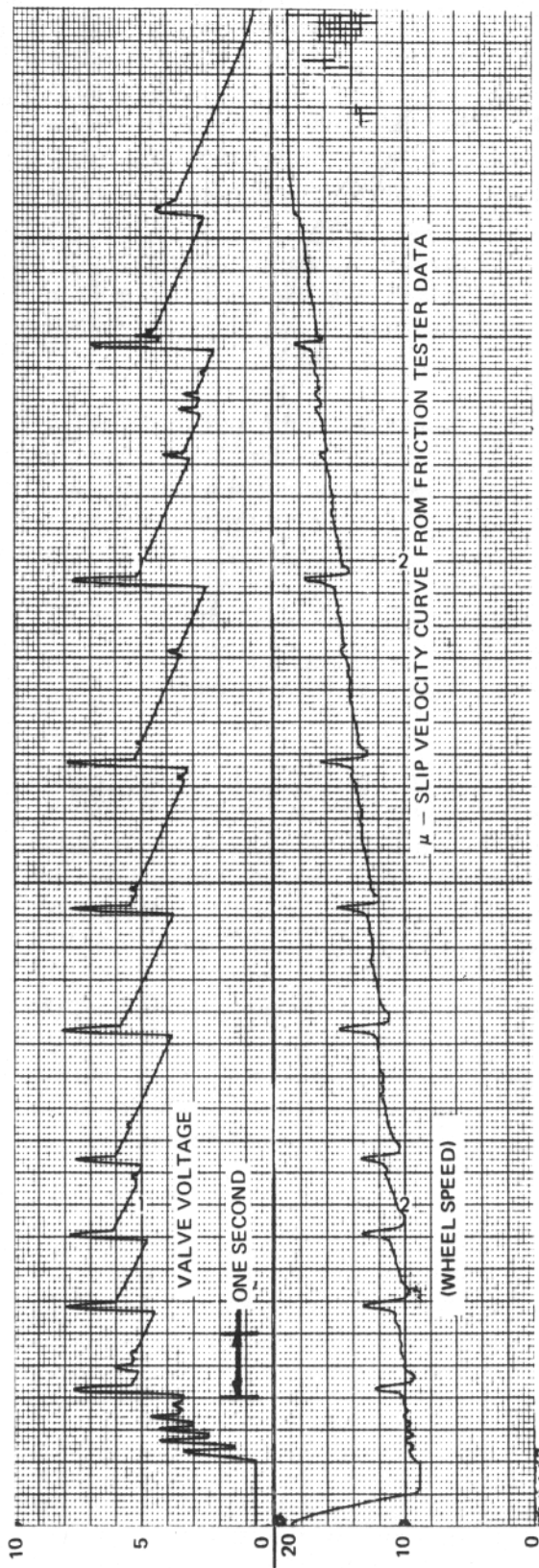


FIGURE V-5. TEST NO. 424 SIMULATOR PERFORMANCE WITH TWO DIFFERENT μ -SLIP CURVES

THE μ_{MAX} VS VELOCITY RELATIONSHIP USED IN THE SIMULATION

The correlation of anti-skid simulator results with the DC-7 phototheodolite data and oscillograph test records was poor when the μ_{MAX} vs velocity relationship obtained from the friction tester tests was used directly. The magnitude of the coefficient of friction obtained in these friction measuring tests was too high, and the shape of the curve, particularly on a dry runway, was not that required for correlation. This qualitative problem (shape of curve) is probably due to the manner in which the friction measuring tests were run. Here, discrete test points are obtained in constant speed runs; whereas, the aircraft tire makes a continuous run through the entire speed range, so that tire heating and/or anti-skid operation probably effect the μ_{MAX} versus velocity relationship.

The μ_{MAX} versus velocity relationship used in the final correlation runs on the anti-skid simulator was obtained by solving for the effective coefficient of friction required to give the instantaneous deceleration obtained from the photo-scope coverage of the DC-7 braking tests. Equations 2 through 7 and 21 (Appendix VI) were combined and solved for μ_{EFF} , yielding the expression:

$$\mu_{EFF} = \frac{-a \left[M\ddot{X}_1 + K_D (\dot{X}_1 + V_W)^2 - mW \right]}{hM\ddot{X}_1 + (K_d h - K_L b - K_{M_A}) (\dot{X}_1 + V_W)^2 + W(b - mh)}$$

Aircraft pitch and vertical dynamics were neglected (i.e., $\ddot{Z} = \dot{Z} = \ddot{\theta}_1 = \dot{\theta}_1 = 0$). This equation gives the effective μ acting at any instant during the braking runs. Simultaneous values of \ddot{X}_1 and \dot{X}_1 obtained from the photo-scope data were substituted in this equation, yielding the relationship between the effective μ and velocity. This was done for all the DC-7 tests, except Run 425 for which phototheodolite coverage was not available. Plots of μ_{EFF} versus velocity for these tests, separated into dry, minimum wet, and maximum wet categories, are shown in Figures V-6, V-7, V-8, and V-9. The minimum wet runs are plotted in two figures for clarity. Figure V-10 shows the best straight line fit (based on least squares) through the effective μ -velocity curves for each of the three runway conditions. Two curves are shown for the dry condition. The single straight line is the best least squares fit for full velocity range, while the segmented curve was determined by splitting the velocity range in two groups: 20-120 and 100-180 ft/sec. The latter curve best describes the character of the data and hence was used in the correlation. These curves do not describe μ_{MAX} , but only the effective μ , which is μ_{MAX} degraded by anti-skid system efficiency.

The final μ_{MAX} versus velocity curve was obtained by beginning with the μ_{EFF} versus velocity curves of Figure V-10 and adjusting until the simulator's velocity and deceleration output traces matched the phototheodolite data. Because anti-skid efficiency was almost constant throughout the runs, the character of the μ_{MAX} curves did not change significantly from that of the μ_{EFF} curves.

VERIFICATION

When utilizing these friction relationships in the simulator, the velocity and distance time-histories duplicated those obtained from the phototheodolite data taken during the aircraft tests. The frequency and depth of the skids also matched test data, as can be seen by comparing Figures V-11 and V-12 to Figures V-13 and V-14, respectively.

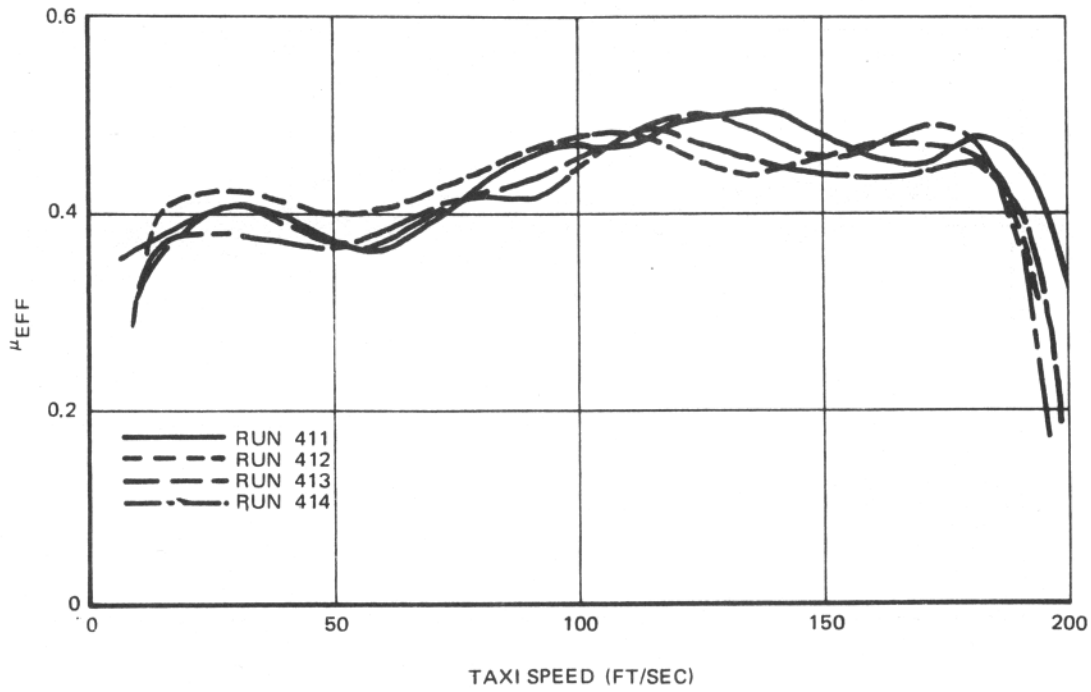


FIGURE V-6. EFFECTIVE FRICTION COEFFICIENT – DRY RUNWAY

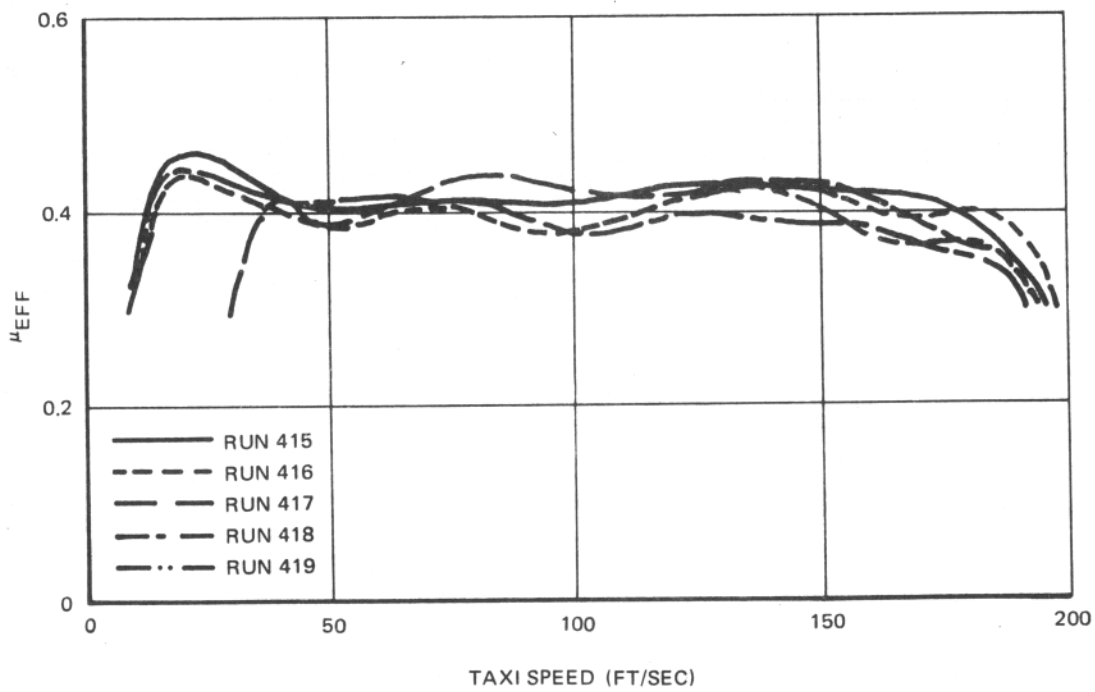


FIGURE V-7. EFFECTIVE FRICTION COEFFICIENT – MINIMUM WET RUNWAY

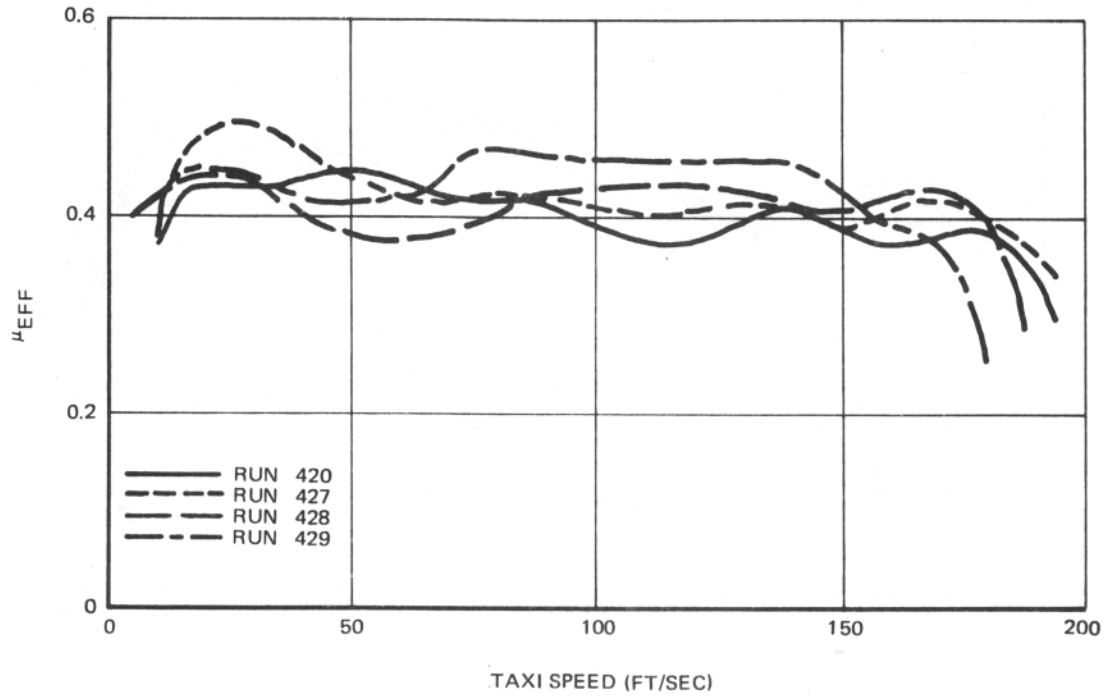


FIGURE V-8. EFFECTIVE FRICTION COEFFICIENT – MINIMUM WET RUNWAY

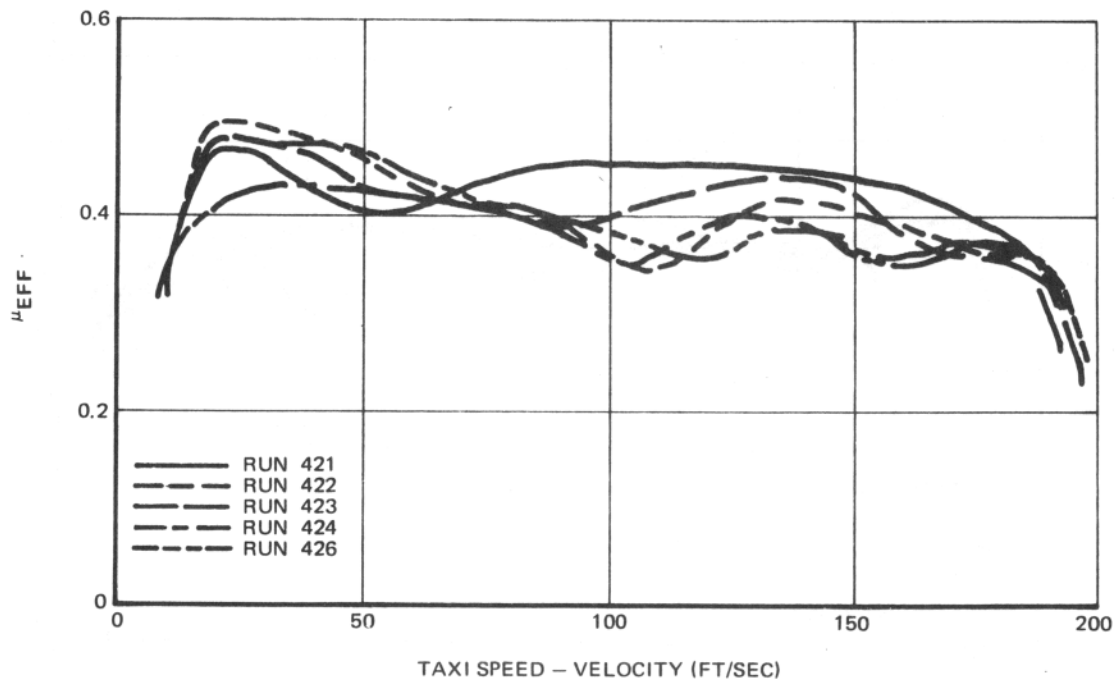


FIGURE V-9. EFFECTIVE FRICTION COEFFICIENT – MAXIMUM WET RUNWAY

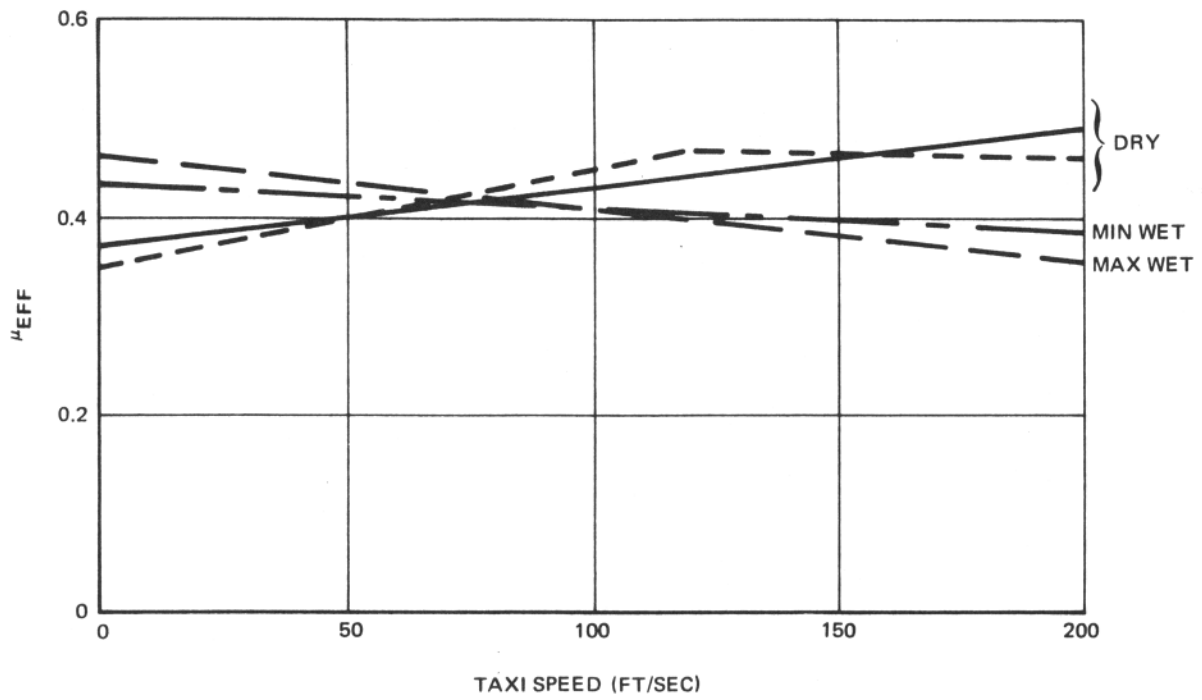
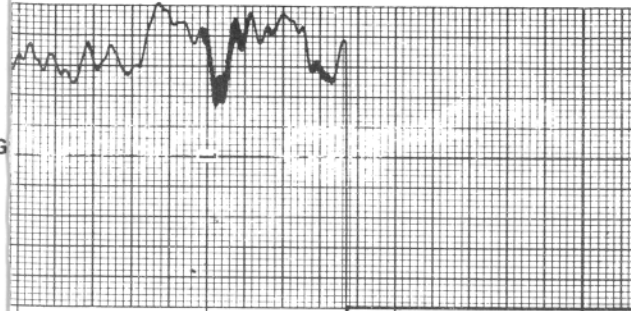
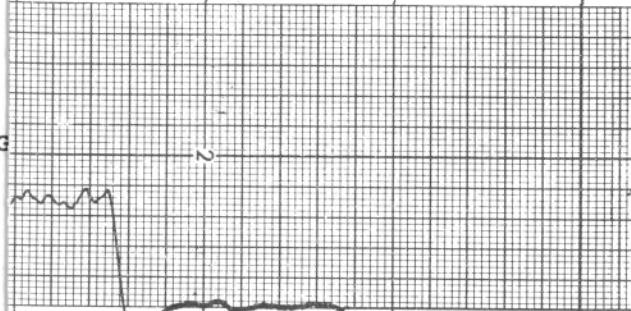


FIGURE V-10. LEAST SQUARES BEST FIT OF EFFECTIVE COEFFICIENT OF FRICTION DATA

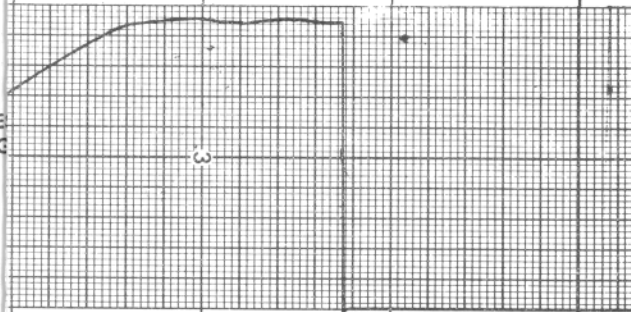
NORMAL FORCE
RIGHT MAIN LANDING G
INBOARD WHEEL
(LBS)



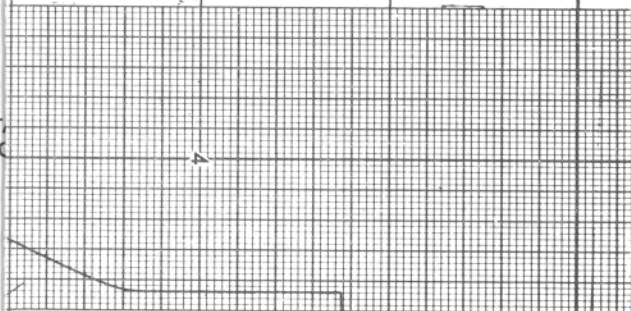
DRAG FORCE
RIGHT MAIN LANDING G
INBOARD WHEEL
(LBS)



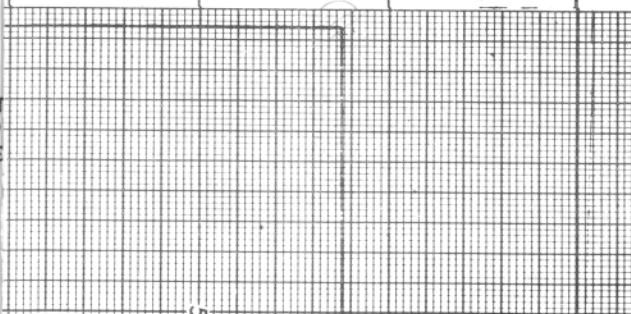
OPERATING BRAKE PRE
RIGHT MAIN LANDING G
INBOARD WHEEL
(PSI)



ANTISKID VALVE VOLT
RIGHT MAIN LANDING G
INBOARD WHEEL
(VOLTS)

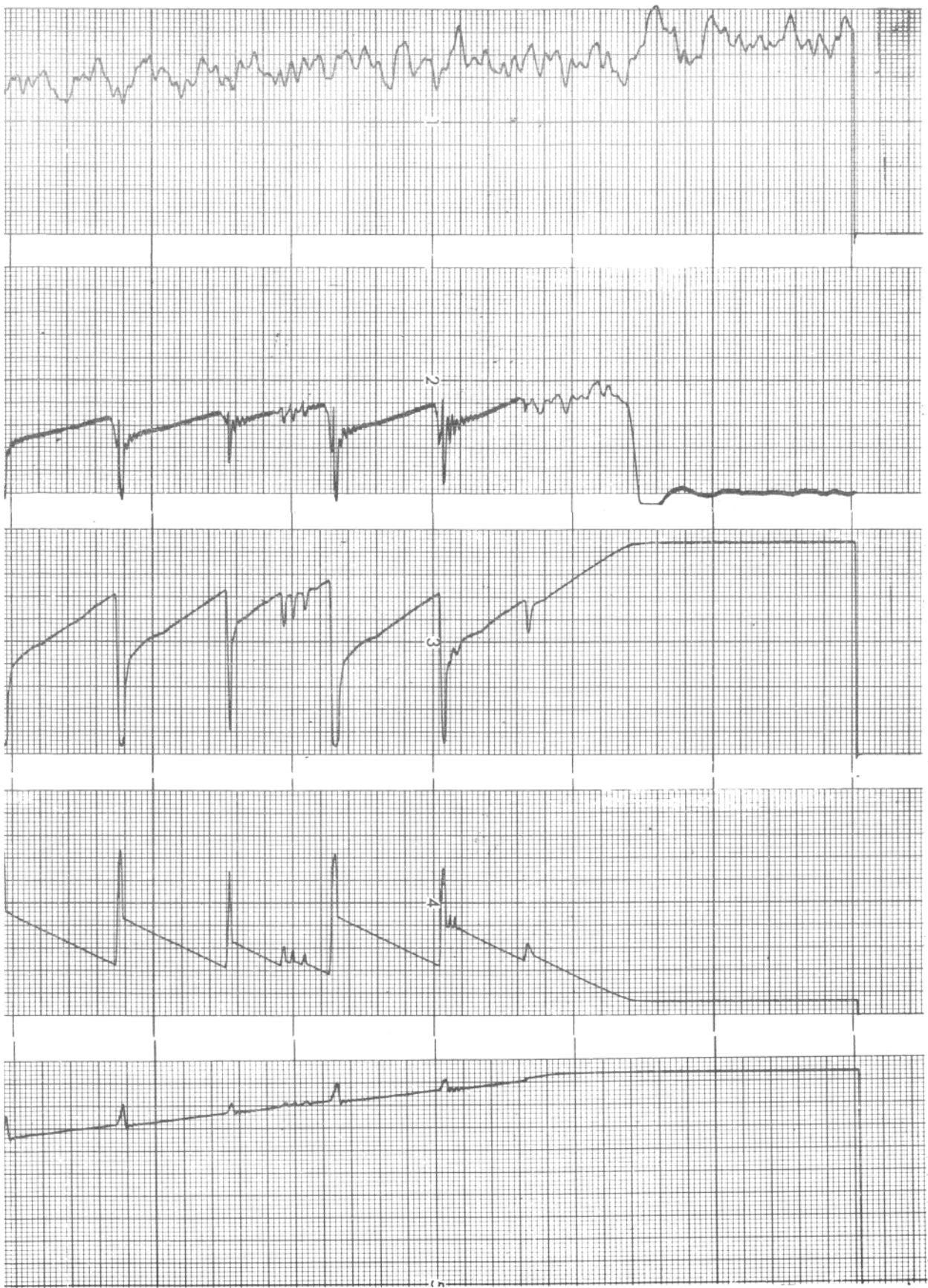


ANTISKID ACTIVE VOLT
(WHEEL VELOCITY)
RIGHT MAIN LANDING G
INBOARD WHEEL
(VOLTS)



20 25

E V-11. SIMULATION TIME HISTORY - DRY PAVEMENT

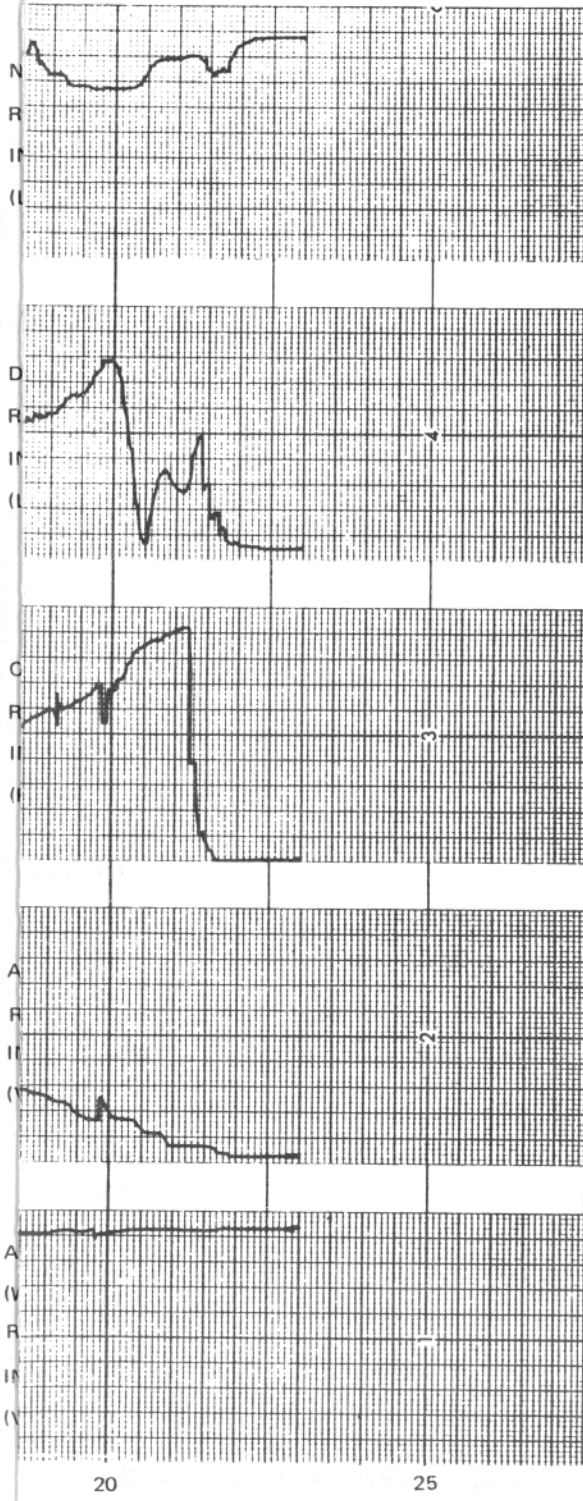


15

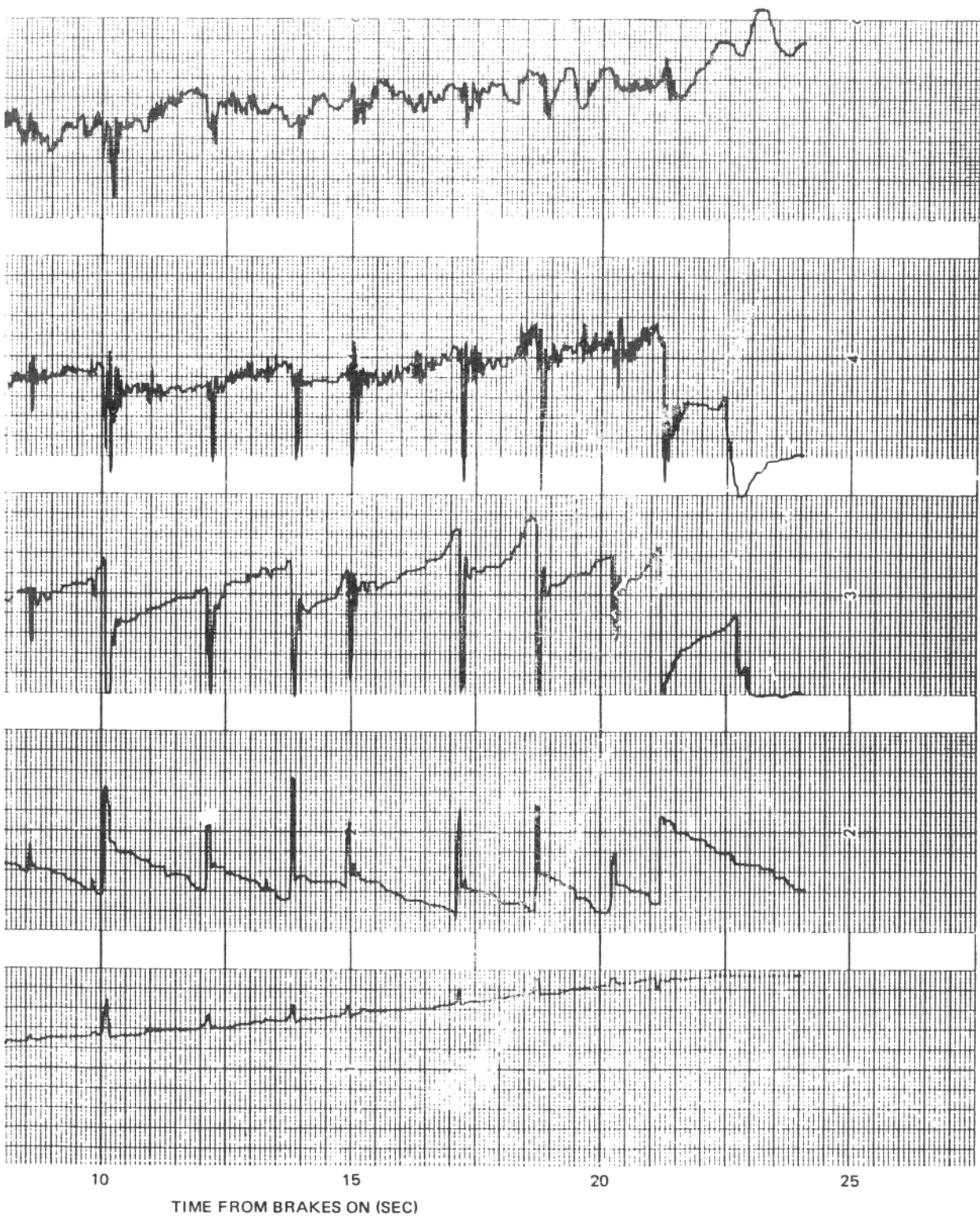
20

25

TIME FROM BRAKES ON (SEC)



HISTORY - DRY PAVEMENT (TEST NO. 412)



REFERENCES

1. R. F. Smiley and W. B. Horne, Mechanical Properties of Pneumatic Tires with Special Reference to Modern Aircraft Tires, NASA TR-R-64, 1960.

APPENDIX VI

ANALOG COMPUTER SIMULATION OF THE TEST AIRCRAFT

INTRODUCTION

The following is a description of the mathematical model that was used for the test aircraft anti-skid braking system hardware simulation. Also included are a block diagram (Figure VI-1) showing the entire simulator system and the computer circuit diagrams (Figure VI-2).

Numerical values for parameters are given in Table VI-1. From analysis of the nonbraking runs it was found that the combined net engine thrust and rolling drag force could be approximated by $0.14 \dot{X}_1^2$. To minimize the number of inputs to the computer, this coefficient was added to the aerodynamic drag coefficient and input to the computer as a single value (K_D). Scale plots of the necessary functions are included in the text.

Initial conditions are specified for Aircraft Velocity ($\dot{X}_1(0)$); Aircraft Vertical Position, $Z(0)$; and Aircraft Pitch, $\theta_1(0)$. All other initial conditions are zero.

The tire model basically follows that which was presented in Reference (1); however, modifications that have been found necessary for correlation with DC-9 flight test data were incorporated.

SIMULATION EQUATIONS

AIRCRAFT

See Figure VI-3 for aircraft geometry and force diagram.

MAIN LANDING GEAR

Figure VI-4 shows the forces acting on the main landing gear.

BRAKE-PRESSURE-TORQUE RELATIONSHIP

Brake torque is assumed to be the product of two functions:

$$T_B = f_1(\dot{\theta}_3) \times f_2(\bar{P}_B)$$

$f_1(\dot{\theta}_3)$ is an empirical function that introduces the effect of brake torque variation with brake rotational speed when the brake pressure is held constant. This function is shown in Figure VI-5.

$f_2(\bar{P}_B)$ is an empirical function that introduces the nonlinear relationship between brake torque and brake pressure when the rotational speed is held constant. This function is shown in Figure VI-6.

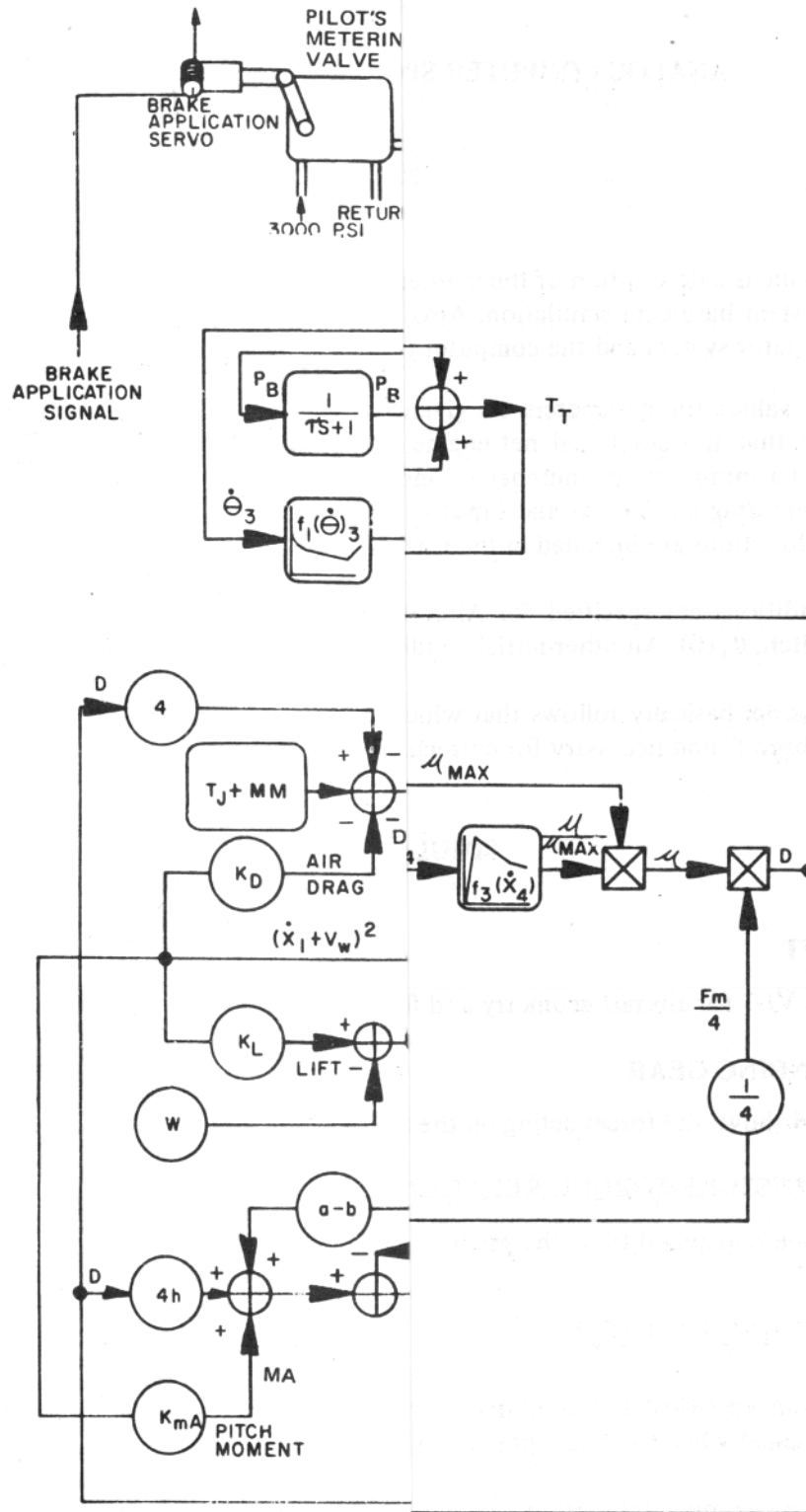


FIGURE VI-1. ANTI-SKID SIMULATION

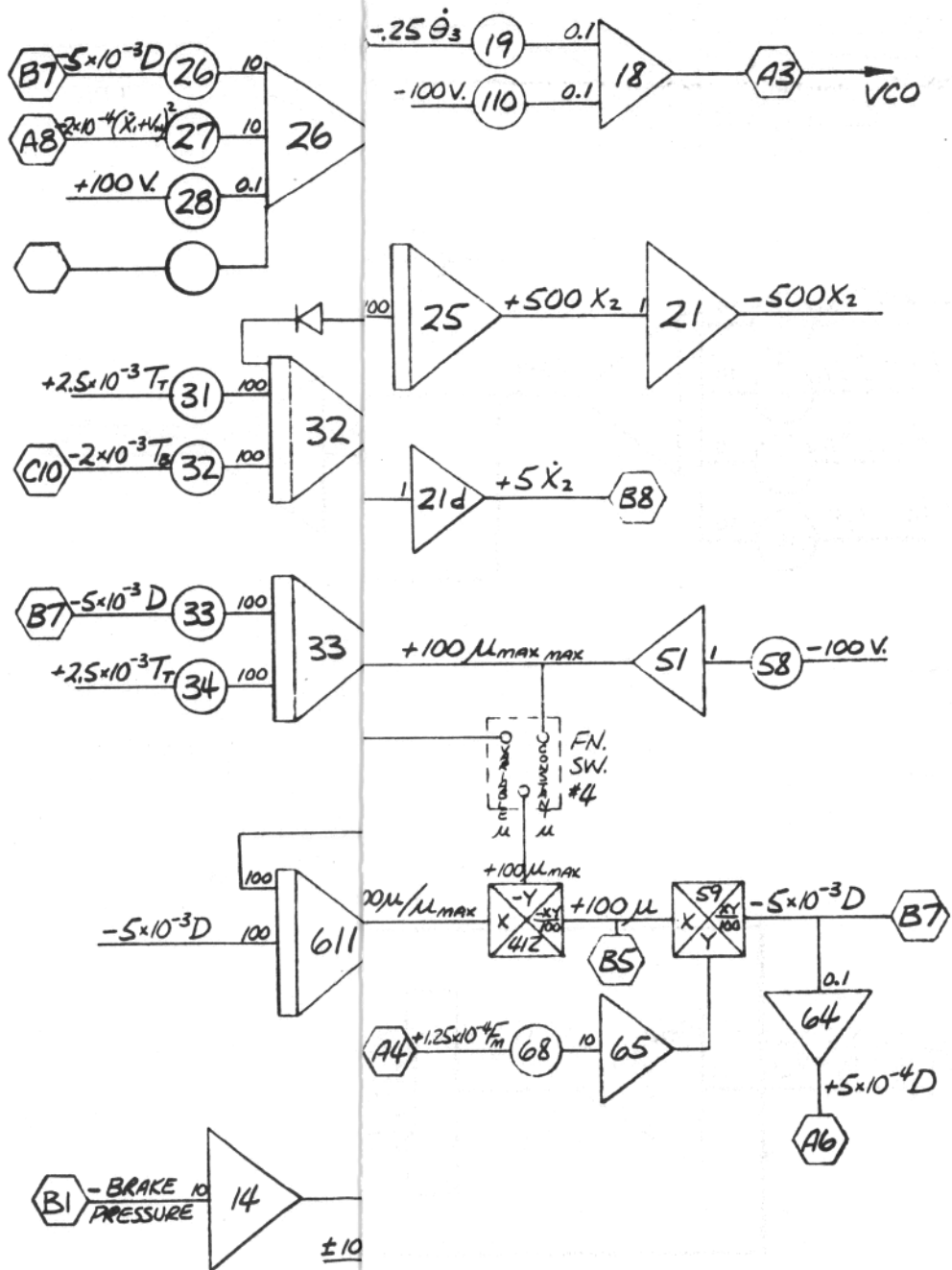
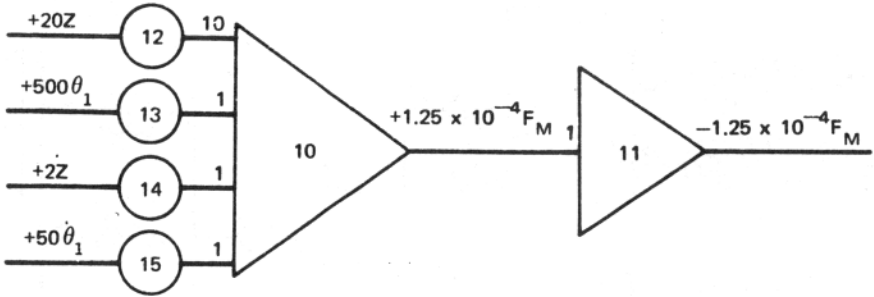
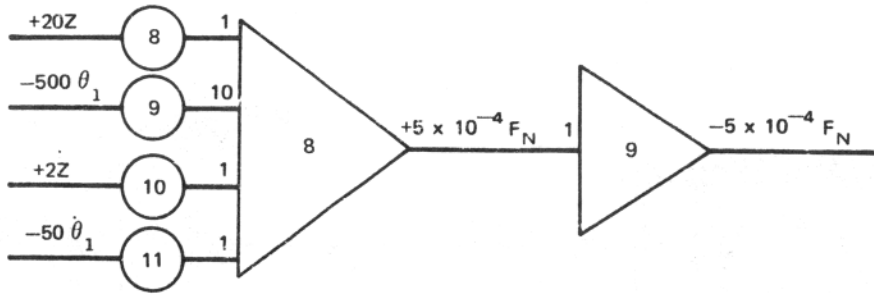


FIGURE VI-2. ANALOG COMPUTER CIRCUIT DIAGRAM (SHEET 1 OF 2)

ER
ION



$-4 (\dot{x}_1 + v_w)^2$

**TABLE VI-1
SIMULATION SYMBOLS AND VALUES**

S Y M B O L S	C O N S T A N T	V A R I A B L E	V A L U E	U N I T S	D E S C R I P T I O N
a	X		36.167	FT	DISTANCE FROM NOSE GEAR TO MAIN GEAR
b	X		31.6	FT	DISTANCE FROM NOSE GEAR TO C.G.
C_M	X		3718	LB/(FT/SEC)	DAMPING COEFFICIENT FOR TWO MAIN GEARS
C_N	X		1650	LB/(FT/SEC)	DAMPING COEFFICIENT FOR NOSE GEAR
C_T	X		500	LB/(RAD/SEC)	TORSIONAL DAMPING COEFFICIENT FOR ONE MLG TIRE
C_X	X		709	LB/(RAD/SEC)	FORE-AFT DAMPING COEFFICIENT FOR ONE MLG TIRE
D		X	-	LB	DRAG LOAD FOR ONE MAIN LANDING GEAR TIRE
D_A		X	-	LB	AERODYNAMIC DRAG ON AIRCRAFT
F_M		X	-	LB	TOTAL NORMAL LOAD ON BOTH MAIN GEARS
F_N		X	-	LB	NORMAL LOAD ON NOSE GEAR
$f_1(\dot{\theta}_3)$		X	-	-	BRAKE TORQUE VARIATION WITH SPEED
$f_2(\bar{P}_B)$		X	-	FT-LB	BRAKE TORQUE VARIATION WITH PRESSURE
$f_3(\dot{X}_4)$		X	-	-	NORMALIZED FRICTION COEFFICIENT VARIATION WITH SLIP VELOCITY
$f_4(\dot{X}_1)$		X	-	-	NORMALIZED WET FRICTION COEFFICIENT VARIATION WITH AIRCRAFT VELOCITY
h	X		8.5	FT	STATIC DISTANCE FROM GROUND TO AIRCRAFT CENTER OF GRAVITY

**TABLE VI-1.
SIMULATION SYMBOLS AND VALUES (CONT)**

S Y M B O L S	C O N S T A N T	V A R I A B L E	V A L U E	U N I T S	D E S C R I P T I O N
I	X		775,160	SLUGS-FT ²	MASS MOMENT OF INERTIA OF AIRCRAFT
I ₃	X		2.0	SLUGS-FT ²	MASS MOMENT OF INERTIA OF THE ROTATING PORTION OF ONE BRAKE, ONE WHEEL, AND PART OF ONE TIRE
I ₄	X		4.86	SLUGS-FT ²	MASS MOMENT OF INERTIA OF THE TREAD PORTION OF ONE TIRE
K _D	X		0.226	LB/(FT/SEC) ²	AERODYNAMIC DRAG COEFFICIENT
K _L	X		0.59	LB/(FT/SEC) ²	AERODYNAMIC LIFT COEFFICIENT
K _M	X		94,800	LB/FT	SPRING CONSTANT FOR TWO MAIN GEARS
K _{MA}	X		14.0	$\frac{LB/FT}{(FT/SEC)^2}$	AERODYNAMIC PITCH MOMENT COEFFICIENT
K _N	X		39,400	LB/FT	SPRING CONSTANT FOR NOSE GEAR
K _T	X		810,000	LB-FT/RAD	TORSIONAL SPRING CONSTANT FOR ONE MLG TIRE
K _X	X		70,920	LB/FT	FORE-AFT SPRING CONSTANT FOR ONE MLG TIRE
K _Z	X		86,400	LB/FT	VERTICAL SPRING CONSTANT FOR ONE MLG TIRE
L		X	-	LB	AERODYNAMIC LIFT ON AIRCRAFT
m	X		0.0038	-	RUNWAY DOWNHILL SLOPE
M	X		•	SLUGS	TOTAL AIRCRAFT MASS
M ₁	X		•	SLUGS	AIRCRAFT SPRUNG MASS
M ₂	X		26.3	SLUGS	UNSPRUNG MASS FOR ONE MAIN LANDING GEAR
M _A		X	-	LB-FT	AERODYNAMIC PITCH MOMENT ON AIRCRAFT
P _B		X	-	LB/IN ²	BRAKE PRESSURE AT THE BRAKE
P̄ _B		X	-	LB/IN ²	LAGGED (FILTERED) BRAKE PRESSURE

*VARIES WITH EACH RUN

TABLE VI-1
SIMULATION SYMBOLS AND VALUES (CONT)

SYMBOLS	CONSTANT	VARIABLE	VALUE	UNITS	DESCRIPTION
r_e		X	-	FT	EFFECTIVE TIRE ROLLING RADIUS
r_o	X		1.638	FT	RADIUS OF FREE MAIN LANDING GEAR TIRE
S		X	-	1/SEC	LAPLACE OPERATOR
T_B		X	-	FT-LB	BRAKE TORQUE
T_J	X		0	LB	ENGINE THRUST
T_T		X	-	FT-LB	TORSIONAL TORQUE OF ONE MAIN LANDING GEAR TIRE
V_W	X		*	FT/SEC	WIND VELOCITY (HEADWIND)
W	X		*	LB	TOTAL AIRCRAFT WEIGHT
X_1		X	-	FT	ELAPSED AIRCRAFT DISTANCE
\dot{X}_1		X	-	FT/SEC	AIRCRAFT VELOCITY
\ddot{X}_1		X	-	FT/SEC ²	AIRCRAFT ACCELERATION
X_2		X	-	FT	DISPLACEMENT (FORE-AFT) OF UNSPRUNG MAIN LANDING GEAR MASS RELATIVE TO AIRCRAFT
\dot{X}_4		X	-	FT/SEC	TIRE TREAD SLIDING VELOCITY
Z		X	-	FT	VERTICAL DISPLACEMENT OF AIRCRAFT C.G.
δ_{11}	X		5.5×10^{-6}	FT/LB	DISPLACEMENT OF UNSPRUNG MAIN LANDING GEAR MASS (FORE-AFT) RESULTING FROM A 1-LB LOAD
δ_{12}	X		4.94×10^{-7}	FT/FT-LB	DISPLACEMENT OF UNSPRUNG MAIN LANDING GEAR MASS (FORE-AFT) RESULTING FROM A 1-FT-LB TORQUE
μ_{MAX}		X	-	-	MAXIMUM FRICTION COEFFICIENT (A FUNCTION OF VELOCITY)
$\mu_{\mu_{MAX}}$		X	-	-	NORMALIZED FRICTION COEFFICIENT
$\mu_{MAX MAX}$	X		-	-	MAXIMUM PAVEMENT FRICTION COEFFICIENT
θ_1		X	-	RAD	AIRCRAFT PITCH ANGLE

*VARIES WITH EACH RUN

**TABLE VI-1
SIMULATION SYMBOLS AND VALUES (CONT)**

S Y M B O L S	C O N S T A N T	V A R I A B L E	V A L U E	U N I T S	D E S C R I P T I O N
$\dot{\theta}_3$		X	-	RAD/SEC	ANGULAR VELOCITY OF WHEEL HUB
$\dot{\theta}_4$		X	-	RAD/SEC	ANGULAR VELOCITY OF TIRE TREAD
τ	X		0.01	SEC	LAGGED BRAKE PRESSURE TIME CONSTANT
ζ_1	X		0.08	-	CRITICAL DAMPING RATIO FOR FORE-AFT MOTION ON UNSPRUNG MASS OF MAIN LANDING GEAR
$\dot{X}(0)$	X		*	FT/SEC	INITIAL AIRCRAFT VELOCITY
$Z(0)$	X		*	FT	INITIAL AIRCRAFT VERTICAL POSITION
$\theta_1(0)$	X		*	RAD	INITIAL AIRCRAFT ANGULAR POSITION

*VARIES WITH EACH RUN

To account for a time delay between brake torque change and brake pressure change \bar{P}_B is determined from the relationship:

$$\dot{\bar{P}}_B = \frac{1}{\tau} (P_B - \bar{P}_B)$$

Where P_B is the measured brake pressure at the brake.

TIRE

The tire model (Figure VI-7) consists of two rotational parts:

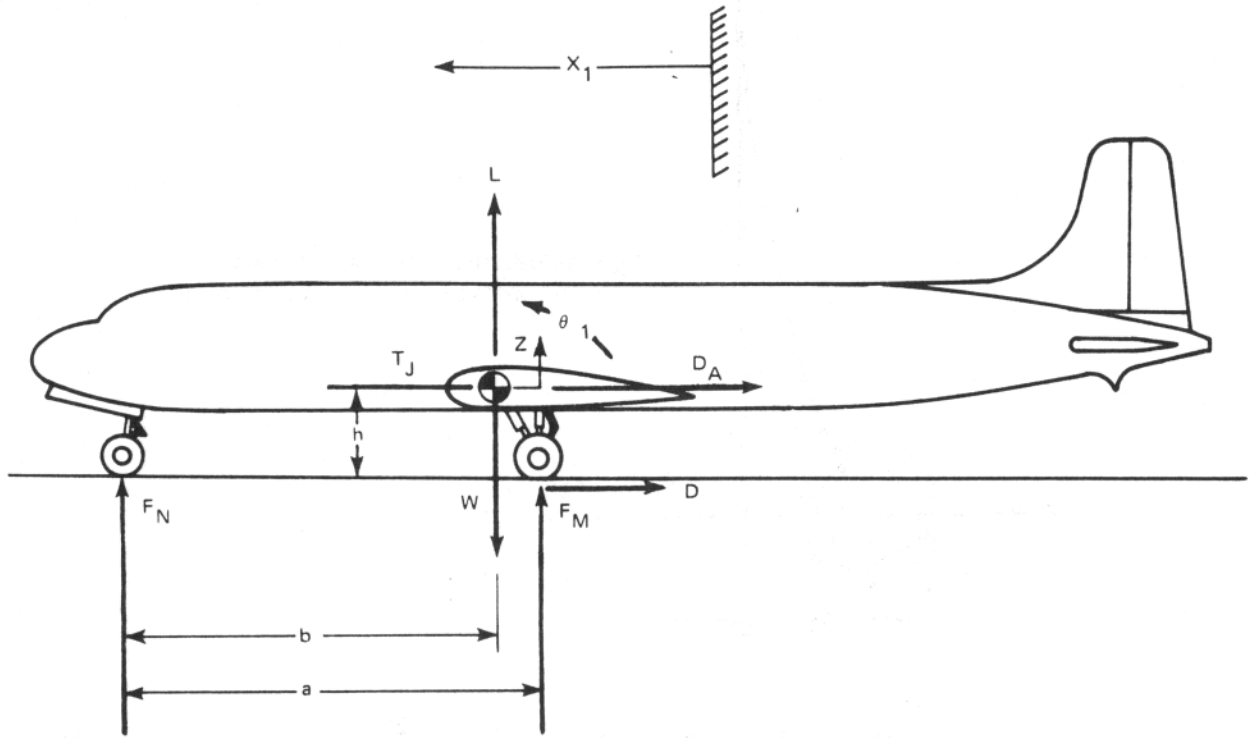
I_4 : Tire tread portion

I_3 : Hub portion including wheel and rotating portion of brake

These parts are connected via a torsional spring K_T and torsional viscous damper C_T .

As the tire tread rolls into contact with the pavement it experiences:

1. A compressive strain because the chord distance is less than the arc.
2. A tension strain because the tread stretches just prior to pavement contact.



$$\ddot{X}_1 = \frac{1}{M} (T_J - D_A - 4D + mW) \quad (2)$$

$$\ddot{Z} = \frac{1}{M_1} (F_N + F_M + L - W) \quad (3)$$

$$\ddot{\theta}_1 = \frac{1}{I} [F_M (a-b) - F_N b + 4Dh + M_A] \quad (4)$$

$$L = K_L (\dot{X}_1 + V_W)^2 \quad (5)$$

$$D_A = K_D (\dot{X}_1 + V_W)^2 \quad (6)$$

$$M_A = K_{M_A} (\dot{X}_1 + V_W)^2 \quad (7)$$

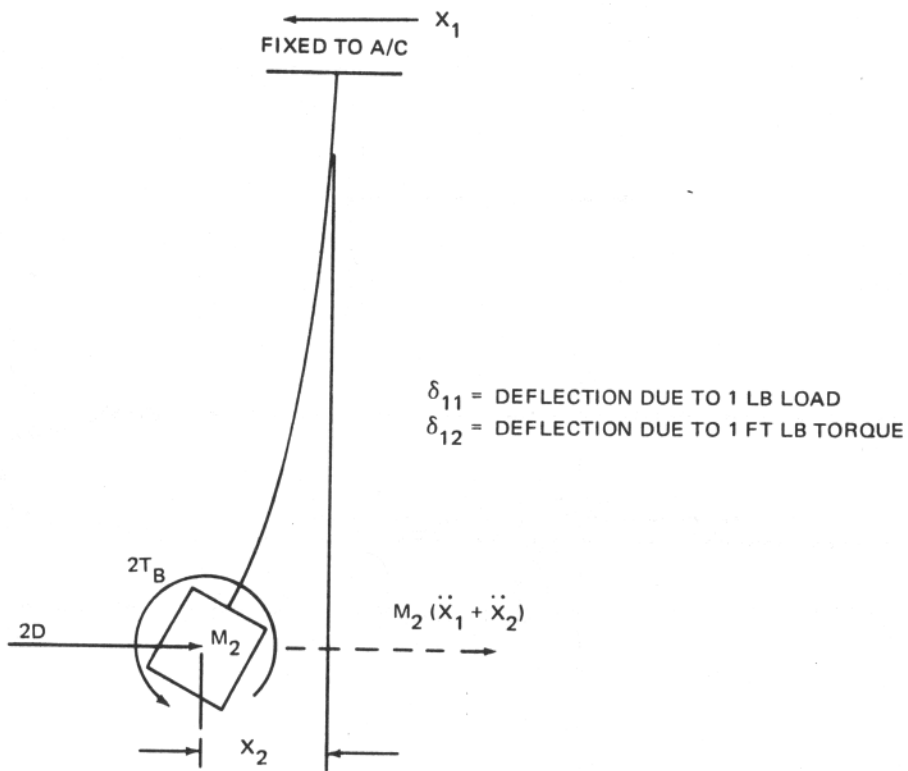
$$F_M = -K_M [Z + (a-b)\theta_1] - C_M [\dot{Z} + (a-b)\dot{\theta}_1] \quad (8)$$

$$F_N = -K_N [Z - b\theta_1] - C_N [\dot{Z} - b\dot{\theta}_1] \quad (9)$$

$$Z(0) = \frac{[(a-b)^2 K_M + b^2 K_N] (L - W) - [(a-b) K_M - b K_N] M_A}{2 a K_M K_N} \quad (10)$$

$$\theta_1(0) = \frac{[(a-b) K_M - b K_N] (W - L) + (K_M + K_N) M_A}{2 a K_M K_N} \quad (11)$$

FIGURE VI-3. AIRCRAFT GEOMETRY AND FORCE DIAGRAM



$$x_2 = -2D\delta_{11} - 2T_B\delta_{12} - M_2(\ddot{x}_1 + \ddot{x}_2)\delta_{11} - 2\xi x_2 \sqrt{M_2\delta_{11}} \quad (12)$$

WHERE

ξ = CRITICAL DAMPING RATIO FOR STRUT

OR

$$M_2\delta_{11}\ddot{x}_2 + 2\xi\sqrt{M_2\delta_{11}}\dot{x}_2 + x_2 = -2D\delta_{11} - 2T_B\delta_{12} - M_2\delta_{11}\ddot{x}_1 \quad (13)$$

$$\ddot{x}_2 = -\frac{2\xi\dot{x}_2}{\sqrt{M_2\delta_{11}}} - \frac{x_2}{M_2\delta_{11}} - \frac{2D}{M_2} - \frac{2T_B\delta_{12}}{M_2\delta_{11}} - \ddot{x}_1 \quad (14)$$

FIGURE VI-4. FORCES ACTING ON MAIN LANDING GEAR

The relative velocity between the tire tread and the pavement at the interface, \dot{X}_4 , is:

$$\dot{X}_4 = \dot{X}_1 + \dot{X}_2 - r_e \dot{\theta}_4$$

Drag load is calculated by:

$$D = \frac{F_m}{4} \times \frac{\mu}{\mu_{MAX}} \times \mu_{MAX}$$

The ratio μ/μ_{MAX} is an empirical function of \dot{X}_4

$$\frac{\mu}{\mu_{MAX}} = f_3(\dot{X}_4)$$

This function is shown in Figure VI-8.

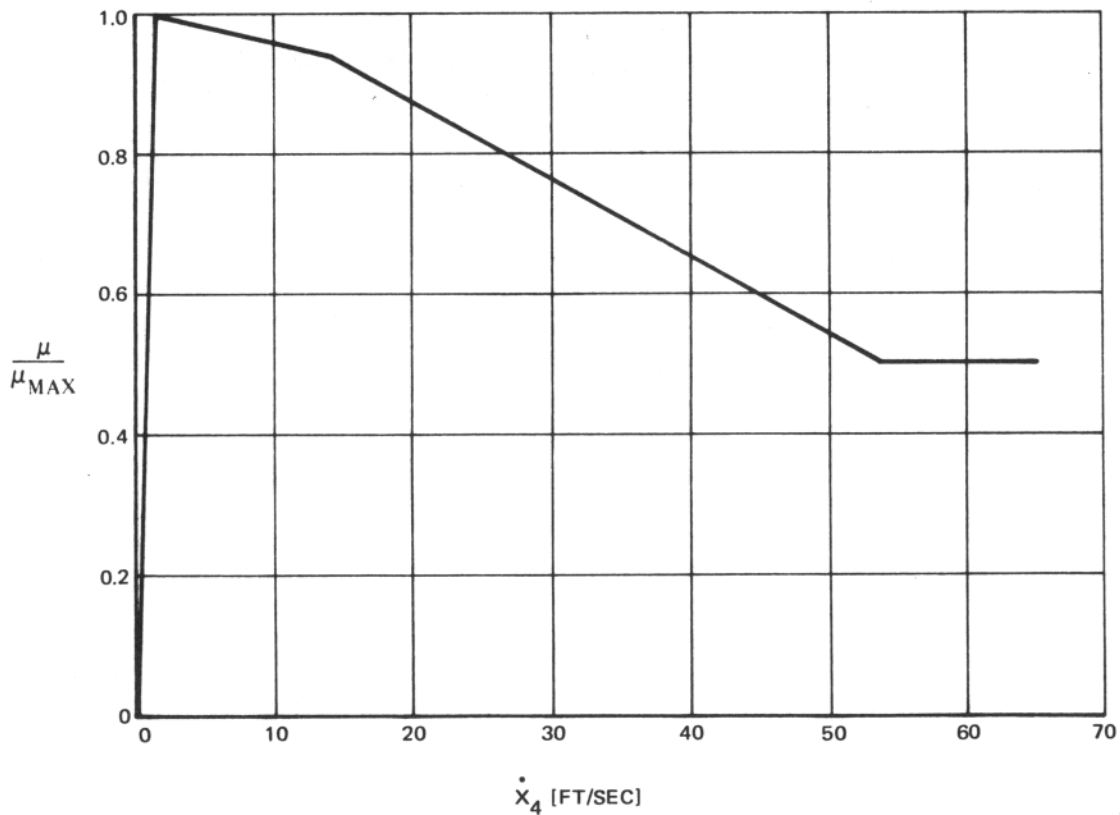


FIGURE VI-8. TREAD SLIP CURVE

The maximum friction coefficient is a function of airplane velocity, \dot{X}_1 , as is shown in Figure VI-9.

$$\mu_{MAX} = \mu_{MAX_{MAX}} \times f_4(\dot{X}_1)$$

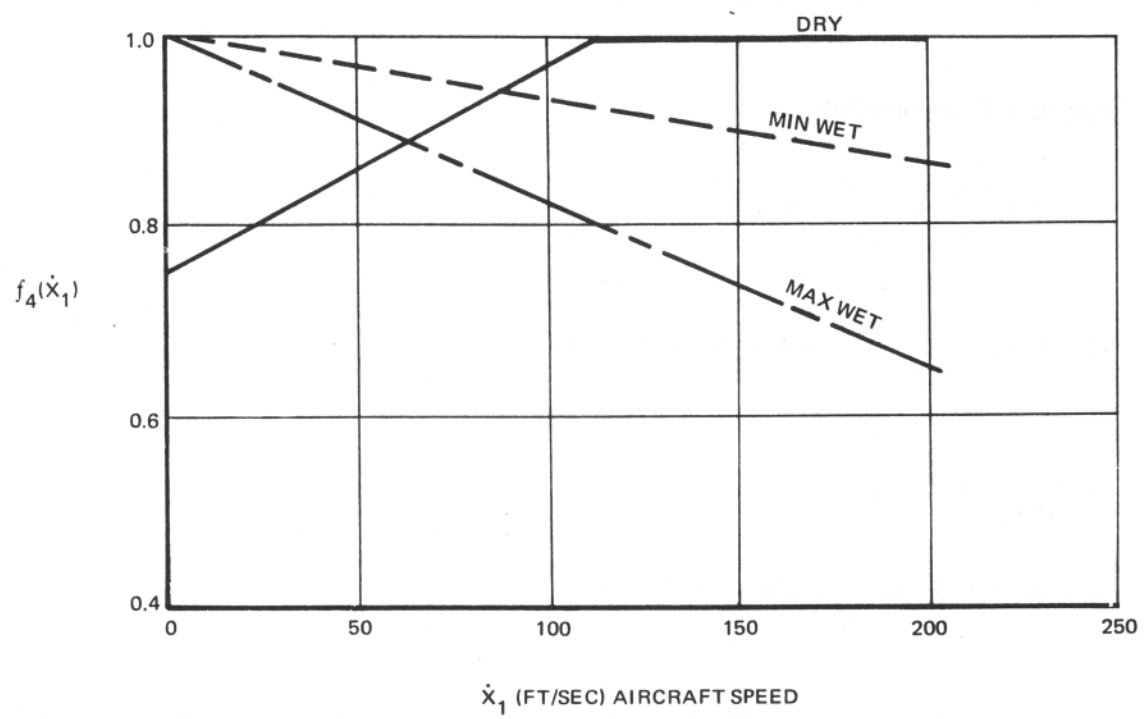


FIGURE VI-9. μ_{MAX} VELOCITY RELATIONSHIP

REFERENCES

1. R. F. Smiley and W. B. Horne, Mechanical Properties of Pneumatic Tires with Special Reference to Modern Aircraft Tires, NASA TR-R-64, 1960.

APPENDIX VII

COMPARATIVE METHODS USED TO DETERMINE RELATIONSHIP BETWEEN FRICTION COEFFICIENTS OF THE FRICTION TESTER AND THE AIRCRAFT.

This appendix describes, discusses, and gives results for comparative methods used to find relationships between the maximum friction coefficient available to the aircraft and that measured by the FAA Variable Slip Runway Friction Tester.

METHOD I – COMPARISON OF AIRCRAFT STRAIN GAGE DATA WITH FRICTION TESTER DATA

The test data recorded during the aircraft tests used for correlation were: (1) phototheodolite results of acceleration, velocity, and distance versus time; (2) aircraft accelerometer data, (3) drag, torque, and normal load on the wheels of the right-hand main landing gear; and (4) anti-skid performance data, primarily individual brake pressures and wheel speeds for all wheels.

This data was not satisfactory. The phototheodolite accelerations were consistent with the aircraft accelerometer data. However, the strain gage drag load information from the instrumented gear yielded maximum friction coefficients that were greater than unity even on some wet surfaces. Consequently, the drag load data were further analyzed.

As stated above, brake pressures were recorded on all tires. The brake pressures recorded for the left gear (only the right gear was strain gaged) were significantly higher than the right gear as shown by Figure VII-1. This implied that the drag loads on the left gear were greater than the right.

To investigate the accuracy of the drag data, and to determine if a new strain gage calibration could be applied to correct it, the inboard and outboard drag loads of the right gear were integrated over time for four aircraft runs. These values were then combined with the integral of aerodynamic drag in four different ways, shown in Figure VII-2, to obtain an equivalent velocity change throughout the aircraft run. The first method utilized four times the outboard value. Had these results correlated, it would have indicated that the inboard drag load data was not correct. The second method used four times the inboard drag load. A third method utilized twice the inboard and twice the outboard, essentially, averaging the results. The fourth method, similar to the third method, established that the actual drag loads during tests were approximately 74 percent of the recorded values.

The relationship shown in Figure VII-3 was obtained by comparing aircraft friction, based on strain gage vertical and corrected drag load data, with friction tester data obtained during the runway tests. This data scatters more than that given in Figure 19 of the main text, but the average value, 0.62, is about the same.

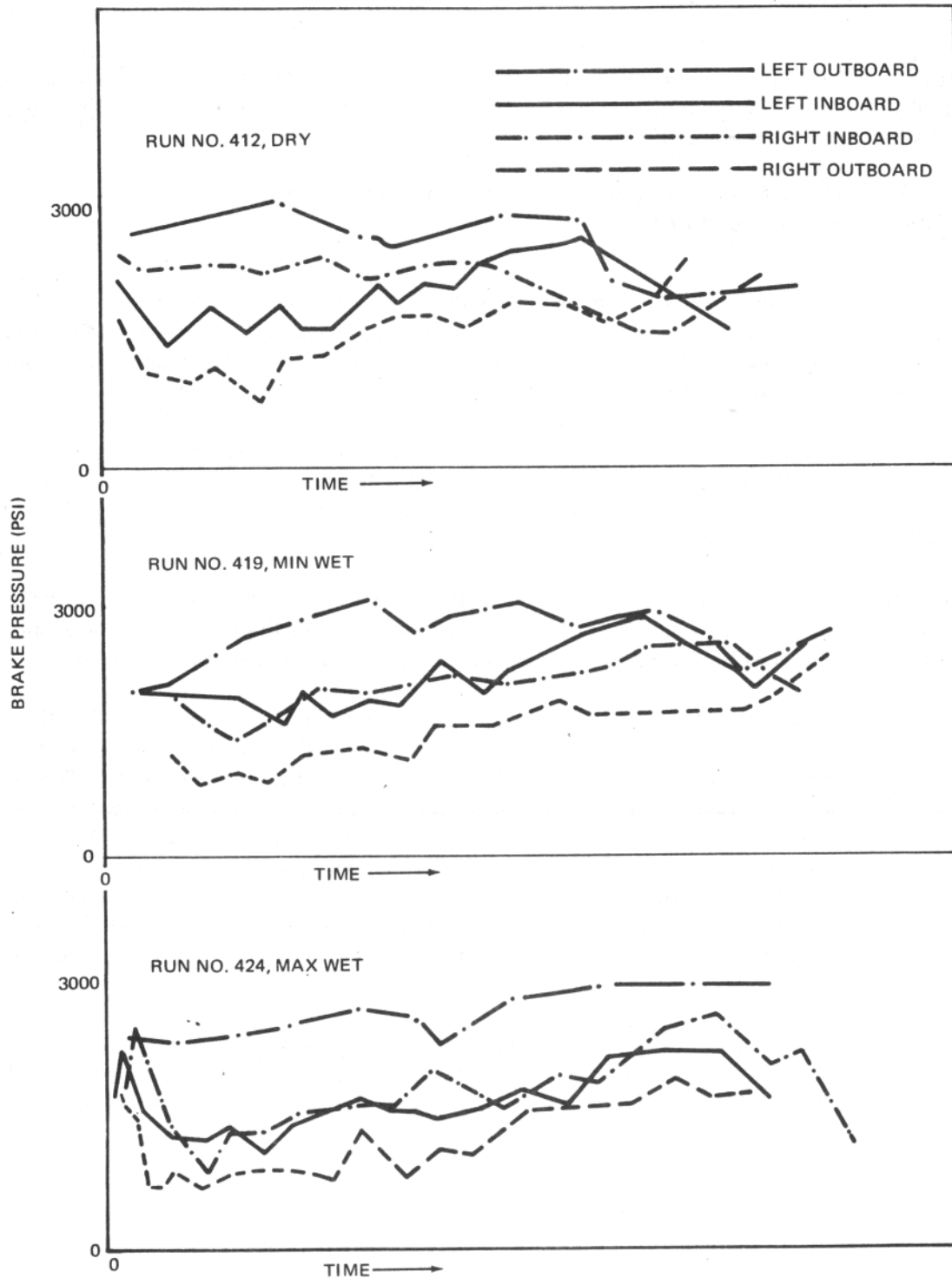


FIGURE VII-I. TEST AIRCRAFT BRAKE PRESSURES

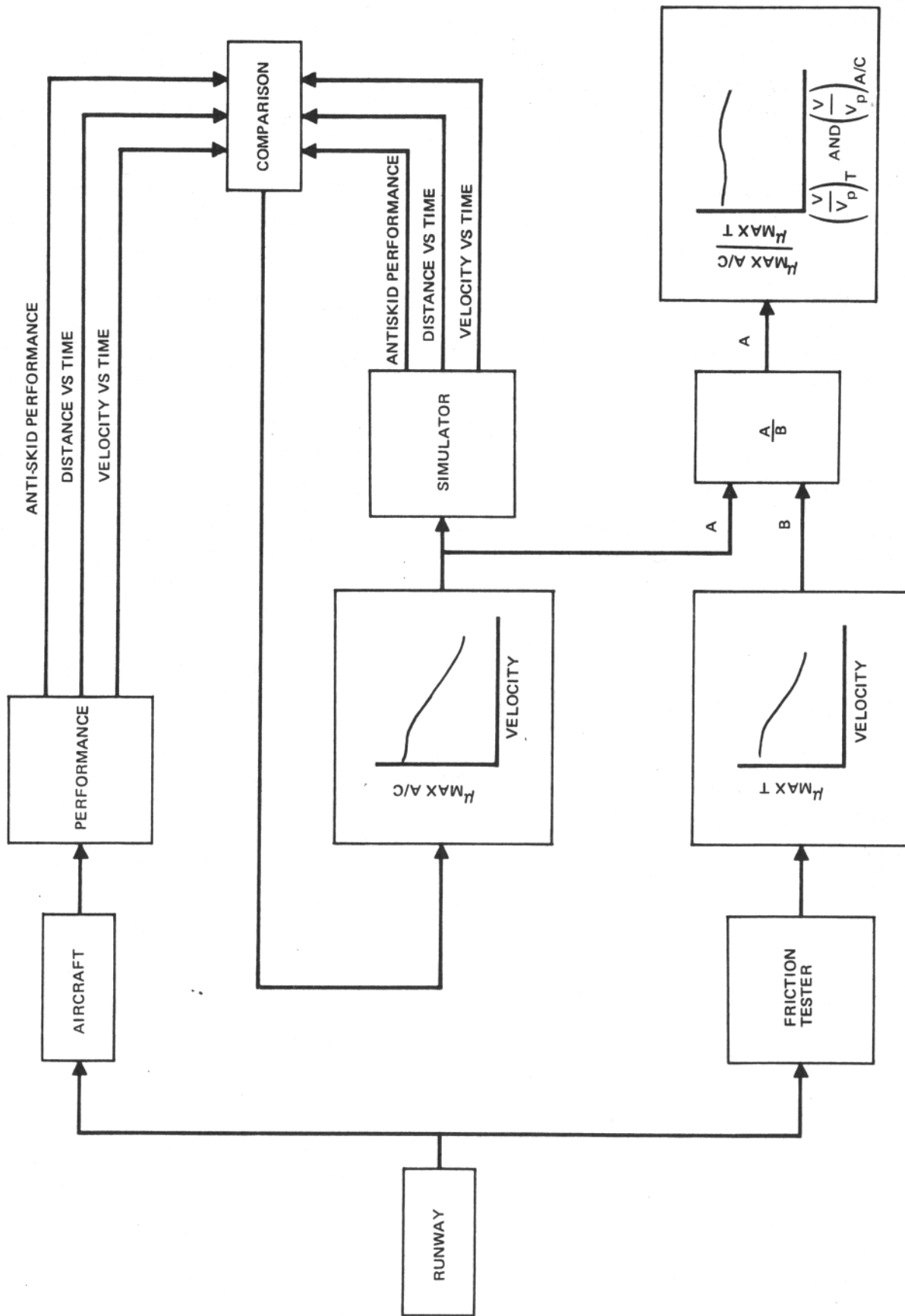


FIGURE VII-4. CORRELATION METHOD II

COMPARATIVE RESULTS

The results of this program indicate that at the Long Beach Airport under dry, minimum wet, and maximum wet conditions, the maximum friction coefficients of the friction tester when reduced by a factor of 0.59 (independent of velocity) give a reasonable approximation to the maximum coefficients experienced by the test aircraft.

This runway had excellent wet friction characteristics as shown by the small differences between wet and dry performance values.

Friction tester performance on wet and flooded surfaces requires further consideration. The data from Reference (1) offer some insight on what to expect under these conditions. Paper 3 of this compendium, Comparative Braking Performance of Various Aircraft on Grooved and Pavements at the Landing Research Runway, NASA Wallops Station, by Thomas J. Yager gives Convair 990 brake test data in the form of μ_{EFF} versus velocity. Paper 23, Joint NASA-British Ministry of Technology Skid Correlation Study, by Walter B. Horne and John A. Tanner gives the results of the Penn State Braking Trailer in the form of μ_{MAX} versus velocity. The Penn State Trailer is similar to the FAA Variable Slip Runway Friction Tester. Data were obtained on nine different runway surfaces and under wet and puddled, and flooded conditions. The μ_{EFF} data were converted to $\mu_{MAX A/C}$ data by the relationship shown in Figure VII-4. The relationships obtained between $\mu_{MAX A/C}$ and $\mu_{MAX T}$ are estimated in Figure VII-5 for the wet and puddled condition. The results show that the tester performance is affected by the type and wetness of the surface.

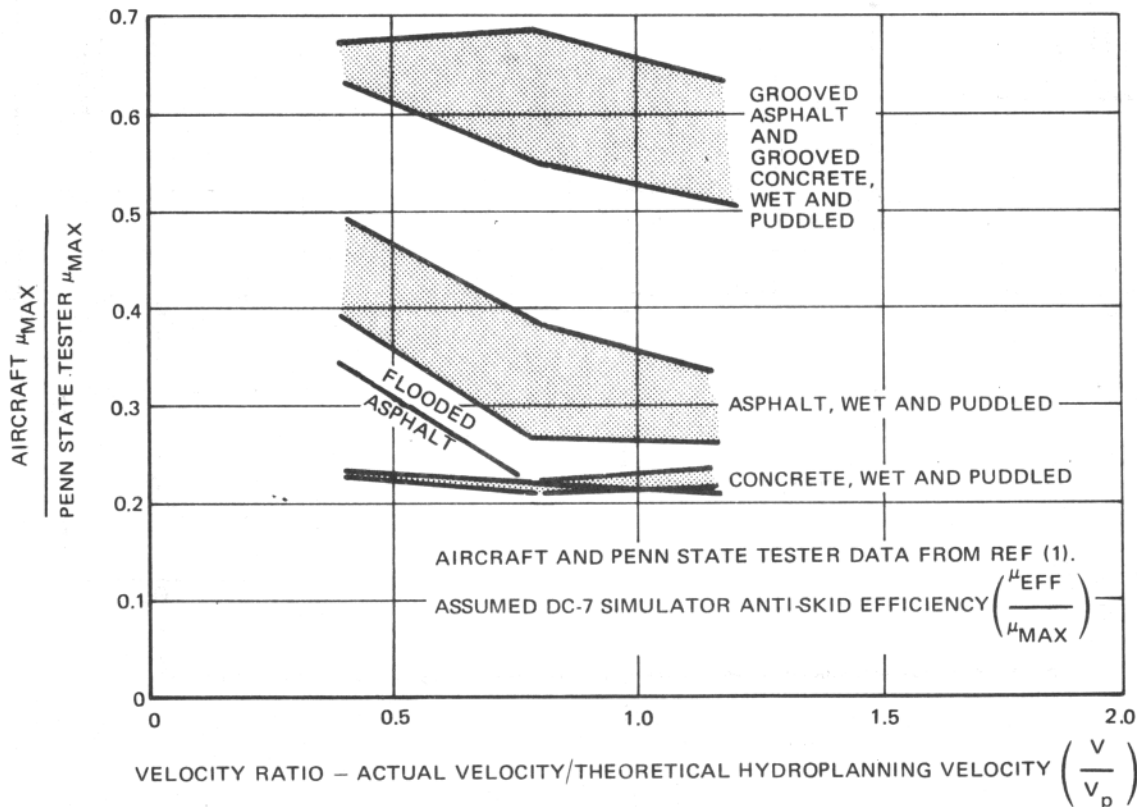


FIGURE VII-5. ESTIMATED RELATIONSHIPS BETWEEN AIRCRAFT AND TESTER FRICTION COEFFICIENTS ON WET/PUDDLED/FLOODED RUNWAYS

REFERENCES

1. Pavement Grooving and Traction Studies, NASA SP-5073, 1969.

APPENDIX VIII

DEFINITIONS

Active voltage	Anti-skid control voltage proportional to wheel speed.
ASTM	American Society of Testing Materials.
C_D	Aerodynamic drag coefficient.
CG	Center of gravity.
C_L	Aerodynamic lift coefficient.
C_m	Aerodynamic pitch moment coefficient.
D_I	Drag on RH inboard wheel.
D_O	Drag on RH outboard wheel.
F_X	Drag load.
F_Z	Normal load.
g	Acceleration of gravity (32.2 ft/sec ²).
K_{AVE}	Average ratio of actual brake drag to two times the sum of the recorded right-hand gear inboard and outboard brake drag.
K_Z	Vertical tire spring constant.
K_X	Fore-and-aft tire spring constant.
μ	Coefficient of friction.
μ_{EFF}	Effective μ of Aircraft.
μ_{MAX}	Maximum μ available.
$\mu_{MAXA/C}$	Aircraft μ_{MAX} obtained by dividing drag load by vertical load.
μ_{MAXMAX}	Maximum μ_{MAX} over entire speed range of aircraft.
μ_{MAXT}	μ_{MAX} measured by FAA Variable Slip Runway Friction Tester.
Phototheodolite	Photo tracker recording aircraft position and time.

PR	Ply rating.
r_{EFF}	Effective rolling radius of the unbraked tire.
rms	Root mean square.
r_0	Radius of undeflected tire.
Slip	The difference between the angular velocity of a braked wheel and that of an unbraked wheel.
Slip ratio	Slip expressed as a percentage of the unbraked wheel speed.
Slip velocity	Slip expressed in translational terms. (V_S)
$\dot{\theta}_3$	Wheel rotational speed (radians/sec).
$\dot{\theta}_4$	Angular velocity of tire.
V	Velocity.
Valve voltage	Voltage input to anti-skid valve to control brake pressure.
V_H	Hub velocity (horizontal velocity of wheel axle).
V_P	Friction tester and aircraft theoretical hydroplaning velocities (assuming equation developed for 10-ply aircraft tires: nine times the square root of the inflation pressure).
V_S	Wheel slip velocity.
\dot{X}_4	Tire tread slip velocity.

Note: For definitions of symbols used in equations describing the analog computer simulation, refer to Table VI-1, Appendix VI.